APPROXIMATE ANALYSIS AND CONDITION ASSESMENT OF REINFORCED CONCRETE T-BEAM BRIDGES USING ARTIFICIAL NEURAL NETWORKS

A THESIS SUBMITTED TO
THE GRADUATE SCHOOL OF NATURAL AND APPLIED SCIENCES
OF
MIDDLE EAST TECHNICAL UNIVERSITY

BY

TAHA DUMLUPINAR

IN PARTIAL FULFILLMENT OF THE REQUIREMENTS
FOR
THE DEGREE OF MASTER OF SCIENCE
IN
CIVIL ENGINEERING

JULY 2008

Approval of the thesis:

APPROXIMATE ANALYSIS AND CONDITION ASSESMENT OF T-BEAM BRIDGES USING ARTIFICIAL NEURAL NETWORKS

submitted by **TAHA DUMLUPINAR** in partial fulfillment of the requirements for the degree of **Master of Science in Civil Engineering Department, Middle East Technical University** by,

Prof. Dr. Canan Özgen _____
Dean, Graduate School of **Natural and Applied Sciences**

Prof. Dr. Güney Özcebe _____
Head of Department, **Civil Engineering**

Assist. Prof. Dr. Oğuzhan Hasançebi _____
Supervisor, **Civil Engineering Dept., METU**

Examining Committee Members:

Prof. Dr. Mehmet Polat Saka _____
Engineering Sciences Dept., METU

Assist. Prof. Dr. Oğuzhan Hasançebi _____
Civil Engineering Dept., METU

Assoc. Prof. Dr. Murat Dicleli _____
Engineering Sciences Dept., METU

Assist. Prof. Dr. Ahmet Türer _____
Civil Engineering Dept., METU

Assist. Prof. Dr. Özgür Kurç _____
Civil Engineering Dept., METU

Date: July 30, 2008

I hereby declare that all information in this document has been obtained and presented in accordance with academic rules and ethical conduct. I also declare that, as required by these rules and conduct, I have fully cited and referenced all material and results that are not original to this work.

Name, Last name: Taha Dumlupınar

Signature :

ABSTRACT

APPROXIMATE ANALYSIS AND CONDITION ASSESMENT OF REINFORCED CONCRETE T-BEAM BRIDGES USING ARTIFICIAL NEURAL NETWORKS

Dumlupınar, Taha

M.Sc., Department of Civil Engineering

Supervisor : Assist. Prof. Dr. Oğuzhan Hasançebi

July 2008, 135 pages

In recent years, artificial neural networks (ANNs) have been employed for estimation and prediction purposes in many areas of civil/structural engineering. In this thesis, multilayered feedforward backpropagation algorithm is used for the approximate analysis and calibration of RC T-beam bridges and modeling of bridge ratings of these bridges.

Currently bridges are analyzed using a standard FEM program. However, when a large population of bridges is concerned, such as the one considered in this project (Pennsylvania T-beam bridge population), it is impractical to carry out FEM analysis of all bridges in the population due to the fact that development and analysis of every single bridge requires considerable time as well as effort. Rapid and acceptably approximate analysis of bridges seems to be possible using ANN approach. First part of the study describes the application of neural network (NN) systems in developing the relationships between bridge parameters and bridge responses. The NN models are trained using some training data that are obtained

from finite-element analyses and that contain bridge parameters as inputs and critical responses as outputs.

In the second part, ANN systems are used for the calibration of the finite element model of a typical RC T-beam bridge -the Manoa Road Bridge from the Pennsylvania's T-beam bridge population - based on field test data. Manual calibration of these models are extremely time consuming and laborious. Therefore, a neural network- based method is developed for easy and practical calibration of these models. The ANN model is trained using some training data that are obtained from finite-element analyses and that contain modal and displacement parameters as inputs and structural parameters as outputs. After the training is completed, field-measured data set is fed into the trained ANN model. Then, FE model is updated with the predicted structural parameters from the ANN model.

In the final part, Neural Networks (NNs) are used to model the bridge ratings of RC T-beam bridges based on bridge parameters. Bridge load ratings are calculated more accurately by taking into account the actual geometry and detailing of the T-beam bridges. Then, ANN solution is developed to easily compute bridge load ratings.

Keywords: Artificial Neural Networks, T-Beam Bridges, Approximate Analysis, Calibration, Bridge Ratings.

ÖZ

BETONARME T-KİRİŞ KÖPRÜLERİN YAPAY SİNİR AĞLARINI KULLANARAK YAKLAŞIK ANALİZİ VE DURUM TESPİTİ

Dumlupınar, Taha
Yüksek Lisans, İnşaat Mühendisliği Bölümü
Tez Yöneticisi : Assist. Prof. Dr. Oğuzhan Hasançebi

Temmuz 2008, 135 sayfa

Son yıllarda, yapay sinir ağları (YSA) inşaat/yapı mühendisliğinde etkili tahminler yapmakta oldukça geniş bir alanda kullanılmıştır. Bu tezde de, çok katmanlı, ileri beslemeli, geri yayınım algoritmalı YSA mimarisi betonarme T-kiriş köprülerin yaklaşık analizinde, kalibrasyonunda ve bu köprülerin köprü reytinglerinin modellemesinde kullanılmıştır.

Günümüzde sonlu eleman metodu köprülerin analizinde yaygınca kullanılan bir yöntemdir. Fakat bu çalışmada olduğu gibi birçok köprüden oluşan bir popülasyon düşünüldüğünde (Pennsylvania T-kiriş köprü popülasyonu) sonlu eleman yöntemini bütün köprülerin analizinde kullanmak aşırı derecede zaman ve zahmet alacağından pratik olmamaktadır. Buna rağmen hızlı ve doğru analiz yapmak yapay sinir ağlarıyla mümkün gibi görünmektedir. Bu çalışmanın ilk kısmında, yapay sinir ağları (YSA) kullanılarak köprü parametreleriyle köprü analiz sonuçları arasında bir ilişki bulunmaya çalışılmıştır. YSA modelleri girdi olarak köprü parametrelerinden

çıktı olarak da köprü analiz sonuçlarından oluşan ve sonlu eleman metoduyla üretilmiş eğitim setiyle eğitilmiştir.

İkinci kısımda, Yapay Sinir Ağları (YSA) tipik betonarme T-kiriş köprülerin - Pennsylvania T-kiriş köprülerinden Manoa Road Köprüsünün- analitik modelinin arazi test sonuçlarını dayalı kalibrasyonunda kullanılmıştır. Bu modellerin kalibrasyonu fazlasıyla zaman alıcı ve zahmetlidir. Bu nedenle, bu modelleri kolay ve pratik bir şekilde kalibre etmek için YSA ya dayalı bir yöntem geliştirilmiştir. YSA Modeli girdi olarak modal ve yer değiştirme parametrelerinden çıktı olarak da yapısal parametrelerden oluşan ve sonlu eleman metoduyla üretilmiş eğitim setiyle eğitilmiştir. Eğitim bitikten sonra arazi test sonuçları Sinir Ağlarına (SA) sunulmuştur. Analitik model Sinir Ağlarının verdiği yapısal parametre tahminleriyle güncellenmiştir.

Son kısımda betonarme T-kiriş köprü reytinglerinin yapay sinir ağları (YSA) kullanılarak köprü parametrelerine dayalı modellenmesi yapılmıştır. Köprü reytingleri köprünün gerçek geometrisini ve detaylarını hesaba katarak yeniden hesaplanmıştır. Sonra, sinir ağlarını kullanarak bu köprü reytingleri kolayca hesaplanması için bir model geliştirilmiştir.

Anahtar Kelimeler: Yapay Sinir Ağları, T-Kiriş Köprüler, Yaklaşık Analiz, Kalibrasyon, Köprü Reytingleri.

ACKNOWLEDGMENTS

I would like to express my sincere gratitude to my thesis supervisor Assist. Prof. Dr. Oğuzhan Hasançebi for his support, valuable criticism, and endless patience throughout my study.

I would also like to thank Assist. Prof. Dr. Ahmet Türer for his suggestions and comments and TUBITAK for their high education scholarship during this study.

Special thanks go to Ömer Burak Yücel for his kind assist and support.

Finally, I would like to express my special thanks to my family for their endless love and patience throughout my study.

TABLE OF CONTENTS

LIST OF TABLES

LIST OF FIGURES

LIST OF SYMBOLS

AI	Artificial Intelligence
ANN(s)	Artificial Neural Network(s)
BC	Boundary Conditions
DF	Distribution Factor for Live Loads
DIITSI	Drexel Intelligent Infrastructure and Transportation Safety Institute
FE	Finite Element
FEA	Finite Element Analysis
FEM	Finite Element Modeling
FRFs	Frequency Response Functions
FWD	Falling Weight Deflectometer
I	Impact factor
LMS	Least Mean Square
LRFD	Load and Resistance Factor Design
MAC	Modal Assurance Criterion
MFLN	Multilayer-functional-link Neural Network
MSE	Mean Square Error
NBI	National Bridge Inventory
NN(s)	Neural Network(s)
N-R	Newton-Raphson
PA	Pennsylvania
PennDOT	Pennsylvania Department of Transportation
RC	Reinforced Concrete
SSF	Submatrix Scaling Factors
TSD	Tunable Steepest Descent Algorithm

θ	Threshold in ANN
f	Activation function
α	Momentum term
η	Learning parameters
r	Coefficient of correlation
w	Weight in ANN
t	Target or desired value of the network output
u	Input to ANN
E	Error between the output of the network and its target value
i	Input layer
j	Hidden layer
k	Output layer
a	Input to a node
x	Output of a node
N	Number of patterns

CHAPTER 1

INTRODUCTION

Over the past years, computers have become an integral part of the day-to-day activities in engineering studies and they have been used in various applications to assist engineers in improving their works. Although computers are utilized to model a variety of engineering activities, the main focus of computer applications is still the areas in which a set of rules are established. The use of computer in the some areas of decision making process where there are no defined rules is very limited. In recent years, Artificial Neural Networks (ANN) has emerged as a promising candidate in modeling some of the human activities in many areas of science and engineering. Unlike expert systems, ANN systems do not need any rules. They are suitable particularly for problems that are too complex to be modeled and solved by classical mathematics and traditional procedures. One of the distinct characteristics of the ANN is its ability to learn and generalize from experience and examples to produce meaningful solutions to problems even if the input data contains error or is incomplete or even fuzzy. These characteristics of ANNs make them a promising tool for modeling some of the engineering problems (Rafiq et al., 2001). Their computing abilities have also been proven in the fields of civil/structural engineering (Adeli, 2001). In this thesis, some of the possible applications of ANN will be explored in conjunction with RC T-beam bridges. In this framework, the three objectives of the thesis are set as follows: (i) to achieve acceptably approximate analysis of RC T-beam bridges using neural networks; (ii) to investigate calibration of RC T-beam bridges using neural networks; and (iii) to model the bridge load ratings of these bridges based on neural networks.

The thesis is organized in eight chapters. Chapter 1 presents general information on the purpose of the study. The scope and objective of subsequent chapters are briefly explained. In Chapter 2, previous applications of ANNs in the literature are reviewed in the fields of approximate structural analysis and structural identification, which are also the major concerns of the thesis. Chapter 3 introduces the fundamentals of Artificial Neural Networks (ANNs). First, inspiration of Artificial Neural Networks from the biological neural networks is explained. Then, a popular network type, the feed-forward network, is introduced in detail and key points that are important for understanding of their implementations are emphasized. One of the most popular learning algorithms, i.e. the backpropagation algorithm, for feed-forward neural networks is presented in the final section of the chapter. In Chapter 4, development of FE model of a typical T-beam bridge of Pennsylvania's bridge population is described. Firstly, general information on the bridge population is presented. Next, the finite element modeling of a typical T-beam bridge is explained using a bridge (selected from the entire population) with average structural and geometrical parameters.

Chapter 5 focuses on the approximate analysis of single span T-beam bridges in Pennsylvania using Neural Networks. Pennsylvania has the third largest reinforced concrete (RC) T-beam population with 2,440 T-beam bridges in the US and 1,899 of which are single span. Especially, when a large population of bridges is concerned, a rapid and reliable estimate of actual response computations is essential and possible using ANN approach. Available analysis methods and tools are insufficient to cope with large population of bridges. Currently, FEM analysis procedure is the most frequently used method in the analysis of bridges. However, it is impractical to carry out FEM analysis of all bridges in the population due to the fact that development and analysis of every single bridge requires considerable time as well as effort. Recent progress in neural computing technology has provided an ideal and reasonable method which enables to reliably predict actual response of a bridge with a trivial computational effort. In this chapter, the inherent structural behavior of T-beam bridges is modeled using neural networks. It is realized that the bridges in the Pennsylvania T-beam bridge population have a common set of

geometrical and structural parameters. Amongst them, the governing ones are identified and used as inputs to the networks to simulate the behavior of T-beam bridges. A group of bridge samples are randomly generated using different combinations of these parameters within the ranges of possible variations to ensure that the ANN model trained using these samples can predict, within an acceptable accuracy, the structural behavior exhibited by majority of the bridges within the population. In order to obtain the outputs of bridge samples, all bridges in the bridge set are modeled using a standard FEM program and analyzed for structural responses. The bridge data acquired are divided into three sets; the training set, the cross validation set and the test set. The training set is used to establish intrinsic relationships between the bridge parameters and responses. The cross validation set is used to avoid overfitting, which is the case of poor generalization. The test set is used to evaluate the performance of the network. Several network designs are examined to determine one with a reasonable performance. Once trained successfully, the network can confidently be used to predict accurate output values for new input data. The analysis results can be obtained from the trained neural network with a trivial computational time and effort and without a need to construct and analyze a new model for each parameter set.

Chapter 6 discusses the calibration of the finite element model of the Manoa Road Bridge, a typical T-beam bridge from the Pennsylvania's bridge population, based on field test data and neural networks. Calibration can be defined as the process of modifying the input parameters to a model until the output from the model matches an observed set of data. Manual calibration of T-beam bridge models are extremely time consuming and laborious. A neural network- based method is developed here for an efficient and practical calibration of these bridges. Artificial neural network (ANN) is trained to learn the pattern between the output and input data sets of an analytical model in reverse direction. The training samples consist of structural parameters to be updated and their corresponding modal and displacement parameters obtained from the FE analyses. Modal and displacement parameters are used as the input data to train the network. The outputs introduced in the training session are the structural parameters. After the training of the ANN model, the

model calibration procedure begins with feeding measured modal and displacement parameters (field-measured data set) into the trained ANN model. The outputs of the ANN model are the predicted structural parameters. These predicted structural parameters are then fed into the FE model to produce a set of calculated modal and displacement parameters. A comparison between the calculated and measured modal and displacement parameters is conducted. If these two sets of parameters differ significantly, then the ANN model is retrained. This procedure is repeated until the calculated and measured responses correlate well. Preparing input and output data sets for such a neural network would take a considerable amount of time; nevertheless, once a neural network is successfully trained and a relationship between the inputs and outputs is established, the same system can be used efficiently and quickly for calibration of the analytical model any time in future, following the testing of actual bridge.

Chapter 7 discusses the modeling of bridge load ratings of RC T-beam Bridges based on Artificial Neural Networks (ANNs). In the current load capacity rating practice, an individual beam is taken out as a free-body, idealized as simply-supported, and the continuity of the bridge in the transverse direction is indirectly accounted for by means of axle-load distribution factors. It has been found that this approach significantly underestimates the contribution of deck slab to lateral load distribution for many bridge geometries. This contribution is properly simulated when a properly constructed, geometric replica 3D FE model is used for analysis. Hence, the load rating of the bridges obtained by using AASHTO and FEM-based analysis methods are different. In this chapter, bridge load ratings are calculated more accurately by taking into account the actual geometry and detailing of the T-beam bridges. Then, Artificial Neural Network solution of bridge load ratings is obtained to easily compute the highest utilizable capacity of any T-beam bridge while still strictly conforming to the AASHTO standards and provisions. The bridge data acquired in the Chapter 5 is used to obtain the training set for the ANN systems. The analysis results of FE models are utilized to obtain the bridge ratings of these bridges. The training samples consist of the same bridge parameters discussed in Chapter 5 and their corresponding FEM based bridge ratings. The

training samples are used to establish intricate relationships between the bridge parameters and bridge ratings. Once the training is successfully completed, the developed ANN model can be used efficiently to retrieve the bridge ratings from another set of bridge parameters within the range of the training set.

Finally, the conclusions of the study are given in Chapter 8.

CHAPTER 2

LITERATURE SURVEY

In this chapter, previous applications of ANN in structural engineering are overviewed. The first article reporting the use of neural networks in a civil/structural engineering application was published by Adeli and Yeh (1989). Since then, a large number of articles have been published on the topic, which is summarized in a review article by Adeli (2001). The chapter is organized in two subsequent sections as; approximate structural analysis studies and structural identification and model updating studies based on ANNs.

2.1 Approximate Structural Analysis Studies

In 1997, Cattan and Mohammadi (Cattan and Mohammadi, 1997) used artificial neural networks to investigate the relationship between the bridge rating and several bridge parameters. In this study, railroad bridges from the Chicago metropolitan area were used as database. A total of 405 rail bridges in the Chicago metropolitan area were selected from the entire population since these bridges had complete information for all the parameters. A statistical analysis of bridge parameters was conducted to determine the variability in each parameter and the representation of the entire bridge population. Based on statistical analysis, the common 12 bridge parameters, such as bridge type, substructure type, deck type, span length, etc. were selected to be used as inputs to the networks. Data set containing 405 rail bridges was divided into two sets: training set and test set. Training set contains 307 bridges and was used to map the relationship between bridge rating and bridge parameters. Test set contains 98 bridges and was used to evaluate the performance of the network. Several network designs were examined to arrive at one with a reasonable

performance. Finally, 45 nodes in input layer, two hidden layers with 45 nodes each, and 4 nodes in the output layer with the learning coefficient of 0.60 and the momentum coefficient 0.85 was arrived as the one having the best performance. The network was then used to predict ratings for several bridges outside the training and test data sets. The overall performance of the network is 73.47%. This study shows that neural network can be trained and used successfully in estimating ratings of a bridge population.

Özkaya and Pakdemirli (2002) investigated the applicability of ANN systems in predicting the natural frequencies of suspension bridges based on common physical parameters of the bridges. In the study, parameters affecting the frequencies are determined as span length, moment of inertia of the bridge cross-section, initial horizontal component of cable tension, dead weight of the bridge per unit length of the span, cables' cross-sectional area, modulus of elasticity of the bridge deck and the cables. The first three natural frequencies were calculated using Newton-Raphson (N-R) method for different physical parameters to prepare data set for training of the network. In the network, these five physical parameters were used as inputs and the first three natural frequencies were predicted as outputs. The ANN architecture used is a 5:12:12:3 multi-layer, feed-forward and back-propagation architecture with momentum coefficient of 0.9 and learning rate of 0.7. A total of 493 examples in the data set were used to train the network and error was minimized to beneath the tolerable level. An additional 15 test patterns were generated using N-R method to test the ANN. For the test patterns, the maximum error between the ANN results and N-R method results is less than 1.02%. The engineering importance of the study was demonstrated by predicting the frequencies for the test values with a considerable low error without spending much effort and time.

Jenkins (1999) investigates the use of neural networks for the structural re-analysis of two-dimensional trusses. In the study, a simple two-layer configuration network is used. The inputs describe the structure, geometry, material properties, applied loads and supports, in the initial states. The output from the net will be the

displacements due to applied loads. The displacements at the outputs nodes are processed using the geometrical and material properties of the members to produce forces at the structural joints. A back-propagation algorithm is used to solve the structural equilibrium equations at the joints and then the member forces are computed. The network is then applied to the linear and non-linear analysis. The network is capable of carrying out the linear analysis and simple non-linear analysis to a desired degree of accuracy. Further work is recommended by the writer in application of the network to complex non-linear analysis.

In 2002, Jenkins presents another study which is a neural network iterative method for structural reanalysis. The network is a simple back-propagation neural network in which the weights under iterative updating are retained and updating resumed as each structural modification is made. The network has two layers, namely input and output layers. Inputs in the network are the applied loads at the joints. The outputs are the displacements at the joints. The joint displacements are used to calculate the forces at the joints. Considering the applied loads in the equilibrium, the joint forces should be zero for equilibrium. Computed forces represent error. A backpropagation is used to reduce the error by adjusting the weights. This iterative process is continued until the error is reduced to tolerable level. This method is applied to plane truss and space truss for illustration of reanalysis. Design change options such as the insertion of additional joints, insertion of new member, additional load, etc. are introduced into neural network based reanalysis. Analysis results for different design states are presented in the paper. The writer concluded that "the software described is compact, easily portable, and suitable to take advantage of the continuous increase in the processing speed and memory capacity of the modern computer".

In 2000, Consolazio presented a technique for enhancing finite-element analysis equation solvers for particular problem domains, i.e., particular classes of structures such as highway bridges. In the technique, artificial neural networks are merged with a preconditioned conjugate gradient iterative equation-solving algorithm to seed the initial solution vector and to precondition the matrix system using

customizable and trainable neural networks. This technique is applied to the particular domain of flat-slab highway bridge analysis. Eighteen networks are trained using the load-displacement data from FE analysis to encode the load (Fz, Mx, My)-displacement (Tz, Rx, Ry) relationships for concrete flat-slab highway bridges. In the combined algorithm, neural networks are used to predict approximate displacements under at each iteration, while overall iterative preconditioned conjugate gradient process guides convergence to the exact solution. This study showed that combining the Neural networks with preconditioned conjugate gradient is very effective for accelerating the convergence of iterative methods.

In 2005, Rogers developed the guidelines to create a neural network that can simulate the structural analysis in the optimization process to reduce the amount of time that an optimization process takes to converge to an optimum design. These guidelines were applied to optimize the shape of a beam to minimize the weight while satisfying the stress constraints. Several network designs were trained using a set of training sample consisting of the design variables as inputs and values of the constraints and objective function as outputs to arrive at one with a reasonable performance. Finally, combination of the selecting the training pairs based on hypercube method and 46 nodes in hidden layer was found to yield better approximation. Further studies on this network design show that it is possible to reduce the overall time required for convergence from 198 min (required by reference optimization process) to 159 min. The results indicate that by selecting the right network parameters and properly constructing and training the NN model, it is possible to reduce the amount of time it takes an optimization process to converge to an optimum design.

C W Tang et al (2003) investigate the use of the artificial neural networks in predicting the confinement efficiency of concentrically loaded reinforced concrete (RC) columns with rectilinear transverse steel. For this purposes, a database of 55 square columns was retrieved from existing literature. In the study, a multilayer-functional-link neural network (MFLN) which is a modification of the standard

backpropagation neural network was used to estimate the maximum axial stress and strain of confined concrete. After a comprehensive study, six major variables - cylinder compressive strength of concrete, area of concrete in the core, volumetric ratio of transverse steel in concrete core, the distance between the laterally supported longitudinal bars, spacing of transverse steel, and yield strength of transverse steel- were discovered to be effective in capturing the underlying behavior of confined RC columns. In other words, the input layer of the neural network consists of six processing units representing these six variables, and the output layer includes two neurons representing the maximum axial stress and strain of confined concrete. Of 55 examples, 45 were used for training of the 6-14-2 architecture network with various network parameters and the rest were used for testing to find the best network. Results were compared with the several analytical models such as Park et al. Model, Yong et al. Model, Sheikh and Uzumeri Model. The overall predictions from the neural network MFLN model were found to be better than analytical models.

Oreta and Kawashima (2003) explore the feasibility of using artificial neural networks (ANNs) to predict the confined compressive strength and corresponding strain of circular reinforced columns. A total of 38 examples for network training were obtained from the past experiments. In the network, seven variables - the unconfined compressive strength, core diameter, column height, and yield strength of lateral reinforcement, volumetric ratio of lateral reinforcement, tie spacing, and longitudinal steel ratio - were used as input parameters. Of 38 examples, twenty-nine data pairs were used as training data and the remaining nine data pairs were used as test data. After examining several architectures, 7-4-2 model with sigmoid transfer function was found to have better performance. The results were compared with the analytical models. There is an average difference of between 1% and 3% for the confined compressive strength and corresponding strain of circular concrete columns. It was seen that only with a sufficient number of data, it is still possible to develop ANNs which can completely model the complex interactions among the multiple variables.

2.2 Structural Identification and Model Updating Studies

C. C. Chang et al (2000) proposed a model updating methodology based on an adaptive neural network (NN) model. This method was applied to the structure model which is a scaled version of the Humen suspension bridge in China. Modal properties such as natural frequencies and mode shapes were used as inputs to a neural network model to predict the structural parameters as outputs. Structural parameters are the parameters such as the modulus of elasticity, the mass density, the cross sectional area, etc. that significantly affect the modal parameters of the structure. The neural network model has feedforward architecture. In this study, 16 nodes (first eight natural frequencies and corresponding mode shapes) in the input layer, 39 and 16 nodes in the first and second hidden layer respectively and 8 nodes (eight structural parameters) in the output layer were used with a modified backpropagation training algorithm with a dynamically adjusted learning rate and a jump factor to improve the convergence performance of the network training. Network was trained using 33 examples obtained from the FE analysis and first estimation of the structural parameters is obtained by feeding the modal parameters into trained NN model. The first predicted structural parameters are then fed into FE model for the calculation of modal parameters. If the difference between the measured and predicted modal parameters does not satisfy the given criterion, training samples are adjusted and the process is repeated. Retraining procedure is repeated until a set of satisfactory result is obtained. This study showed that it is possible to reduce the difference between the measured and the predicted frequencies from a maximum of 17% to 7% for the first eight vertical modes.

Chen (2005) proposed a neural network-based method for determining the dynamic characteristic parameters of structures from field measurement data. Structural responses were used to train an ANN to determine the frequencies, damping ratios and modal shapes. The architecture of proposed ANN model is single hidden layer with 16 nodes. In the model, n (lags in the output) = 2 and m (lags in the input) = 8. The technique was employed to determine the dynamic characteristics of two bridges. First one is the arch pylon of a cable-stayed bridge. In this bridge, ANN

was trained using the Randomdec signatures to identify the dynamic characteristics of the arch pylon such as the natural frequencies, modal damping ratios and modal shapes of first five modes. The results are reasonably consistent with the results of the finite element analysis. Second bridge is a three-span highway bridge. In the bridge, ANN was trained using the velocity responses to identify the natural frequencies, modal damping ratios and modal shapes of six modes in transverse direction. The results show a very good agreement with ambient vibration test results.

Barai and Pandey (1995) presented vibration signature analysis of steel bridge structures based on artificial neural networks (ANN) for the purpose of damage identification. This strategy was applied to a typical structure idealized as a simply supported steel truss bridge with a pinned joint. In order to generate a structural response, a moving load was simulated to travel on the bridge structure and the vibration signatures at various nodes of the bridge structure were obtained for various position of the load. Vertical displacements at several nodes at a certain time interval were used as inputs to the network and structural identification parameters such as cross-sectional area of the members representing the stiffness in damage state formed the outputs of the network. A total of 16 examples were generated using FEM program to train the network and additional five examples were generated to test the network. After an extensive study on number of hidden layer , number of hidden units per layer, learning parameter, momentum parameter and error tolerance, 69-(21-21)-21 architecture was found to have better performance with learning parameters of 0.9 , momentum parameters of 0.7 and error tolerance of 0.01. Based on this architecture, the average percent error in the identification of stiffness of members was found to be less than 4%. This study shows that ANN has great potential in damage identification.

In 2000, Yun and Bahng studied substructure identification using neural networks. In this study, neural network is used to estimate the stiffness parameters of a complex structural system using the natural frequencies and mode shapes as inputs to the network. For the identification of a structure, the structure is subdivided into

several substructures to reduce the size of the system to concentrate the identification at critical locations of the structure. Then, modal data on the substructure of interest and corresponding submatrix scaling factors (SSF) are obtained to train the network. The first four modes are used as input patterns to the neural networks and the corresponding SSFs are estimated as output. Finally, trained networks are tested using the testing patterns to measure the generalization performance of the neural networks. The proposed neural network-based method was applied to a two-span truss and a multi-storey frame. For two examples, the average relative estimation errors for testing data set were found to be in the range of 9±15%, which shows the applicability of the present method for the identification of large structural systems.

Fang et al. (2005) presented a structural damage detection method based on neural network with learning rate improvement. In the study, frequency response functions (FRFs) are used as input data to the back-propagation neural network to estimate the location and severity of damage as the outputs. In order to increase the training effectiveness, efficiency and robustness without increasing the algorithm complexity, a tunable steepest descent algorithm (TSD) was used in determining an optimal learning rate. The frequency response functions (FRFs) of the intact and the damaged state are directly used as input data to the TSD based neural network. Structural damage is designated as stiffness loss in one or multiple elements and the network outputs are designed as the relative stiffness ratio, that is, the ratio of the stiffness of the damaged structure with respect to the stiffness at the intact state. This method was applied to a cantilevered beam. In the application, the beam is equally divided into 20 elements and the elements are numbered in sequence. Structural damage causes stiffness loss in one or multiple elements. The natural frequencies and modal shapes of the intact and damaged structures were recorded and a total of 30 numerical stiffness loss cases were obtained to train the network. A three-layer feedforward network with 78 input nodes, 40 hidden nodes, and 5 output nodes was used in training process. Then, the trained network was tested using 4 unseen cases which gave maximum 17.7% error which is very high accuracy in

predicting damage location and severity. This study has showed that neural network can assess damage conditions successfully.

CHAPTER 3

ARTIFICIAL NEURAL NETWORKS

3.1 General

Artificial Intelligence (AI) is a very versatile and potential area in the field of computing technology. It enables computer users in various fields to solve problems which cannot be formulated using algorithmic approaches and which normally requires human intelligence and expertise. Artificial Neural Networks (ANNs) which is one of the best known manifestations of AI has today gained immense credibility and acceptance in many professional fields (Fausett, 1994).

An Artificial Neural Network (ANN) is an information processing paradigm that is inspired by the way biological nervous systems process information. The key element of this paradigm is the novel structure of the information processing system. It is composed of a large number of highly interconnected processing elements (neurons) working in unison to solve specific problems. ANNs, like people, learn by example. An ANN is configured for a specific application, such as pattern recognition or data classification, through a learning process. Learning in biological systems involves adjustments to the synaptic connections that exist between the neurons. This is true of ANNs as well.

Biologically inspired methods of computing are the major advancement in the computing industry. Even simple animal brains are capable of functions that are currently impossible for computers. While computers do rote things well, like keeping ledgers or performing complex math, they have trouble recognizing even simple patterns much less generalizing those patterns of the past into actions of the

future (Anderson and McNeill, 1992). What makes such a difference is neither due to the processing ability of the computers nor due to their processing speed. Today's processors are much complicated and have a speed 10^6 times faster than neurons. The difference is mainly because of the structural and operational trend. While the instructions are executed sequentially in a complicated and fast processor in a conventional computer, the brain is a massively parallel interconnection of relatively simple and slow processing elements (Halıcı, 2004).

3.2 From Biological to Artificial Neuron Model

3.2.1 Biological Neuron

Neurons are the basic computational unit in the nerve system. It is estimated that there are $1{,}3x10^{10}$ neurons in the human central nerve system and about $1x10^{10}$ of them takes place in the brain. The power dissipation due to firing of neurons is estimated to be in the order of 10 watts. When asleep, about $5x10^7$ nerve impulses per second are being relayed back and forth between the brain and other parts of the body and this rate is increased significantly when awake (Fischer, 1987).

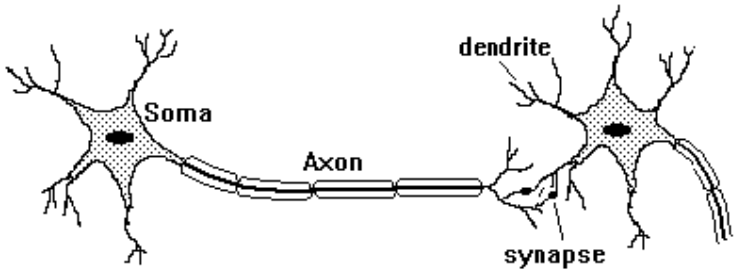

Figure 3.1 Typical Neuron (Halıcı, 2004)

A typical neuron is shown in Figure 3.1. Most of the neural computation occurs in the cell body (soma of the neuron) which includes the neuron's nucleus. The signals generated in soma are transmitted to other neurons through an extension on the cell body called axon or nerve fibres. Dendrites are another kind of extensions around

the cell body like bushy three. They are responsible from receiving the incoming signals generated by other neurons. The axon is separated into several branches and at the very end the axon enlarges and forms terminal buttons. Terminal buttons are placed in special structures called the synapses which are the junctions transmitting signals from one neuron to another. In terminal buttons, the synaptic vesicles which hold several thousand molecules of chemical transmitters take place. When a nerve impulse arrives at the synapse, some of these chemical transmitters are discharged into synaptic cleft. Synaptic cleft is the narrow gap between the terminal button of the neuron transmitting the signal and the membrane of the neuron receiving it. The membrane of the post-synaptic cell gathers the chemical transmitters, which cause either decrease or increase in the efficiency of the local sodium and potassium pumps depending on the type of the chemicals released into the synaptic cleft. The synapses, whose activation decreasing the efficiency of the pumps cause depolarization of the resting potential. On the other hand, the synapses increasing the efficiency of pumps results in hyper-polarization. The first kind of synapses which encourage depolarization is called excitatory and the others which discourage it are called inhibitory synapses. If the decrease in the polarization is adequate to exceed a threshold, then the post-synaptic neuron fires (Halıcı, 2004).

3.2.2 Artificial Neuron Model

As mentioned in the previous section, the transmission of a signal from one neuron to another through synapses is a complex chemical process in which specific transmitter substances are released from the sending side of the junction. The effect is to raise or lower the electrical potential inside the body of the receiving cell. If this graded potential reaches a threshold, the neuron fires. It is this characteristic that the artificial neuron model proposed by McCulloch and Pitts, (1943) attempt to reproduce. The neuron model shown in Figure 3.2 is the one that is widely used in artificial neural networks with some minor modifications on it.

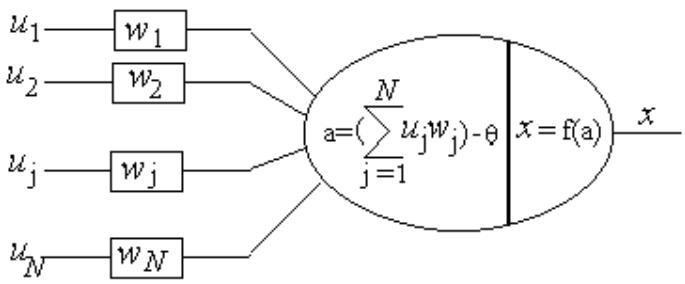

Figure 3.2 Artificial Neuron

The artificial neuron given in this figure has N input, denoted as $u_1, u_2, \ldots u_N$. Each line connecting these inputs to the neuron is assigned a weight, which is denoted as $w_1, w_2, \ldots w_N$ respectively. Weights in the artificial model correspond to the synaptic connections in biological neurons. The threshold in artificial neuron is usually represented by θ and the activation corresponding to the graded potential is given by the formula:

$$a = \left(\sum_{j=1}^{N} w_j u_j \right) + \theta \tag{3.1}$$

The inputs and the weights are real values. A negative value for a weight indicates an inhibitory connection while a positive value indicates an excitatory one. Although in biological neurons, θ has a negative value, it may be assigned a positive value in artificial neuron models. If θ is positive, it is usually referred as bias. For its mathematical convenience we will use (+) sign in the activation formula. Sometimes, the threshold is combined for simplicity into the summation part by assuming an imaginary input $u_0 = +1$ and a connection weight $w_0 = \theta$. Hence the activation formula becomes:

$$a = \left(\sum_{j=0}^{N} w_j u_j \right) \tag{3.2}$$

The output value of the neuron is a function of its activation in an analogy to the firing frequency of the biological neurons:

$$x = f(a) \tag{3.3}$$

Furthermore the vector notation

$$a = \mathbf{w}^{\mathrm{T}}\mathbf{u} + \theta \tag{3.4}$$

is useful for expressing the activation for a neuron. Here, the j^{th} element of the input vector **u** is u_j and the j^{th} element of the weight vector of w is w_j. Both of these vectors are of size N. Notice that, $\mathbf{w}^{\mathrm{T}}\mathbf{u}$ is the inner product of the vectors **w** and **u**, resulting in a scalar value. The inner product is an operation defined on equal sized vectors. In the case these vectors have unit length, the inner product is a measure of similarity of these vectors.

Originally, the neuron output function, *f*(*a*), in McCulloch-Pitts model was proposed as threshold function, however, sigmoid, hyperbolic tangent, and linear functions formulated in Equations 3.5-3.7 are also widely used output functions. These functions are graphically represented in Figure 3.3.

$$f(a) = sgm(a) = \frac{1}{1 + \exp(-\mathrm{a})} \tag{3.5}$$

$$f(a) = tanh(a) = \frac{\exp(\mathrm{a}) - \exp(-\mathrm{a})}{\exp(\mathrm{a}) + \exp(-\mathrm{a})} \tag{3.6}$$

$$f(a) = purelin(a) = a \tag{3.7}$$

where; sgm(·) is *sigmoid* function, tanh(·) is hyperbolic tangent function (Morshed and Kaluarachchi, 1998), and purelin(·) is linear function.

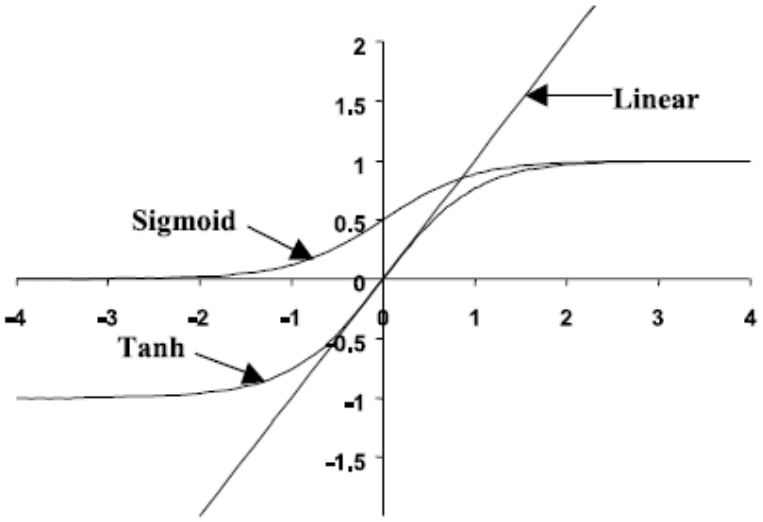

Figure 3.3 Transfer Functions of Artificial Neurons (Rafiq, 2001)

3.3 Network Structure

3.3.1 Network of Neurons

Since a single artificial neuron is not able to implement some boolean operations, the problem is overcome by connecting the outputs of some neurons as input to the others, so constituting a neural network. Supposing that many artificial neurons introduced in Section 3.2.2 are connected to form a network, there appears several neurons in the system. Hence, indices are assigned to the neurons to discriminate them. Then, to express the activation i^{th} neuron, the above formulas are modified as follows:

$$a_i = \left(\sum_{j=1}^{N} w_{ji} x_j \right) + \theta_i \tag{3.8}$$

where x_j may be either the output of a neuron determined as

$$x_j = f_j(a_j) \tag{3.9}$$

or an external input determined as:

$$x_j = u_j \tag{3.10}$$

In some applications the threshold value θ_i is determined by the external inputs. Due to the equation (3.8) sometimes it may be convenient to think that all the inputs are connected to the network only through the threshold of some special neurons called the input neurons. They are just conveying the input value connected to their threshold as $\theta_j = u_j$ to their output x_j with a linear output transfer function $f_j(a) = a$.

For a neural network a state vector **x** can be defined in which the i^{th} component is the output of i^{th} neuron, that is x_i. Furthermore a weight matrix **W** can be defined, in which the component w_{ji} is the weight of the connection from neuron j to neuron i. Therefore the system can be represented as:

$$\mathbf{x} = \mathbf{f}(\mathbf{W}^{\mathbf{T}}\mathbf{x} + \theta) \tag{3.11}$$

Here θ is the vector whose i^{th} component is θ_i and **f** is used to denote the vector function such that the function f_i is applied at the i^{th} component of the vector.

3.3.2 Network Architectures

In the previous sections, we discussed the properties of the basic processing unit in an artificial neural network. This section focuses on the pattern of connections between the units and the propagation of data. There are two well-known network

architectures, namely feed-forward networks and recurrent networks, which mainly differ from each other in terms of pattern of connections.

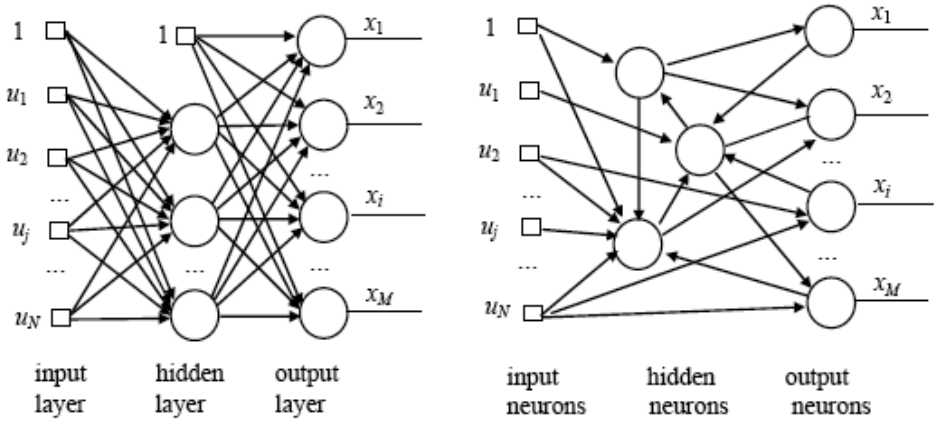

Figure 3.4 a) Layered Feedforward Neural Network b) Nonlayered Recurrent Neural Network

- Feed-forward Networks (Figure 3.4 (a)) allows the data to travel one way only; from input to output. Data flow is strictly feedforward. The data processing can extend over multiple (layers of) units, but there is no feedback connections i.e. connections extending from outputs of units to inputs of units in the same layer or previous layers (Kröse and Smagt, 1996).

- Recurrent Networks (Figure 3.4 (b)) allows the data to travel in both directions. Contrary to feed-forward networks, they contain feedback connections and the dynamical properties of the network are important. In some cases, the activation values of the units undergo a relaxation process during which the network evolves to a stable state where these activations do not change anymore. In other applications, the change of the activation values of the output neurons is significant, such that the dynamical behavior constitutes the output of the network (Pearlmutter, 1990).

3.4 Feed-forward Neural Network

The network consists of several layers of neurons (Figure 3.5). The input vector distributes the inputs to the input layer. There is no processing in input layer; rather it can be conceived as a sensory layer, where each neuron receives a sole component of the input vector **U**. The last layer is the output layer which outputs the processed data. The output of each neuron in this layer corresponds to a component of the output vector **X**. The layers between the input and output ones are referred to as hidden layers. Hidden layer(s) may have any number of neurons; however they should be chosen scrupulously to achieve some special effects in some cases.

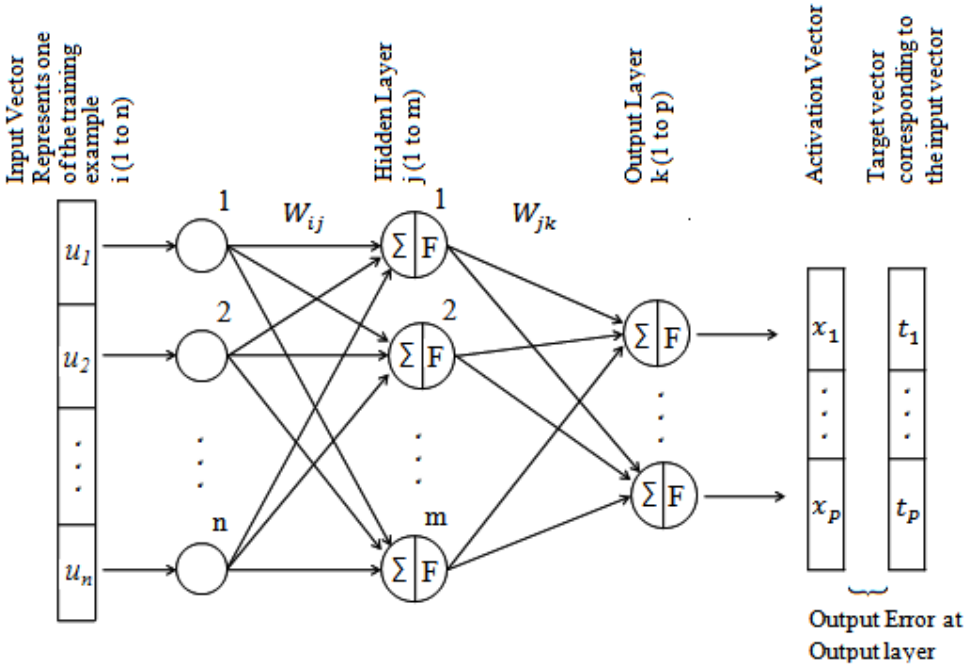

Figure 3.5 Single Hidden Layer Feedforward Neural Networks (Pandey and Barai, 1993)

Shown in Figure 3.5 is a straight feedforward network where each neuron in a layer is connected to all the neurons of the previous and next layers by weighted

connections. Except for the first sensory layer, the outputs of all neurons from the previous layer are received as an input to each neuron. Each neuron performs a nonlinear transformation of the weighted sum of the incoming inputs to produce the output of the neuron which is given to other neurons or outside the network.

3.4.1 ANN Definitions and Concepts

The ***training*** process in the multilayer feedforward networks involves presenting to the network a set of training data (examples) consisting of a selected number of known input and output pairs. During training the system adjusts the weights of the internal connections to minimize errors between the network output and target output. However, it is not always advantageous to continue training until the errors reach a minimum level. This situation is referred to '***overfitting***' in the nomenclature of ANN, where the network learns the 'noise' presented in the training data and not the required general pattern. When this happens, the network performs very well over the data set used for training, but shows poor predictive capabilities when supplied with data other than the training patterns. This case can be thought as "memorization" rather than "learning". One of the simplest and most widely used means of avoiding overfitting is to divide the training data into two sets: a training set and a **validation** set. Training set is used for computing the error gradient and updating the network weights and biases, and the validation set is used at some interval for calculation of error. The error on the validation set is monitored during the training process. The validation error will normally decrease during the initial phase of training, as does the training set error. However, when the network begins to overfit the data, the error on the validation set will typically begin to rise. The network starts memorizing the training patterns. When the validation error increases for a specified number of iterations, the training is ***stopped***, and the weights and biases at the minimum of the validation error are returned. Schematic learning curves showing error on the training and validation sets are shown in Figure 3.6. To avoid overfitting, it is necessary to stop the training at time *t*, where performance on the validation set is optimal.

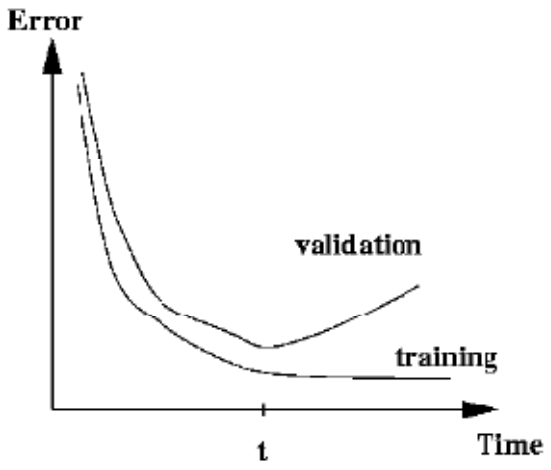

Figure 3.6 The learning error and the validation error as a function of the time

After the training is completed, usually, the network error is minimized. The network output shows similarities with the target output. However, a set of unseen patterns, ***test set***, must be selected and the network should be tested using these patterns to make sure that the network training has been satisfactorily completed and the network is capable of generalization (Rafiq, 2001).

Two modes of training are present in neural network training: ***supervised*** and ***unsupervised*** learning.

In ***supervised learning,*** there is an external teacher, a training set of data or an observer who grades the performance, to control the learning and incorporate global information. Training requires examples whose target output is known. Therefore, we must have a training set for which we already know 'the answer' to our questions to the network. While learning, weights are adjusted according to the input/output samples. Examples of supervised learning algorithms are the least mean square (LMS) algorithm and its generalization, known as backpropagation algorithm, and radial basis function network. (Fausett, 1994).

Unsupervised learning is sometimes referred to as self-organizing, i.e. learning to classify without being taught. There is no external teacher. Therefore, the system must organize itself by external criteria and local information designed into the network. Unsupervised learning involves no target values, only the input samples are available and the network classifies the input patterns into different groups. Kohonen network is an example of unsupervised learning (Konar, 1999).

Initialization is required for the weights of the neural network. Before training, the network weights are initialized to small random values. The random values are usually drawn from a uniform distribution over the range [-r,r] (usually in the range of -1 to +1). Selection of initial weights influences whether the network reaches a global (or only a local) minimum of the error and how quickly it converges.

Presenting the entire set of training patterns to the network is called an ***epoch***. The number of 'epochs', number of times that the whole set of patterns is presented to the network, affects the performance of the network. This number depends on many factors such as number of training data, number of hidden layers, number of neurons in hidden layers and number of dependent output parameters.

Training a NN involves gradual reduction of the error between NN output and the target output. Generally, there are two different modes of training NN, namely ***batch*** mode and ***pattern*** mode. In a batch mode, when an epoch is completed a single average error is calculated and the weights in the network are adjusted according to that error. In a pattern mode, the error is calculated after each pattern is presented to the network, and network weights are adjusted. Choosing between the two modes is generally problem specific.

Data scaling is another essential step for network training. For example, upper and lower limits of output from a sigmoid transfer function are generally 1 and 0 respectively. Scaling of the inputs to the range [0, +1] greatly improves the learning speed, as these values fall in the region of the sigmoid transfer function where the output is most sensitive to variations of the input values (Figure 3.3). It is therefore

recommended to normalize the input and output data before presenting them to the network.

Choosing a topology for the network is a difficult task. If the number of hidden units is too small, than the network may not be sufficient to develop the required internal representation of the problem and therefore may not be able to perform the necessary recognition task. On the other hand if the number of hidden unit is too large, then the network can overfit the data. The appropriate selection of ***layers*** and ***nodes*** is problem dependent and the optimum layout can be arrived by trial and error approach.

3.4.2 Learning in Feedforward Neural Networks

Although the method of storing and recalling information in brain is not fully understood, experimental research has enabled some understanding of how neurons appear to gradually modify their characteristics as a result of exposure to particular stimuli. The most obvious changes have been observed to occur in the electrical and chemical properties of the synaptic junctions. For example the quantity of chemical transmitter released into the synaptic cleft is increased or reduced, or the response of the postsynaptic neuron to receive transmitter molecules is altered. The overall effect is to modify the significance of nerve impulses reaching that synaptic junction on determining whether the accumulated inputs to post-synaptic neuron will exceed the threshold value and cause it to fire. Thus learning appears to effectively modify the weightings of the synaptic connections that exist between the neurons.

A single-layer network has severe restrictions, and the class of tasks that can be accomplished using this network is very limited (Kröse and Smagt, 1996). A multi layer feed-forward network can overcome many restrictions, but did not present a solution to the problem of how to adjust the weights from input to hidden (Minsky and Papert, 1969). The tool that was missing in those early days of multilayer feedforward networks was what we now call backpropagation learning. The central

idea behind this solution is that the errors for the units of the hidden layer are determined by back-propagating the errors of the units of the output layer (Kröse and Smagt, 1996).

Although usage of the term ***backpropagation*** appears to have evolved in 1985, the basic idea of back-propagation was first described by Werbos in his Ph.D. Thesis (Werbos, 1974), in the context of a more general network. It was rediscovered by Rumelhart et al. (1986), and popularized through the publication of the seminal book entitled "Parallel and Distributed Processing" by Rumelhart and McClelland (1986). Parker (1985) derived a similar generalization of the algorithm independently. A roughly similar learning algorithm was also presented by LeCun (1985).

3.4.3 The Backpropagation Algorithm

Back propagation neural networks are powerful tools for searching regularities, forecasting, and qualitative analysis. They are called back propagation networks because of the learning algorithm they use, in which an error moves from output layer to the input one, i.e. in the direction opposite to that of signal spreading during the normal network operation.

Backpropagation process is conducted by supervised learning because the output of the system delivered is compared to the exact values. In backpropagation algorithm there are two main phases. The first phase is a forward pass, which is also called as activation phase. In that phase, inputs are processed to reach the output layer through the network. After the error is computed, a second phase starts backward through the network, which is also called as error backpropagation.

Back-propagation can also be considered as a generalization of the delta rule for multi layer networks. The derivation of the generalized delta rule is included in the Appendix A. Based on the network shown in Figure 3.5, the main steps involved for implementing the algorithm are given as follows (Pandey and Barai, 1993).

Step 1. Select a number of input nodes (n), output nodes (p) and hidden nodes (m) and first training example (u_i) .

$$\{U_i\} = \begin{Bmatrix} u_1 \\ u_2 \\ u_3 \\ \vdots \\ u_n \end{Bmatrix} \tag{3.12}$$

Step 2. Initialize the weights using random number generator in the range of -0,5 to 0,5

$$[W_{ji}] = \begin{bmatrix} w_{11} & w_{12} & w_{13} & \cdots & w_{1n} \\ w_{21} & w_{22} & w_{23} & \cdots & w_{2n} \\ w_{31} & w_{32} & w_{33} & \cdots & w_{3n} \\ \vdots & \vdots & \vdots & \ddots & \vdots \\ w_{m1} & w_{m2} & w_{m3} & \cdots & w_{mn} \end{bmatrix} \tag{3.13}$$

Step 3. Compute the value of $\{a_j\}$ for the hidden nodes [see eqn (A1.1)]

$$\{a_j\} = \begin{Bmatrix} a_1 \\ a_2 \\ a_3 \\ \vdots \\ a_m \end{Bmatrix} = [W_{ji}]\{U_i\} \tag{3.14}$$

Step 4. Calculate the activation value $\{x_j\}$ for the hidden nodes [eqn (A1.2)]. Here the sigmoid function has been used. The parameter θ_j is to shift the activation function to the left and right along the horizontal axis depending upon its positive or negative values, respectively. Similarly the θ_o is used to modify the shape of the sigmoid.

$$\{x_j\} = \begin{Bmatrix} x_1 \\ x_2 \\ x_3 \\ \vdots \\ x_m \end{Bmatrix} = \begin{Bmatrix} f_1 \\ f_2 \\ f_3 \\ \vdots \\ f_m \end{Bmatrix} \left(\begin{Bmatrix} a_1 \\ a_2 \\ a_3 \\ \vdots \\ a_m \end{Bmatrix} \right) = \begin{Bmatrix} f_1(a_1) \\ f_2(a_2) \\ f_3(a_3) \\ \vdots \\ f_m(a_m) \end{Bmatrix} = \begin{Bmatrix} 1/(1+e^{-(a_1+\theta_1)/\theta_0}) \\ 1/(1+e^{-(a_2+\theta_2)/\theta_0}) \\ 1/(1+e^{-(a_3+\theta_3)/\theta_0}) \\ \vdots \\ 1/(1+e^{-(a_m+\theta_m)/\theta_0}) \end{Bmatrix} \quad 3.15$$

Step 5. Calculate the value of $\{a_k\}$ for the output node

$$\{a_k\} = \begin{Bmatrix} a_1 \\ a_2 \\ a_3 \\ \vdots \\ a_p \end{Bmatrix} = [W_{kj}]\{x_j\} \tag{3.16}$$

Step 6. Calculate the activation value $\{x_k\}$ for the output nodes

$$\{x_k\} = \begin{Bmatrix} x_1 \\ x_2 \\ x_3 \\ \vdots \\ x_p \end{Bmatrix} = \begin{Bmatrix} f_1 \\ f_2 \\ f_3 \\ \vdots \\ f_p \end{Bmatrix} \left(\begin{Bmatrix} a_1 \\ a_2 \\ a_3 \\ \vdots \\ a_p \end{Bmatrix} \right) = \begin{Bmatrix} f_1(a_1) \\ f_2(a_2) \\ f_3(a_3) \\ \vdots \\ f_p(a_p) \end{Bmatrix} = \begin{Bmatrix} 1/(1+e^{-(a_1+\theta_1)/\theta_0}) \\ 1/(1+e^{-(a_2+\theta_2)/\theta_0}) \\ 1/(1+e^{-(a_3+\theta_3)/\theta_0}) \\ \vdots \\ 1/(1+e^{-(a_p+\theta_p)/\theta_0}) \end{Bmatrix} \tag{3.17}$$

Step 7. Calculate the $[\Delta W_{kj}]$ [eqn (A1.24)]

$$[\Delta W_{kj}] = \eta\{t_k - x_k\}\{x_k\}\{x_j\}^T + \alpha[\Delta_p W_{kj}] \tag{3.18}$$

η (learning parameter) and α (momentum parameter) are usually selected from experience.

t = target output and $\Delta_p W$ = previous weight changes

Step 8. Compute the new values of weights between the hidden and output layers

$$[W_{kj}] = [W_{kj}] + [\Delta W_{kj}] \tag{3.19}$$

Step 9. Calculate the $[\Delta W_{ji}]$ for input to hidden weights

$$[\Delta W_{ji}] = \eta\{x_j\}\{t_k - x_k\}\{x_k\} * [W_{kj}]^T\{U_i\}^T + \alpha[\Delta_p W_{ji}] \tag{3.20}$$

Step 10. Calculate the new values of the weights between input and hidden layer

$$[W_{ji}] = [W_{ji}] + [\Delta W_{ji}] \tag{3.21}$$

The algorithm continues for all set until the average system error (ASE) [eqn (A1.7)] between the target output and computed output is close to the tolerance specified.

CHAPTER 4

ANALYTICAL MODELING OF A TYPICAL T-BEAM BRIDGE

4.1 Pennsylvania's T- Beam Bridge Population

The total T-beam bridge population in the US is 38,170 based on the NBI (2001). With 2,440 T-beam bridges, Pennsylvania has the third largest reinforced concrete (RC) T-beam population after California and Kentucky. However, Pennsylvania has the greatest number of structurally deficient and functionally obsolete T-beam bridges in the US (NBI, 2001). The total number of single span T-beam bridges in PA is 1,899 and approximately 60% of this population is older than 60 years, with a maximum age of 101 years. Most of RC T-beam bridges were constructed mostly between 1900's and 1960's by using a standard set of design drawings (Figure 4.1). Therefore, these T-beam bridges share geometry and design details, materials and similar cast-in-place construction.

The Swan Road Bridge and Manoa Road Bridge shown in Figures 4.2 and 4.3 are the two of these bridges, and are used for numerical studies in this thesis. Close-up photographs in Figures 4.2 and 4.3 show the conditions and any damage at critical areas of these bridges.

Swan Road Bridge with 26-ft length (7.93 m) and 26- ft width (7.93 m) was constructed in 1937, has no skew and is supported on 6 T-beams each of which has a depth of 24 in (0.6096 m). Total steel area in the tension region is 12.50 in^2 (80.65 cm^2) for all beams. T-beam web width, beam spacing (flange width) and deck thickness are 15.75 in (0.4001 m), 61 in (1.5494 m) and 8.5 in (0.2159 m), respectively. Bridge has end diaphragm beams at the boundaries and reinforced concrete parapets on both sides through the roadway.

Figure 4.1 Example of a Population of Similar Bridges

The Manoa Road Bridge with 32ft length (9.75 m), 53-ft width (16.15 m) and 15 degree skew, was constructed in 1929, and is supported by 11 T-beams. The depth of beams is 28.5 in (0.7239 m) and total steel area in the tension region is 14.50 in^2 (93.55 cm^2). T-beam web width, beam spacing (flange width) and deck thickness for Manoa Road Bridge are 16.5 in (0.4191 m), 61.5 in (1.5621 m) and 8.5 (0.2159 m) inches, respectively. The secondary structural elements, such as end diaphragm beams at the boundaries and reinforced concrete parapets, are also critical components of the bridge. While the geometry of the Swan Road Bridge may be considered typical, the Manoa Road Bridge represents a particular case of large width. Both bridges feature just two traffic lanes.

Figure 4.2 Swan Road Bridge: General and Close-up Views

Figure 4.3 Manoa Road Bridge: General and Close-up Views

4.2 Analytical Modeling of T-Beam Bridges

It is clear that developing a detailed FE model of each and every bridge of the T-beam population will be impractical, as it requires a considerable time and expertise

for development and interpretation. When a major, long span bridge is considered, this effort is very feasible and valuable. Here in the case of a population, a real bridge with average structural and geometric parameters is selected from the entire population for modeling.

A typical T-beam bridge is in fact an integration of beams and slab along the span of the bridge ending in rigid diaphragm beams. The orthotropically reinforced slab is bounded by stiff edge girders monolithic with parapets in addition to the diaphragm beams. While the girders predominantly transmit forces through uni-axial shear-flexure, the orthogonal flexural response of the slab as a plate, and the axial membrane forces in the slab that arise due to the restraining of the diaphragms at the abutment interfaces are additional mechanisms that contribute to load capacity.

The finite element libraries of modern general-purpose structural analysis software such as SAP 2000 offer various options for 3D FE modeling of a T-beam bridge. Several options are illustrated in Figure 4.4. While all options may permit representing the critical behavior mechanisms of the bridge, the first option based on using solid elements for simulating concrete at the microscopic level and using axial frame elements for simulating individual reinforcing bars on an individual rebar basis offers great advantages in simulating deterioration and damage.

In order to verify the reliability in mixing the solid and frame elements for simulations, a single reinforced concrete T-beam from an existing bridge was modeled by 3D solid and beam elements and the results were compared with the engineering mechanics solution. Figure 4.5 shows two responses for stress and moment compared along the beam from the FE model and the engineering mechanics solution. The study verified that solid elements for the concrete and frame elements for the steel rebars can be connected at the nodes and used for finite element modeling of reinforced concrete T-beams at a microscopic level, given the dimensions for the solid and frame elements shown in Fig. 4.5.

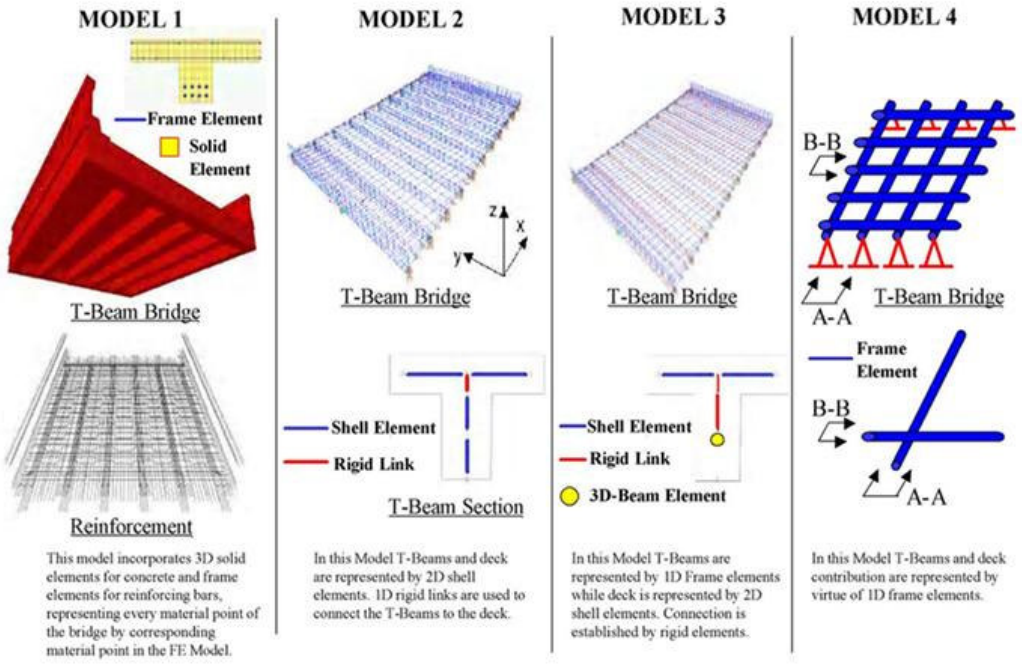

Figure 4.4 Finite Element Modeling Options (DIITSI, 2003)

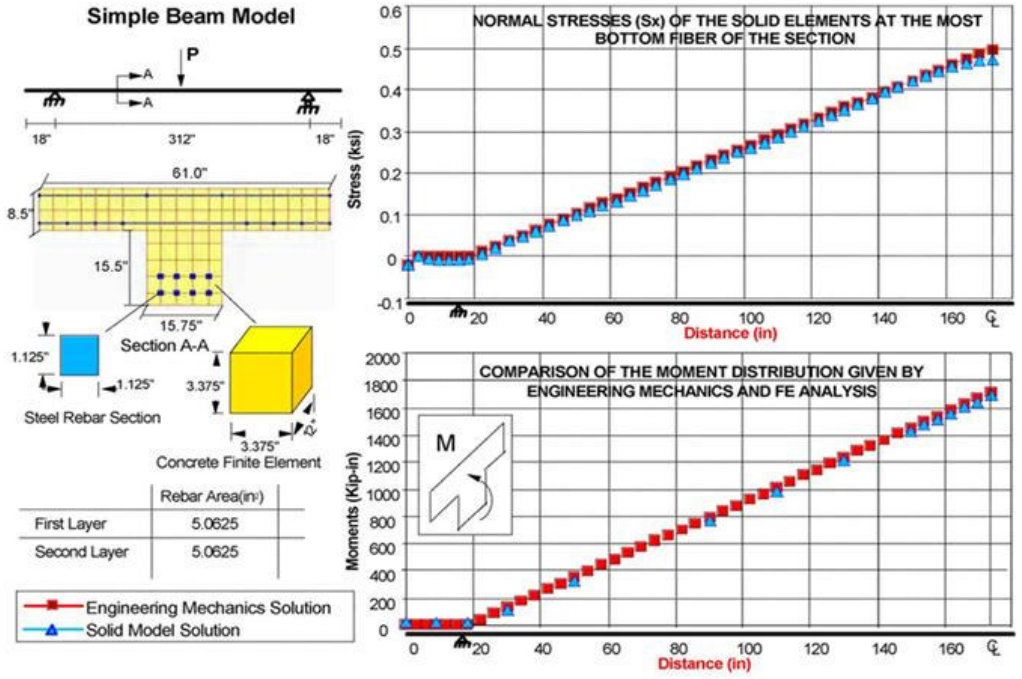

Figure 4.5 Verification Analysis; Solid Modeling of T-beam Section (DIITSI, 2003)

4.2.1 Finite Element Model of the Swan Road Bridge

The Swan Road Bridge in Chester County (Figure 4.6) was selected as a typical T-beam bridge in PA in terms of its nominal design attributes with 6 reinforced concrete T-beams, and a deck thickness of 8.5inches. After identifying the most suitable modeling option, the analytical model can be constructed. A typical 3D FE model that is constructed using solid elements and axial frame elements available in the library of the SAP 2000 V9 software (2002) for a complete and accurate modeling of the geometry, detailing and material properties are illustrated in the example in Figure 4.7. Such a fine microscopic approach to 3D geometric -replica analytical modeling is now practical and enables explicitly simulating every material point of the bridge for an accurate representation of the geometry, the actual behavior mechanisms and any existing deterioration or damage.

Figure 4.6 Swan Road Bridge, Lancaster Co, PA - Average Geometric and Structural Parameters

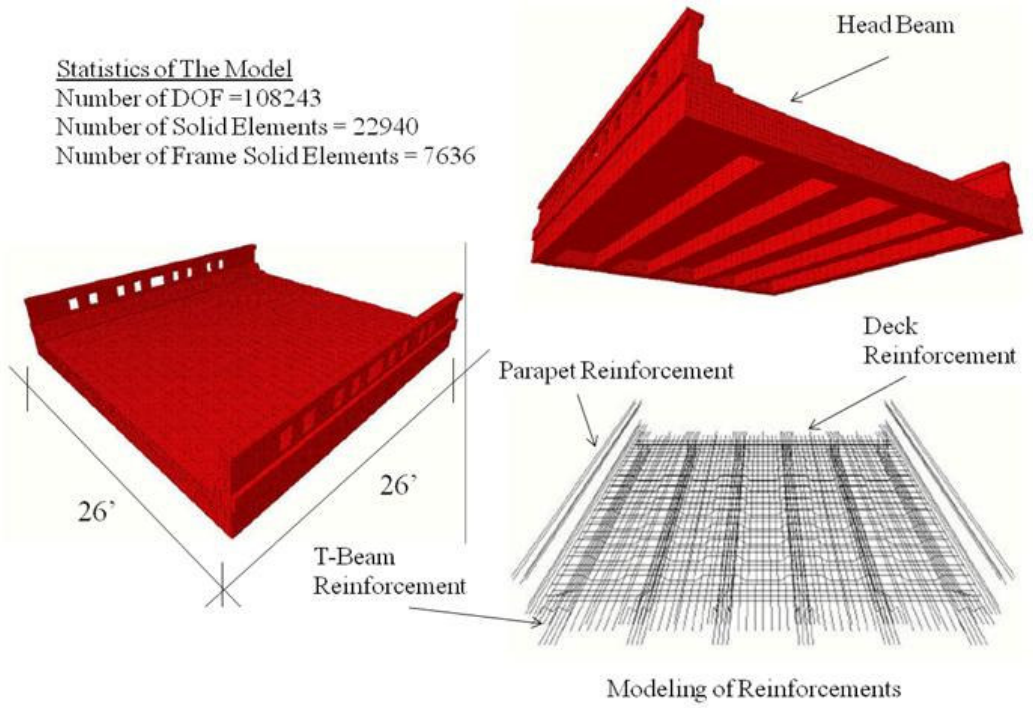

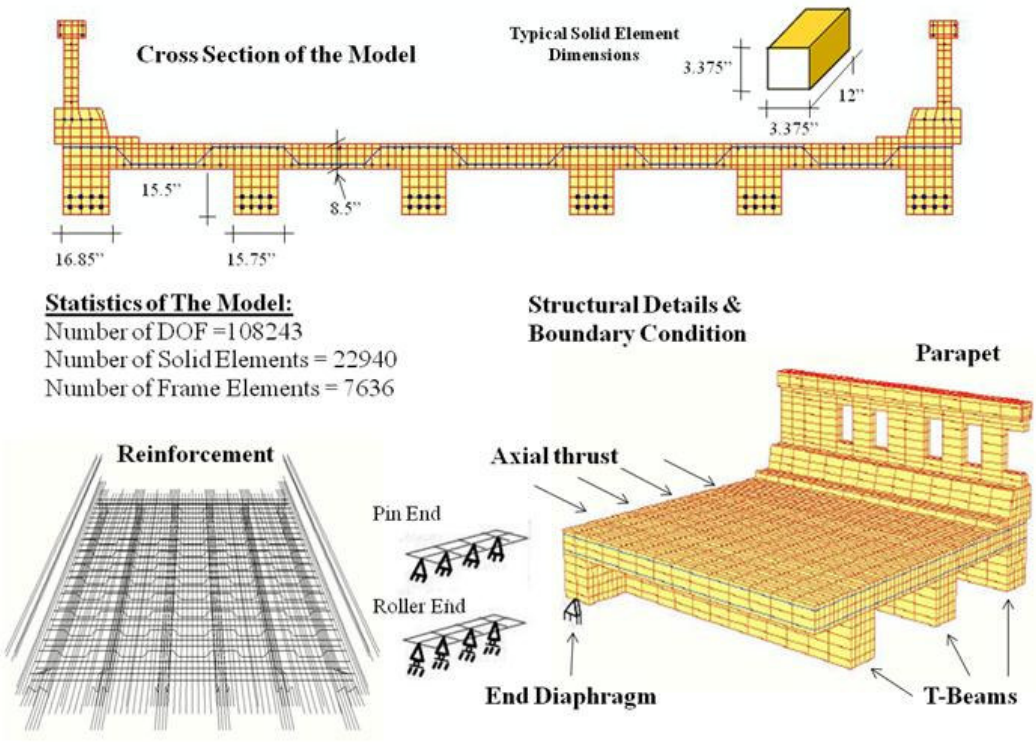

Figure 4.7 Finite Element Modeling of a T-beam Bridge with Solid and Frame Elements

The nominal concrete cylinder stress is 3 ksi and rebar yield stress is 33 ksi. The model features 108,243 degrees of freedom, employing 22,940 solid elements and 7,636 frame elements. Both longitudinal and transverse steel reinforcing bars were modeled on a one-to-one basis using frame elements and connected to the solid elements simulating perfect bond. The parapets and lateral end diaphragm were modeled in detail. Boundary conditions are defined such that all the center nodes on the superstructure-substructure interface at one end of the bridge are modeled using pin supports to simulate restraints due to the dowels, while the center nodes at the other end are modeled with roller supports, allowing both rotation and translation in longitudinal and transverse directions, as shown in Figure 4.7. In addition, the lateral earth pressure on the diaphragm beam can be simulated using linear springs.

In order to investigate the mesh sensitivity, a second model with a finer mesh was also constructed. The second model incorporated a total of 301,887 degrees of freedom as opposed to the 108,243 degrees of freedom of the first model, yet the maximum difference in the deflections and stresses remained within 0.7%. Therefore, to increase the computational efficiency the model with 108,243 degrees of freedom was employed for the reported studies.

CHAPTER 5

APPROXIMATE ANALYSIS OF T-BEAM BRIDGES USING NEURAL NETWORKS

Using present-day computing resources and a finite-element (FE) modeling software, it is possible to routinely apply FE analysis techniques to the evaluation of complex structures systems. Accompanying the use of such modeling software, however, is a substantial increase in the quantity of time required to perform the analysis. In addition, the preparation of such models requires substantial amount of effort. Engineers practicing in certain fields (e.g. highway bridge engineering) often find themselves repeatedly analyzing structures that fall into fairly well-defined categories or "problem domains". Structures falling into this problem domain will exhibit certain common characteristics. Given the increasing use of modeling software, the increasing size of FEA models routinely generated in everyday practice, and the frequent need to analyze structures in well-defined problem domains, it becomes desirable to conceive a strategy wherein the analysis can be accelerated by exploiting structural similarities within particular problem domains.

In this chapter, a technique for enhancing analysis of bridge structures for a particular problem domain is discussed. The strategy described herein consists of restricting bridge structures to a particular problem domain, e.g., a particular type of bridge population, and then using neural networks to approximately encode the basic structural behavior of that class of structures. This strategy was applied to single span RC T-beam bridge population in the Pennsylvania state. ANN systems seem to be applicable to predicting structural responses from bridge parameters. They are capable of learning the relationship between bridge parameters and responses based on the existing data and generalizing this for other bridges not included in the existing set. Firstly, a statistical analysis of bridge parameters is

conducted to determine the variability in each parameter and the degree to which the entire bridge population can be represented. Then, based on these parameters, a group of bridge samples are randomly generated using different combinations of the parameters within the ranges of possible variations to ensure that the ANN model trained using these samples can predict, within an acceptable accuracy, the structural behavior exhibited by majority of the bridges within the population. In order to obtain the outputs of bridge set, all bridges in the set are modeled using a standard FEM program and analyzed for structural responses. The bridge data acquired are divided into three sets; the training set, the cross validation set and the test set. The training set is used to establish relation between bridge parameters and structural responses. The cross validation set is used to avoid overfitting which is the case of poor generalization. The test set is used to evaluate the performance of the network. Finally, several network designs are created and examined to arrive at ones with good generalization capability. If a relationship between bridge parameters and bridge responses can be found, then prediction of a bridge's responses can readily be made just by evaluating its input parameters with a trivial computational time and effort and without a need to construct and analyze a new model for each parameter set.

5.1 Statistical Analysis

There are a large number of parameters controlling the structural behavior of T-beam bridges. Amongst these parameters are the span length, skew angle, width of bridge (number of T-beams), beam depth, beam web width, beam flange width (beam spacing), slab thickness, reinforcement detailing, boundary conditions and existence of reinforced parapets or end diaphragms.

However, not all these parameters are independent owing to the fact that the majority of the T-beam bridges were constructed using a standard set of drawings. In the standard design drawings, the structural details and element dimensions are dependent on the span length and width of the bridges. For example, when a bridge with a certain plan geometry is selected, the beam sizes, reinforcement and all other

details are automatically established. This "mechanistic" dependency greatly reduces the number of independent structural parameters.

A statistical analysis is conducted here to determine the governing and independent structural and geometrical parameters. It has been found that T-beam web width, beam spacing (flange width) and deck thickness are constant for all bridges in the population at values of around 16 in (0.4064 m), 60 in (1.524 m) and 8.5 in (0.2159 m), respectively. Since the bridges were constructed from one set of typical plans, all other parameters such as proportioning and reinforcement detailing were dependent on these parameters. The secondary structural elements, such as end diaphragm beams at the boundaries and reinforced concrete parapets, are critical components of the bridges contributing to the structural behavior. It is noted that not all bridges in the population possess these secondary components. The boundary conditions (BC) of an actual bridge are often complicated. Therefore, they can be idealized as pin roller supports in the analysis models.

As a result of this study, the numbers of governing independent bridge parameters are reduced to six as follows: the span length and skew angle, width of bridges, beam depth and existence of reinforced parapets and end diaphragms.

5.2 Bridge Data

As mentioned in the previous section, the independent bridge parameters are established as the span length, skew angle, width of bridge (number of T-beam), beam depth, and existence of reinforced parapets and end diaphragms. NBI (1998) data and PennDOT database are used to determine the range of variation of each of these parameters within the population. A summary of the results of this study is given as follows:

- span length ; 20 ft (~6 m) – 55 ft (~17 m)
- skew angle ; 0 – 45 degrees
- number of beams ; 5 – 11

- beam depth ; 19 in (~0.48 m) – 40 in (~1.02 m)
- parapet ; exist or not exist
- diaphragm ; exist or not exist

T-beam web width, beam spacing (flange width) and deck thickness are assumed to be constant equal to 15.5 in (0.3937 m), 60 in (1.524 m) and 8.5 in (0.2159 m), respectively for all bridges in the sample set. All other parameters are kept at their nominal values and the boundary conditions are idealized as pin roller supports.

According to Atalla and Inman (1998) the training of the network with a random generation of the bridge parameters within the ranges of possible variations produces the best results. In line with this statement, a total of 140 sample bridges are randomly generated using the aforementioned ranges/values of bridge parameters to generate a representative bridge set, accounting for distinct structural and geometrical features of the bridges in the population. . The dataset used for this study is tabulated in Appendix B.1.

5.2.1 Loading Conditions

Live load is either the standard truck or lane loading corresponding to HS20 truck. For short spanned bridges, such as the ones considered in this study, the governing loading condition is usually the truckload. Therefore, only the live load due to truck loads is simulated in order to generate the maximum absolute member forces. Determining the most critical member forces due to truck loads require a number of sequential analyses such that after determining the number of the design lanes in the bridge, various number of trucks are positioned at different locations in the model. Then, model is analyzed under these truck configurations considering the multiple presence factors for moment and shear. The moments and shears found in this way needs to be compared against each other in order to establish the maximum member forces for the model.

5.2.1.1 Number of Design Lanes and Multiple Presence of Live Load

The number of design lanes in a bridge is determined by taking the integer part of the ratio w/3600, where w is the clear roadway width in mm between curbs and/or functional clear roadway width of the bridge is considered (Figure 5.1). In cases where the traffic lanes are less than 3.6 m wide, the number of design lanes shall be equal to the number of traffic lanes, and the width of the design lane shall be taken as the width of the traffic lane. Roadway widths from 6 to 7.2 m are assumed to have two design lanes, each equal to one-half the roadway width (AASHTO Section 3.6, 1999).

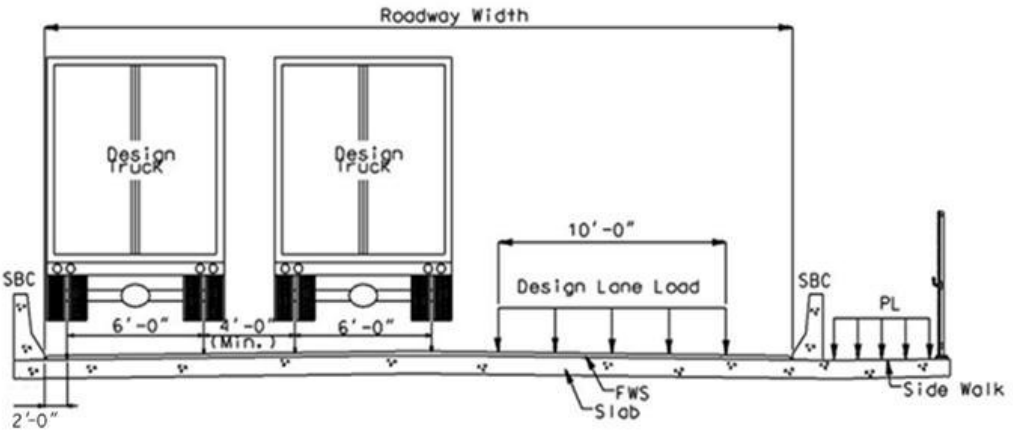

Figure 5.1 Application of Live Load to Lanes

According to AASHTO Specification, bridges in the representative set are composed of one, two, and three lanes depending on the number of beams along their width. These are presented in Table 5.1.

Table 5.1 Number of design lane of bridges in the representative sample set

Number of Beams	Width (mm)	Number of Lanes
5-beam	5151	1
6- beam	6675	2
7- beam	8199	2
8- beam	9723	2
9- beam	11247	3
10- beam	12771	3
11- beam	14295	3

The extreme live load force effect shall be determined by considering each possible combination of number of loaded lanes multiplied by a corresponding multiple presence factor to account for the probability of simultaneous lane occupation of the design truck. The following table gives the multiple presence factors, *m*. (AASHTO Section 3.6, 1999).

Table 5.2 Multiple Presence Factors “m”

Number of Loaded Lanes	Multiple Presence Factors "m"
1	1,2
2	1
3	0,85
>3	0,65

5.2.1.2 Truck load generation

The next step is to define the loads. Mainly, there are two different vehicle loads considered: a) truck loads, and b) lane loads (see Figure 5.2).

The rating-truck "HS20-44" defined in AASHTO was used in this study. An HS20-44 truck is a virtual rating truck. It weighs a total of 320.3kN (72 kips, 36 short tons; one short ton is equal to 2 kips and 0.91 tons), and is composed of three axles. The first two axles are 4.27m (14ft) apart. The distance between the second and third axles can vary between 4.27m (14ft) and 9.14m (30ft). In this study, the rear axle spacing was taken as 4.27m (14ft.) in order to maximize positive bending moment in each span. The width of the truck is assumed to be constant and equal to 1.8m (6ft.) for all axles. The first axle weight is 35.6kN (8kips); the second and third axles are 142.3kN (32kips) each. The term "20" in "HS20-44" notation comes from the summation of the first two axle weights in terms of short tons. The term "44" represents the year 1944 that HS20-44 trucks were first started to be used for bridge design/rating.

AASHTO lane loads are composed of a uniformly distributed lane load of 9.34kN/m/lane (640lbf/ft/lane) together with one or two 80.1kN/lane (18 kips/lane) of concentrated load(s). Lane loading is intended to be a governing case for especially long bridges since uniformly distributed vehicle traffic in a closed road or traffic jam condition can be more critical than a single truck load. One 80.1kN (18 kips) concentrated point load per lane is used to maximize the positive bending moment. This load is located along the bridge to produce the largest positive moment. For members experiencing negative bending (such as members close to the piers), two concentrated loads of 80.1kN/lane (18 kips/lane) must be defined on either side of the support to obtain the largest negative bending moment. Each one of the two 80.1kN (18 kips) loads on each lane should be placed at a location to maximize the negative bending moment.

Since bridges generated for the study fall into the class of short span bridges, the governing loading condition is the truckload. In models, each truck is represented by 96 concentrated loads, sixteen of which represent each tire (Figure 5.3). Concentrated loads are spread over the nodes of solid elements over which the tire is acting. Truck configurations are positioned such that they create the maximum member forces at defined sections in the model as shown in Figure 5.3.

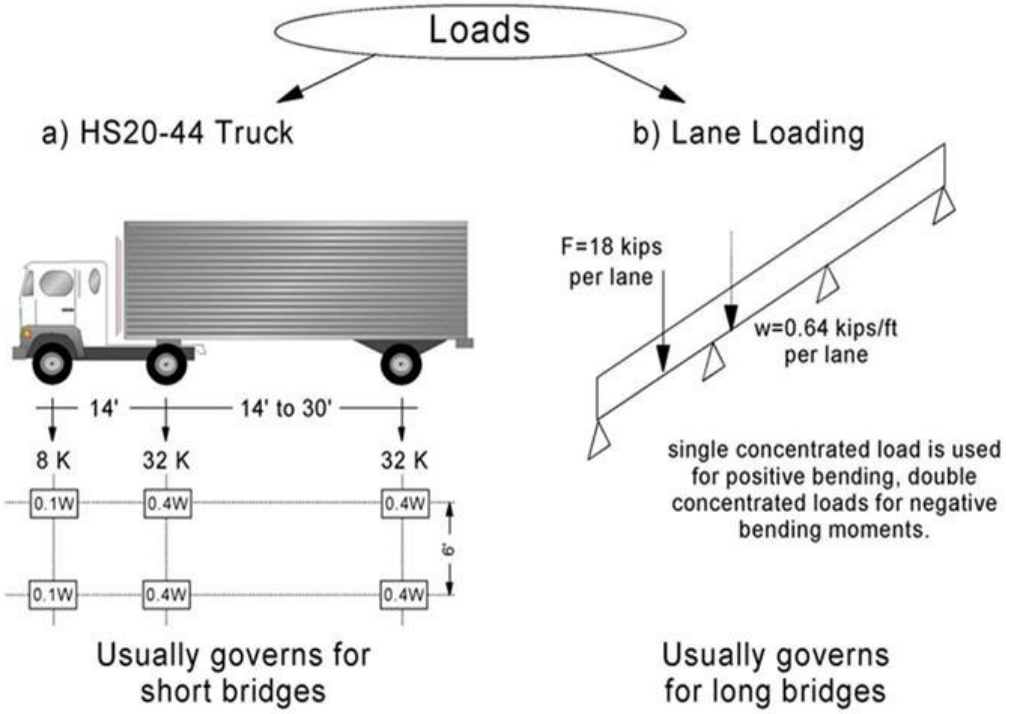

Figure 5.2 Loading Types for AASHTO (Turer, 2000)

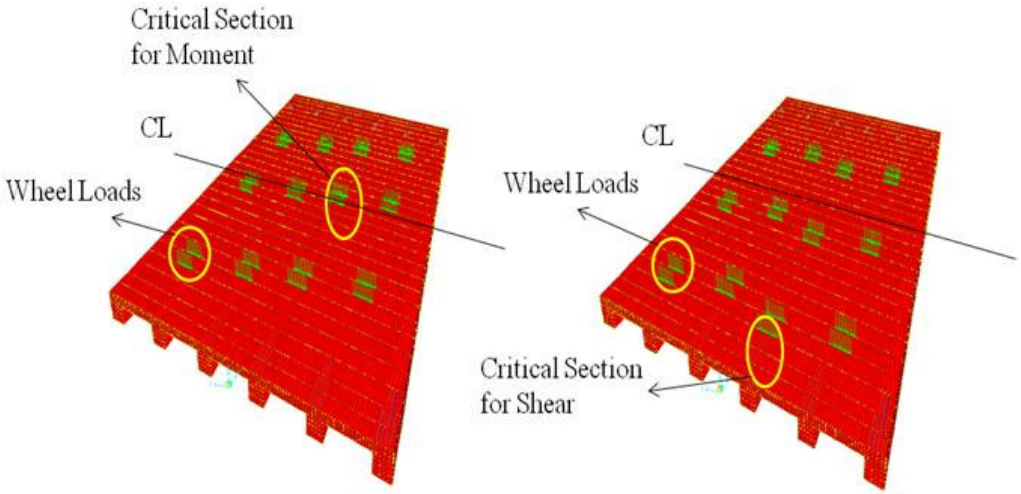

Figure 5.3 Application of Truck Load for Critical Moment and Shear

5.2.2 FE Modeling and Analysis

Finally, randomly generated 140 T-beam bridges are constructed using solid elements and frame elements available in the library of the SAP 2000 V9 software for a complete and accurate modeling of the geometry, detailing and material properties as illustrated in Figure 4.7. Pin-roller type supports are used in all the models to simulate the nominal boundary conditions. All of the 3D FE models are analyzed under various configurations of HS20-44 trucks for critical moment and shear (see Appendix B.1 for analysis results). After analyzing the bridges, the training data for neural network model has been generated. As mentioned before, the training data consists of input and output pairs where the bridge parameters identified in statistical analysis and used to parameterize the models are the inputs, whereas the outputs are the maximum shear and moment developing in bridges.

5.3 Neural Network Modeling

ANN learns from the existing patterns and then makes a prediction for the patterns which are not considered during learning. Therefore, the success of a network is measured by its generalization performance. If the difference between the actual and computed output by ANN is within the acceptable level, then the network can be used for prediction in the similar domain which exhibits certain common characteristics with the existing patterns. The prediction performance of a network usually depends on the network parameters and the topology chosen. The best performance is generally achieved by extensive parametric study on the different network using trial and error approach. In each trial, performance of network is evaluated. This process is repeated until the best architecture with the right network parameters is arrived.

In this study, the Levenberg- Marquardt algorithm (Rao and Kumar, 2007) is used for learning rule of ANN, and the sigmoid function is used for activation function. Since, Levenberg- Marquardt requires less time and epochs to converge, it performs more efficiently compared to other learning rules, which in turn makes it ideal for

trial of different networks. In addition, while almost all learning rules lead to somewhat satisfactory results, Levenberg- Marquardt is the one producing the best results (Yetilmezsoy and Demirel, 2008). The use of sigmoid function requires that the input and output data be scaled to the range [0-1]. In the present study, the input and output data are scaled to a somewhat narrower range between 0.2 and 0.8, resulting in a considerable improvement in learning speed due to increased sensitivity of the sigmoid function within this range. As mentioned before, the training data generated for the application consist of 140 input-output patterns (pairs) and are divided into three sets, namely, the training set, the cross-validation set and the test set. The training set contains 101 patterns and used to detect any relationship between the bridge parameters and responses. The cross-validation set contains 29 patterns and is used to avoid overfitting problem. The test set consists of 10 patterns and is used to evaluate the performance of the networks. Based on defined network parameters, the effect of the number of hidden layers and number of processing elements in hidden layers as well as in output layer are observed using several architectures with the help of Neuro Solutions 5 (www.neurosolutions.com) which is general software developed for neural network applications. After completion of training of each network design, the performance of the network is tested using the test patterns that are not used during the training. The performance is measured by the average maximum error in the testing set. This process is repeated for each network design. In this way, many networks which are capable of generalization at different levels are obtained. Among them, the best network is selected.

5.3.1 Development of the Network Models

Obtaining the best network is a lengthy process which requires trial of different network parameters in several architectures. After a number of trials, appropriate values of the networks parameters are set as follows:

- Number of training examples = 101
- Number of cross-validation examples = 29

- Number of test examples = 10
- Number of input layer neurons = 6
- Number of output layer neuron(s) = 1 or 2
- Type of back-propagation = Levenberg-Marquardt back-propagation
- Activation function = Sigmoid function
- Normalization range = [0.2,0.8]
- Learning rate = 0,01
- Training mode = Batch mode
- Termination rule = minimum cross validation error or maximum epoch

Several architectures are tested in conjunction with the above set of network parameters to find the one having the best prediction performance, that is, the best generalization capability. A typical architecture is designated as "input nodes (n) - [hidden nodes per hidden layer (m)]-output nodes (p)". For example, the notation "6-(7-7)-2" (7-7) indicates that the network architecture consists of an input layer of 6 nodes, an output layer of 2 nodes, and two hidden layers of 7 nodes each.

The following cases are created and studied with respect to the choice of network architecture as well as the selection of network output

Case 1: Network 6-(m-m)-2; m varies from 4 to 11

In case 1, the moment and shear are both considered as network output. The architecture used has two hidden layers with m nodes per layer denoted as 6-(m-m)-2.

Case 2: Network 6-(m-m)-1; m varies from 5 to 11

For case 2, the moment and shear are separately considered as network output. Hence, the network architecture is denoted by 6-(m-m)-1, in which the output node is assigned to either moment or shear.

Case 3: Network 6-(m)-2; m varies from 3 to 9

In case 3, both the moment and shear are considered as network output. The architecture used has one hidden layer with m nodes denoted as 6-(m)-2.

Case 4: Network 6-(m)-1; m varies from 3 to 9

For case 4, the moment and shear are separately considered as network output. The network architecture is denoted by 6-(m)-1, in which the output node is assigned to either moment or shear.

In the current study, the network performance is associated with the maximum error in the moment and shear prediction of the network for all the testing patterns. If the maximum testing error appears to be below the tolerable level, then the performance of network is considered satisfactory.

5.3.1.1 Observations

The results of the study on the network designs has showed that ANN is quite promising in predicting the maximum moment and shear developing in the bridges due to moving truck loads. Some of the typical results have been given in Figures 5.4 through 5.7. The following observations are made based on all examined networks.

1. All the trained networks are able to predict the responses for all the testing patterns with a reasonable accuracy (Figure 5.4 and 5.5). Thus it can be deduced that single span population of T-beam bridge behavior can be modeled through neural networks.

2. While minimum MSE (Mean Square Error) [eqn (A1.8)] is a measure of learning performance, it does not guarantee the best prediction rate (generalization capability). As it is clear from Figures 5.4 to 5.7 that the

prediction performance of the 6-(m)-1 architecture is generally better than that of other architectures for both moment and shear for all the testing patterns, even though some of them have lower MSE.

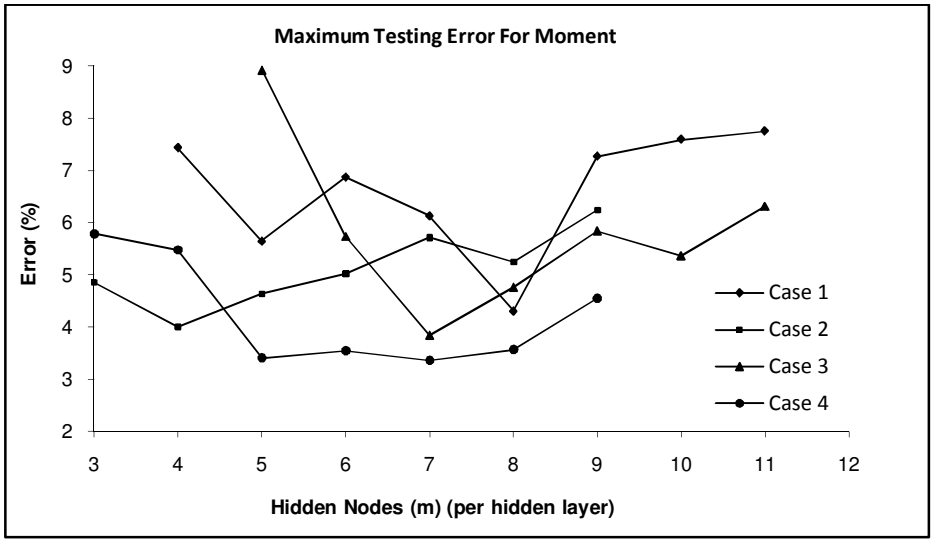

Figure 5.4 Maximum Testing Errors versus Number of Nodes in Hidden Layer(s) for Moment

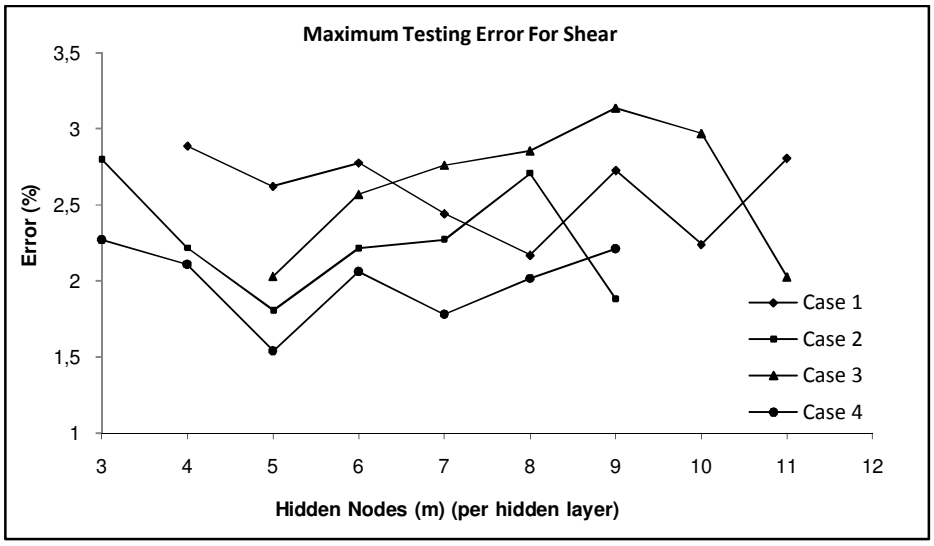

Figure 5.5 Maximum Testing Errors versus Number of Nodes in Hidden Layer(s) for Shear

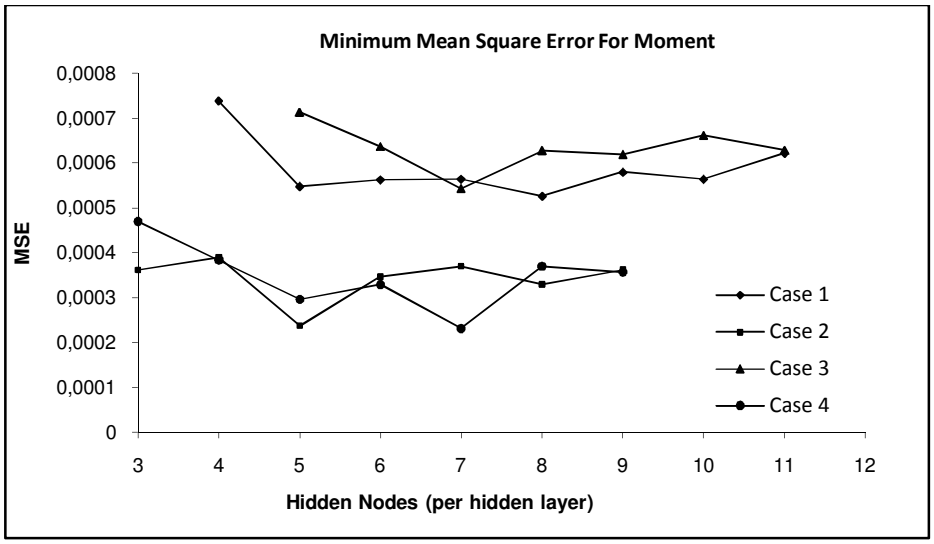

Figure 5.6 Minimum MSE versus Number of Nodes in Hidden Layer(s) for Moment

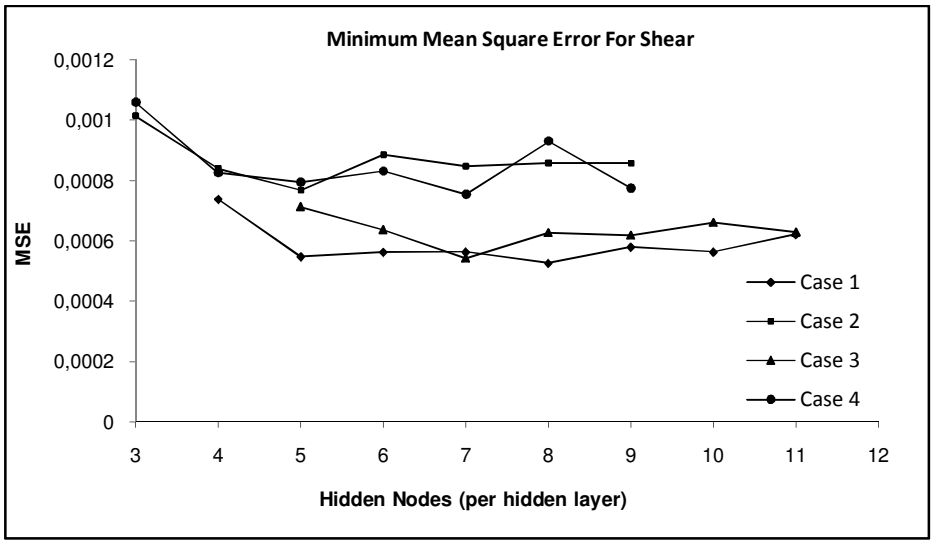

Figure 5.7 Minimum MSE versus Number of Nodes in Hidden Layer(s) for Shear

3. Levenberg- Marquardt learning rule and the sigmoid transfer function are appropriate choices for a successful network application in the current context.

4. The learning and prediction performance of the network vary depending on the number of hidden layers and the number of nodes in the hidden and output layers. A single hidden layer with an optimum number of neurons is sufficient for modeling of this problem. The use of single output node assigned to either moment or shear improves the performance of the networks compared to the cases where two output nodes are used for predicting moment and shear together (Figures 5.4 and 5.5).

5.3.2 Best Neural Network Models

It is clear from Figures 5.6 and 5.7 that almost all networks generate a reasonable MSE value. However, as seen from the Figures 5.4 and 5.5, the best performance in predicting moment is shown by Case 4 with a seven processing elements, resulting in 3.36% maximum average testing error for all testing patterns. Similarly, the best performance in predicting shear is again exhibited by Case 4, yet this time with a five processing elements, resulting in 1.53% maximum average testing error for all testing patterns.

In Figures 5.8 and 5.9, the average MSE in training versus epochs are plotted for moment and shear, respectively. The MSE drops drastically after 10 epochs for moment and carries on running until minimum validation error which is reached at 38th epoch with a MSE error of 0,000231. For shear, the error stabilizes at around 10 epochs and goes on running until minimum validation error which is reached at 79^{th} epoch with a MSE error of 0,000794. To make sure that the network training has been satisfactorily completed and the network is capable of generalization, a set of unseen patterns must be selected and the network should be tested using these patterns. For this purpose, a total of 10 testing patterns are used to observe the prediction performance of all the architectures considered in the study.

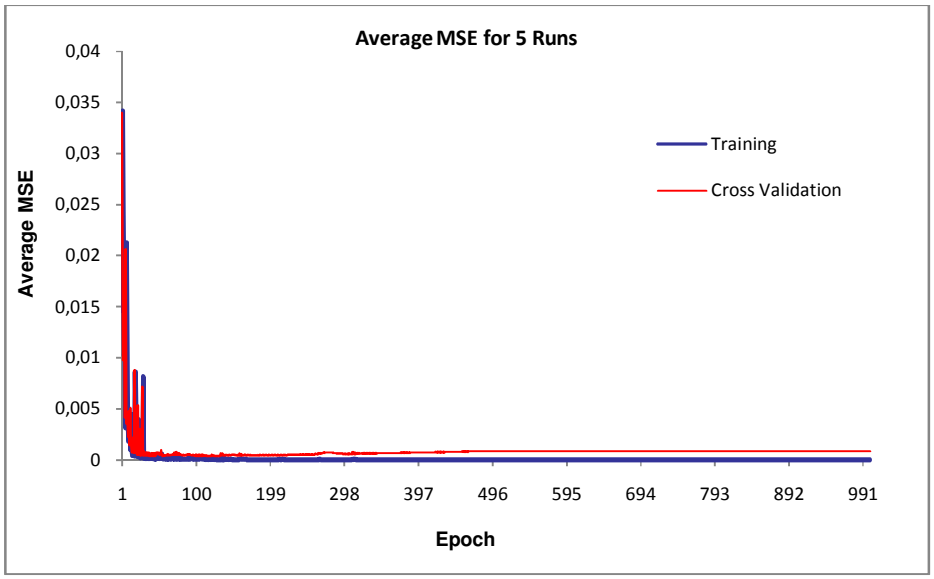

Figure 5.8 Learning Curves for 6-(7)-1 Moment Output Network

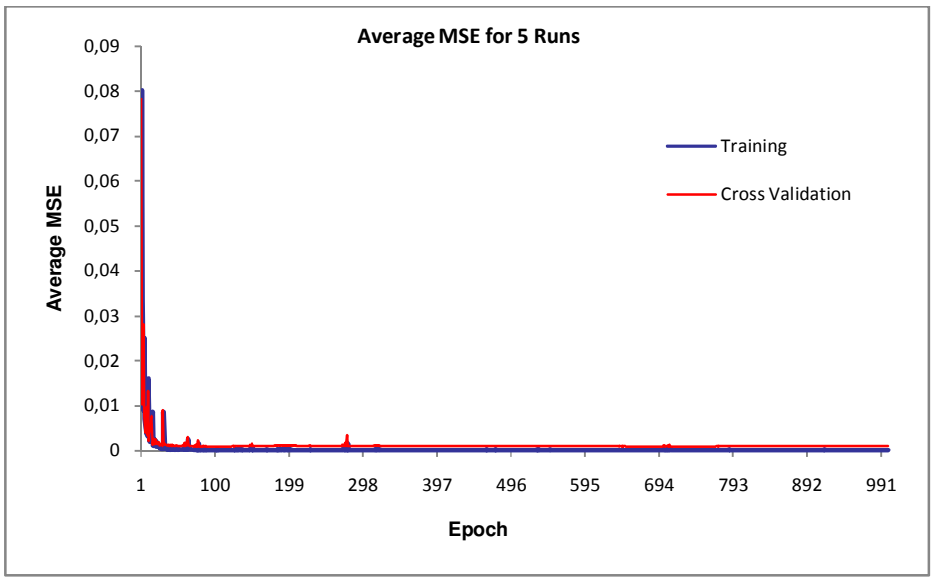

Figure 5.9 Learning Curves for 6-(5)-1 Shear Output Network

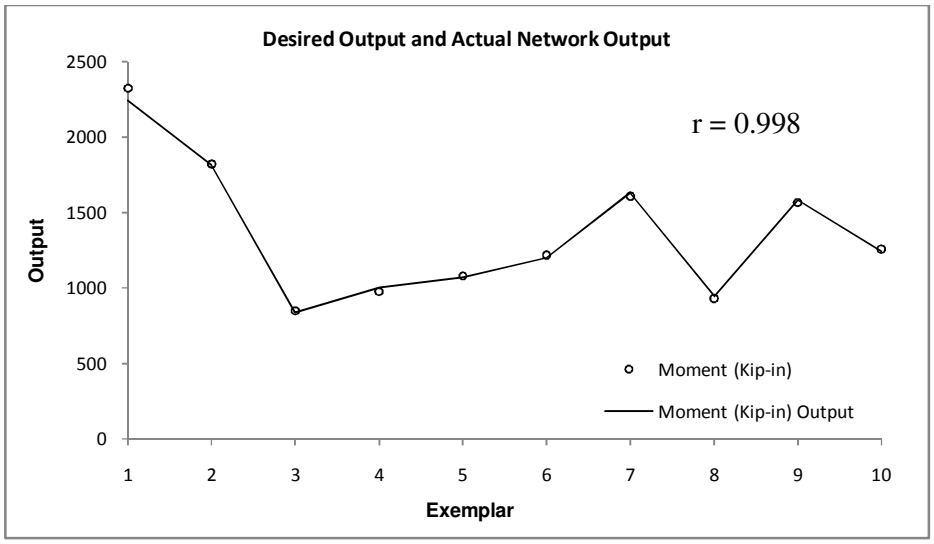

Figure 5.10 FEM Output and Best Network (6-(7)-1) Output for Moment

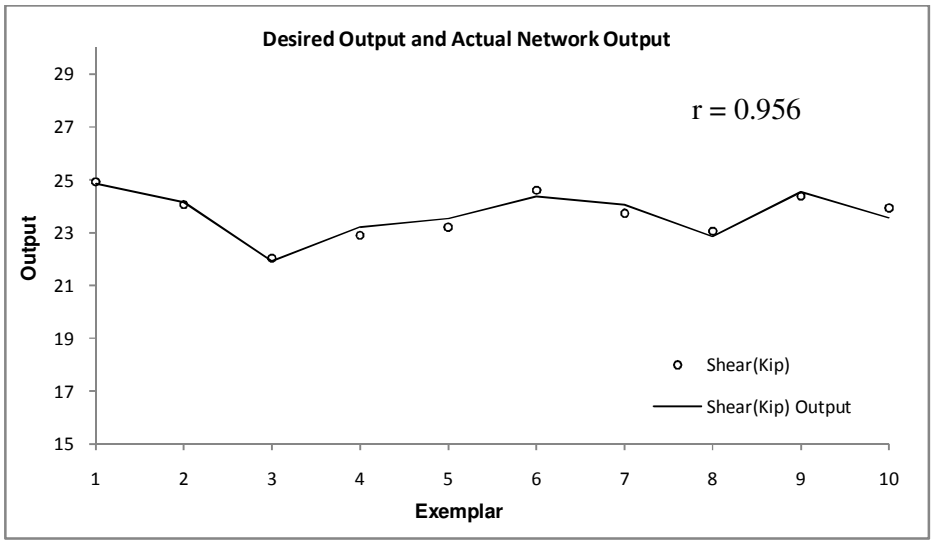

Figure 5.11 FEM output and Best Network (6-(5)-1) Output for Shear

Figures 5.10 and 5.11 show the FE analysis (desired) outputs and best network outputs for all testing patterns. It is clear that the prediction of the best networks for 10 unseen patterns is quite satisfactory. As discussed before, the best network for moment yields maximum error of 3.36%, while the best network for shear yields

maximum error of 1.53% for these patterns under the defined network parameters. This indicates that the networks trained successfully establish the relationship between the bridge parameters and responses and interpolate this relationship for other bridges in the population with an acceptable accuracy. In addition, the coefficient of correlation (see Appendix A.2) between analytical and predicted outputs is 0.998 for moment and 0.956 for shear, indicating that the learning and generalization performance of the network is very good.

5.4 Sensitivity Analysis

Sensitivity analysis is a method for extracting the cause and effect relationship between the inputs and outputs of the network. The basic idea is that each input channel to the network is offset slightly and the corresponding change in the output is reported. To ascertain the influence of the input variables on output variables, sensitivity analysis is also carried out. This testing process provides a measure of the relative importance among the inputs of the neural model and illustrates how the model output varies in response to variation of an input. The first input is varied between its mean +/- a user-defined number of standard deviations while all other inputs are fixed at their respective means. The network output is computed for a user-defined number of steps above and below the mean. This process is repeated for each input. In this study, the number of standard deviations to add and subtract from the mean of an input is 1 and the number of steps to use on each side of the mean is 50. A report was generated which summarizes the variation of each output with respect to the variation in each input and presented in Figure 5.12 for moment and in Figure 5.14 for shear. In addition, a plot was created for each input showing the network output(s) over the range of the varied input. These plots are shown in Figure 5.13 for moment and Figure 5.15 for shear.

It can be clearly seen from the Figure 5.12 and 5.14 that the most important input parameter for moment is the bridge length, while the most important input parameter for shear is skew angle. The least important input for both is parapet.

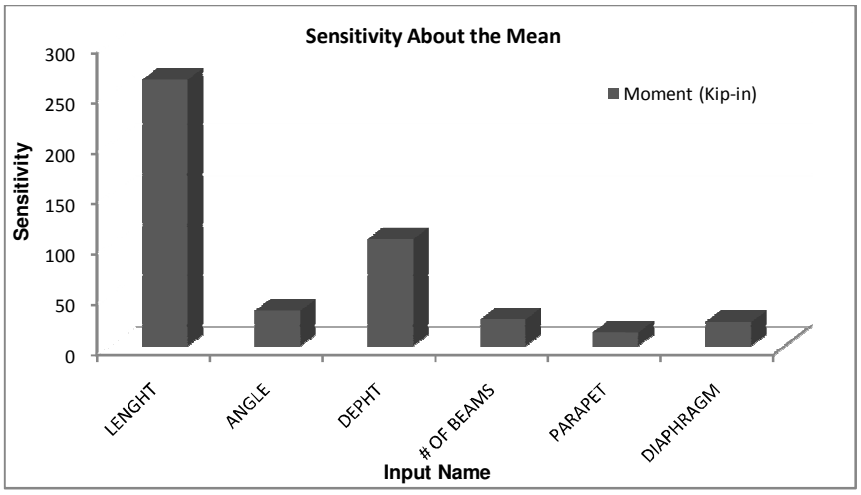

Figure 5.12 Variation of Moment w.r.t. the Variation in Each Input about Its Mean

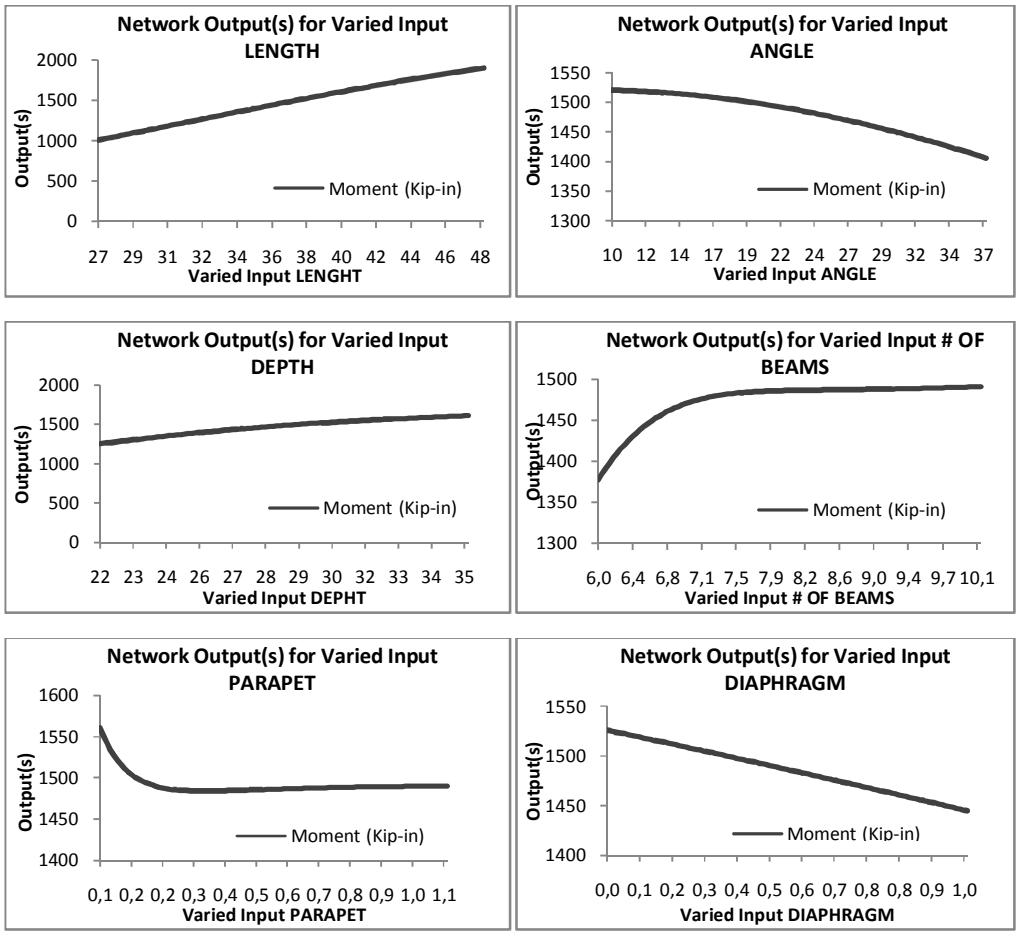

Figure 5.13 Plots Showing the Moment over the Range of the Varied Input

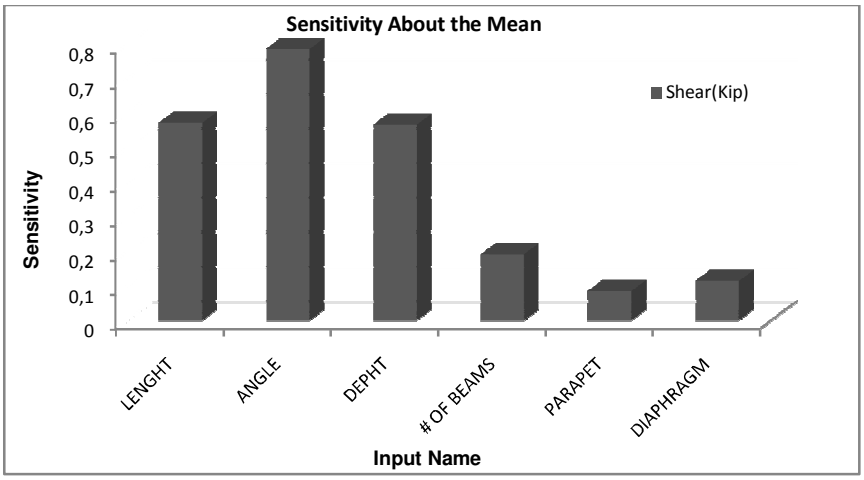

Figure 5.14 Variation of Shear w.r.t. the Variation in Each Input about Its Mean

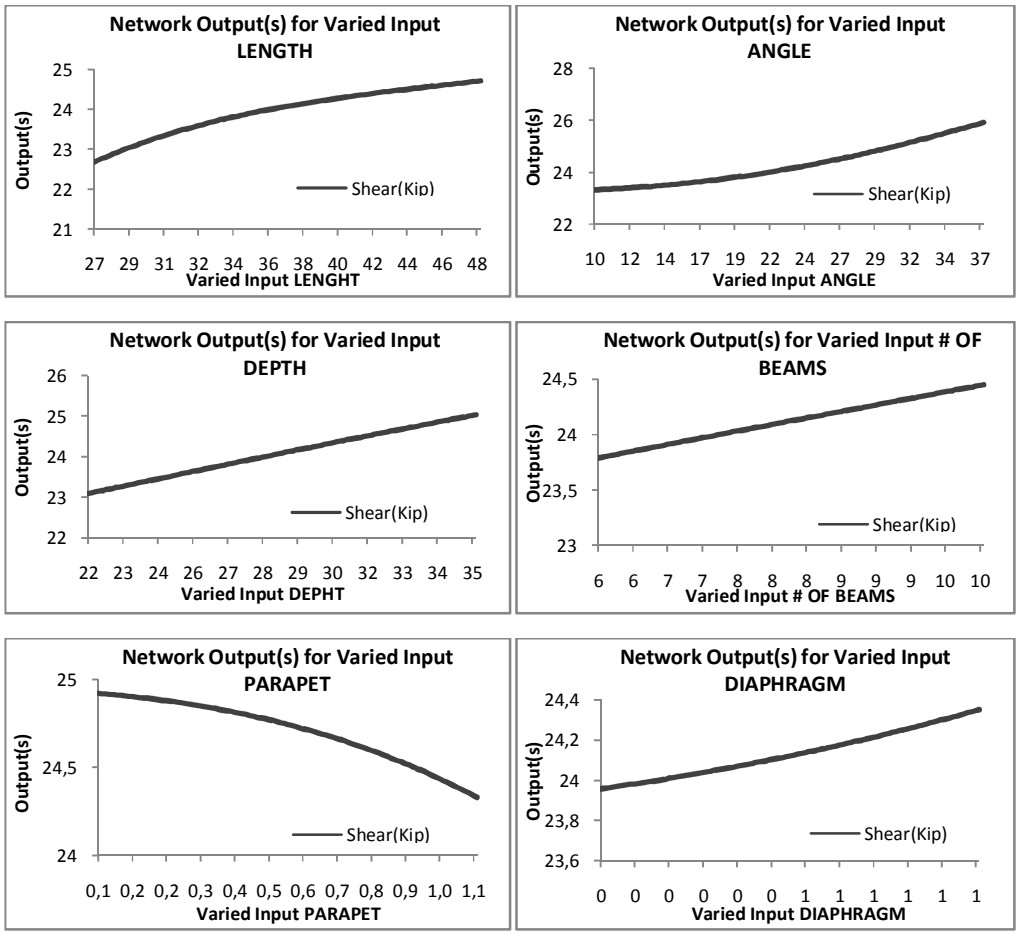

Figure 5.15 Plots Showing the Shear over the Range of the Varied Inputs

As it can be observed from Figure 5.13, moment increases with increasing span length, beam depth and the number of beam, while it decreases with increasing skew angle and existence of parapet and diaphragm. Similarly, Figure 5.15 illustrates that shear increases with increasing span length, skew angle, beam depth, the number of beam and presence of diaphragm while it decreases with the existence of parapet.

5.5 Discussion

The principal objective of this chapter is to show that artificial neural networks can be trained to predict critical structural responses of a population of bridges once governing structural and geometrical parameters are identified. Rapid and accurate analysis is essential, especially when a large population of bridges is concerned, and seems to be possible using ANN approach. This strategy was applied to single span T-beam bridge population in the Pennsylvania state. Common governing bridge parameters of the population were identified. Based on these parameters, a total of 140 representative T-beam bridges was randomly generated and modeled with the help of a standard FEM program and analyzed under HS20-44 trucks for critical moment and shear. Bridge set consisting of bridge parameters as inputs and bridge responses as outputs was divided into three subsets; the training set, the cross validation set and the test set. Based on these sets, we investigated the relationship between bridge parameters and bridge responses in different network designs. The results indicate that by selecting the right input parameters and properly constructing and training the ANN model, it is possible to reduce the differences between the FE analysis results and the ANN results to 3.36% for moment and 1.53% for shear. In addition, the linear coefficient of correlations very high between analytical data and values predicted through neural nets and it is 0.998 for moment and 0.956 for shear. These clearly show that the neural network methodology can be used efficiently to model the structural behavior of single span T-beam bridges. The main advantage of neural networks is that the analysis outputs can be obtained from the trained neural network within seconds without spending much effort and time required in constructing and analyzing of analytical models. Sensitivity

analyses with the trained neural net or during training could provide valuable additional information on the relative influence of various parameters on the bridge systems. From our results, it is obvious that networks are promising in analysis of civil structures and should be investigated further.

CHAPTER 6

CALIBRATION OF T-BEAM BRIDGES USING NEURAL NETWORKS

Structural identification is the process of developing and/or revising an analytical model of a structure such that for a given set of inputs the model can simulate the output response accurately. Structural parameter estimation, one area within the field of structural identification uses optimization to reconcile an analytical model of a structure with full-scale test data. The result is a set of estimated parameters capable of simulating "actual" structural response. Structural identification is an objective tool for condition assessment of structures. The current application is bridge condition assessment. By using structural identification and parameter estimation as a means of determining the actual state properties, performance, and limit states of a structure it is possible to gain an improved understanding of a structure's capacity and typical performance during serviceability. Thus, at any point in time it would be possible to assess the reliability of the structure using the objective results obtained through structural identification.

Today, analysis of very large structures with detailed discretization is possible even with personal computers. Models in each one of the numerical, modal or geometric spaces may contain any number of independent coordinates, representing a structure at different levels of discretization and detail. Moreover, numerical and geometric model spaces may accommodate various types of nonlinearity as well as non-stationarity. Yet there is a great need in civil engineering education, research and practice for emphasis upon the difference between modeling of an actual constructed facility for condition assessment, as opposed to modeling a non-existing one for design purposes. In particular, geometric models in the form of 3D FE models are constructed to assist with identifying the critical regions and behavior

mechanisms of a structure and to estimate the limits of the forces, strains, tilts, displacements and accelerations that may be necessary to measure. It is important that the models are calibrated through system-identification procedures to permit reliable simulations based on the data from a health monitoring implementation. The data needed for system identification of the structure and subsequent calibration of the FE model may be obtained from experiments conducted on the structure.

This chapter discusses the calibration of the finite element model of the Manoa Road Bridge, a typical T-beam bridge from the Pennsylvania's bridge population, based on field test data and neural networks. After a bridge is constructed, it may show significant variations in terms of its structural, geometrical and material properties. Therefore, a FE model should be updated considering the modified parameters of the structure. By this way, the ability of the model to simulate actual behavior is improved. This is called calibration. To calibrate a FE model, first field tests are conducted to collect experimental data, and next FE model is successively changed until the analytical response it produces correlates well with experimental data. Manual calibration of T-beam bridge models are also extremely time consuming and laborious. Therefore, a neural network- based solution strategy is investigated here for easy and practical calibration of these models. First a FE model of the Monoa Road Bridge is developed using the nominal structural parameters and material properties. Sensitivity studies are conducted next to determine the governing parameters affecting the dynamic and static response of the bridge, as well as to determine the sensitivity range of each parameter. Afterwards, a set of training patterns incorporating a selected number of bridge parameters and response are constituted by considering different values/combinations of these parameters generated randomly within their sensitive ranges. Neural network (NN) is then trained to learn the relationship between the bridge parameters and response in a reverse direction such that the inputs are the bridge response and outputs are the bridge parameters. After the training is completed, the field-measured bridge response is fed into the trained neural network system to predict the values of structural parameters representing the as-is condition of the bridge. Structural

parameters are then updated in the FE model in line with the predictions of ANN and the analytical response of the bridge is obtained analyzing the bridge under the predicted parameter set. A comparison between the experimental and analytical response of the bridge is conducted. If these two sets of parameters differ significantly, then the ANN model is retrained. The re-training procedure is continued until the measured and calculated responses do correlate well.

6.1 Bridge Description

The Manoa Road Bridge is a reinforced concrete structure located in E. Karakung Drive 26J07 in Pennsylvania. Its coordinates are 39°58′48″N and 78°16′54″W and is schematically shown in Figures 6.1. The typical cross section of deck is shown in Figure 6.2. The Manoa Road Bridge is 32 ft (9.75 m) long with a 15 degree skew, was constructed in 1929. It is 53 ft (16.55 m) wide and is supported by 11 T-beams, carrying two-way traffic. Each beam has a width of 61.5 in (1.5621 m) and depth of 28.5 in (0.7239 m). T-beam web width and deck thickness are 16.5 in (0.4191 m) and 8.5 in (0.2159 m), respectively. Total steel area in the tension region is 14.50 in^2 (93.55 cm^2). Secondary elements, such as diaphragms and parapets exist in the structure.

Figure 6.1 Manoa Road Bridge

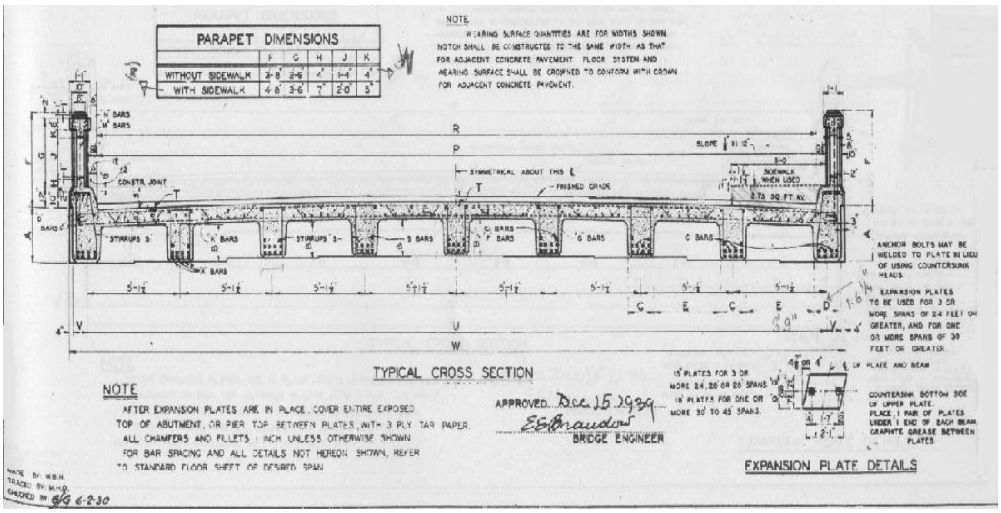

Figure 6.2 Typical cross section of the bridge deck

6.2 Field Investigations

DI3 researchers (DIITSI, 2003) conducted extensive field investigations and experiments on Manoa Road Bridge. The experimental studies included instrumentation and controlled load testing of selected bridges by stationary and crawling trucks and, dynamic testing by impact using an instrumented impact hammer. Researchers also explored possible uses of Falling Weight Deflectometer (FWD) as a practical test method to quantify bridges' as-is stiffness.

In dynamic tests, acceleration of the different points of the bridge due to an impact is recorded to extract dynamic properties of the structure (i.e. mode shapes, natural frequencies). Impact and accelerometer locations were determined prior to the test based on preliminary dynamic analysis of the structure. In controlled static truck load tests, two trucks were simultaneously positioned on the bridge. Truck positions were determined prior to the test in conjunction with the instrumentation plan. Each predetermined location corresponds to a load case, which can also be simulated in the FE model. Displacement data is separately recorded for each load case.

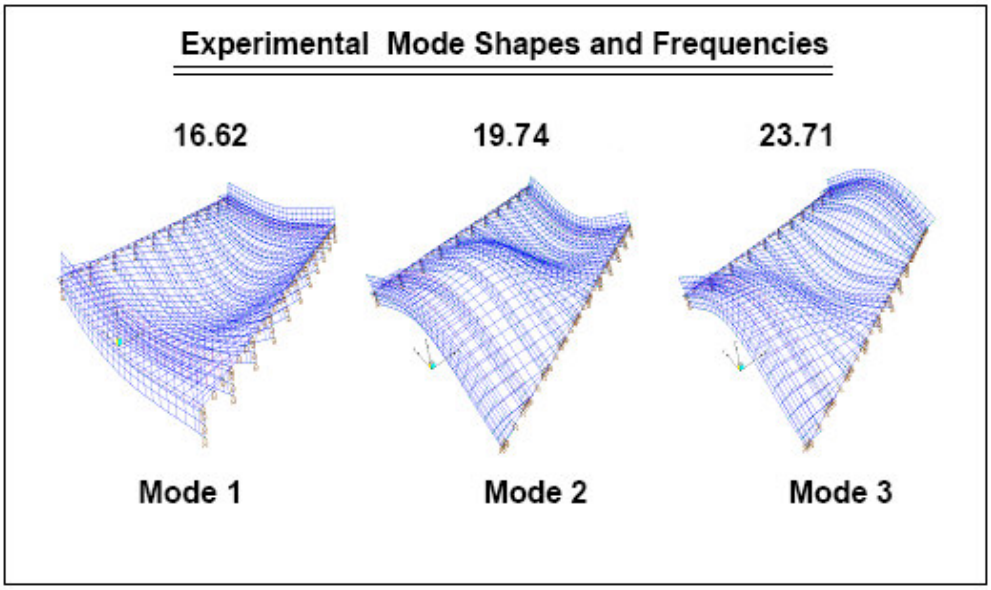

Figure 6.3 Dynamic Test Results of Manoa Road Bridge (DIITSI, 2003)

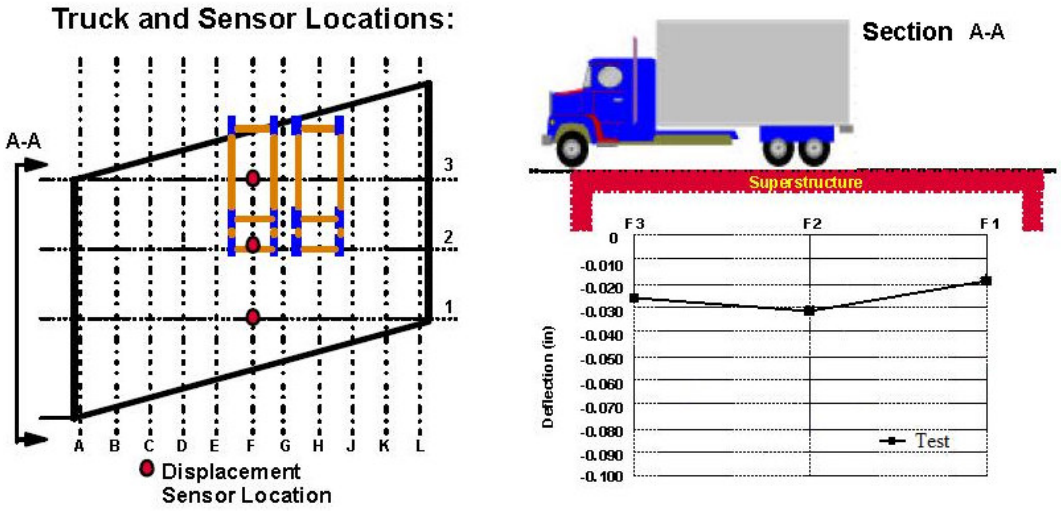

Figure 6.4 Deflections of the Beam "F" From the Field Test for Manoa Road Bridge

In this study, the measured response of the Manoa Road Bridge obtained from field tests is used for the calibration of the analytical model of the bridge. The measured response consists of the first three modes and natural frequencies of the bridge as illustrated in Figure 6.3 as well as the vertical displacements recorded at three locations along the length of the center beam as visualized in Figure 6.4.

6.3 Bridge Modeling

SAP2000 is used to model and analyze the Manoa Road Bridge. Accordingly, a 3-D numerical model of the Manoa Road Bridge is developed using the 9th version of the software. The key dimensions and geometry of bridge members were extracted from the plans. A typical 3D FE model that is constructed using solid elements and frame elements for a complete and accurate modeling of the geometry, detailing and material properties are illustrated in the example in Figure 4.7. Each reinforcing bar and its bond with concrete are explicitly simulated. Such a fine microscopic approach to 3D geometric -replica analytical modeling is now practical and enables explicitly simulating every material point of the bridge for an accurate representation of the geometry, the actual behavior mechanisms and any existing deterioration or damage.

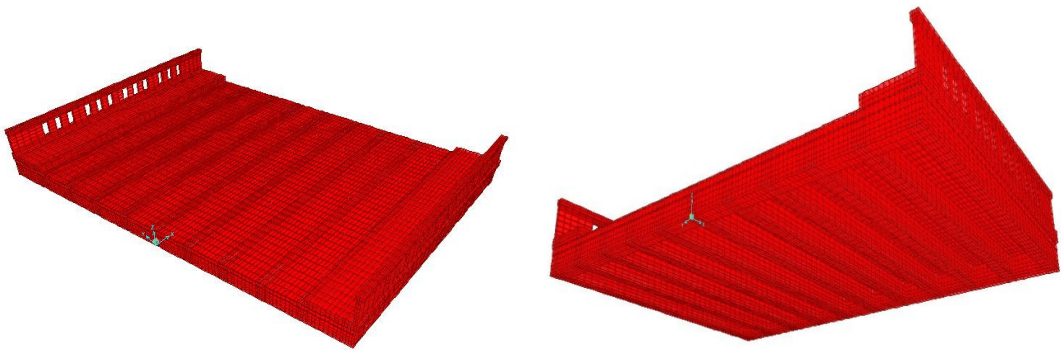

Figure 6.5 3-D Views of the Entire Bridge

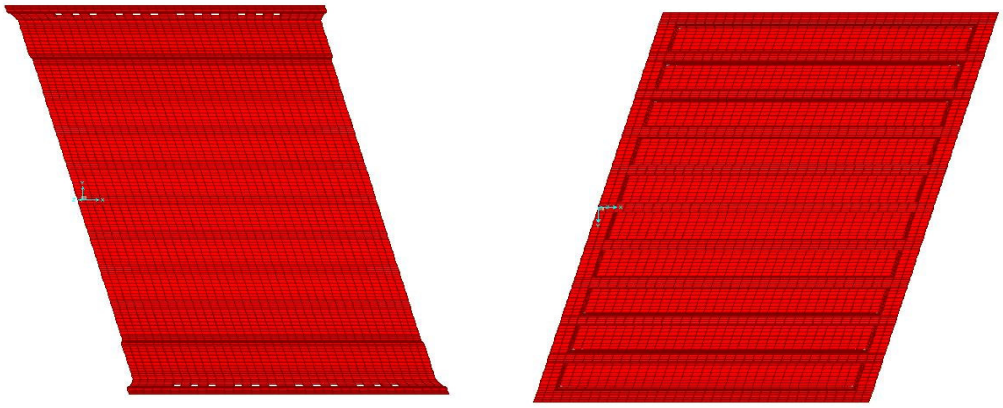

Figure 6.6 Top and Bottom Views of the Entire Bridge, respectively

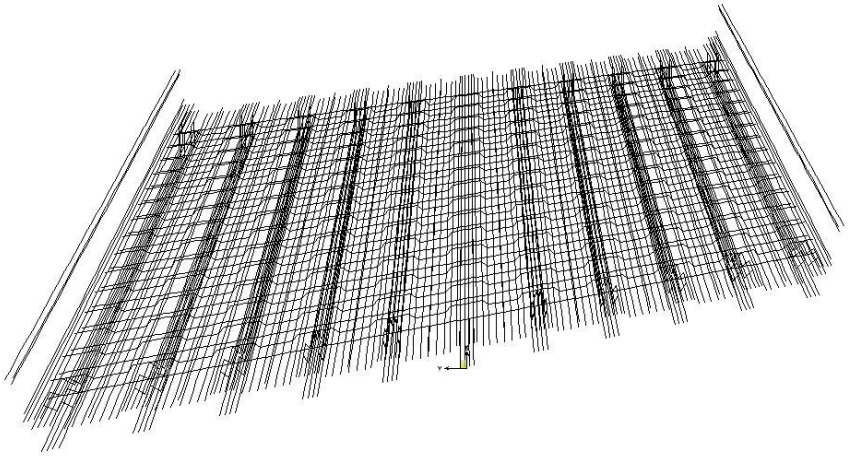

Figure 6.7 Reinforcement of the Entire Bridge

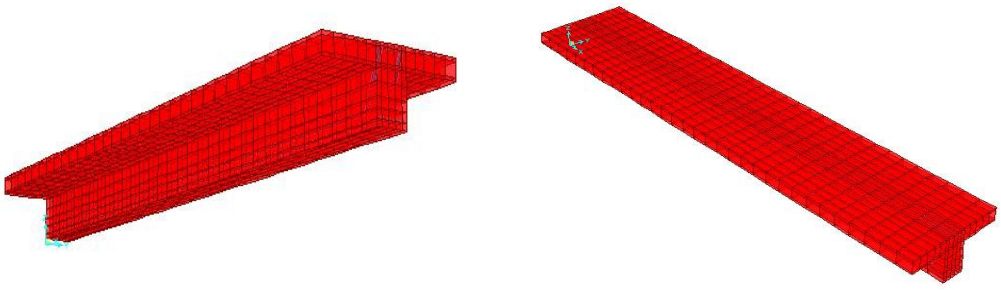

Figure 6.8 3-D Views of a Single T-Beam

Various outlooks of the Manoa Road Bridge model with explicit modeling of all main components are presented in Figures 6.5 to 6.8. The bridge was modeled based on the geometries and material data from as-built drawings. In the FE model, axial frame elements were adopted for reinforcement and solid elements were adopted for concrete. The complete FE model of the entire bridge has a total of 40935 joints, 12161 frame elements, 31060 solid elements, resulting in 154419 degrees of freedom. Both longitudinal and transverse steel reinforcing bars were modeled on a one-to-one basis using frame elements and connected to the solid elements simulating perfect bond. The parapets and lateral end diaphragm were modeled in detail. Boundary conditions were defined such that all the nodes on the superstructure-substructure interface at the ends of the bridge are modeled using linear springs. As observed during visual inspections, there are effective lateral restraints at the ends of the bridges due to earth pressure and pavement thrust. Therefore, the lateral earth pressure on the diaphragm beam is also simulated using linear springs. Thickness of asphalt overlay on top of the concrete deck is accounted for by distributing the total mass of the asphalt to the joints on the surface of the concrete deck.

6.4 Parametric Studies

Sensitivity studies are conducted to asses the governing bridge parameters affecting most the dynamic and static response of the structure, as well as to determine the sensitivity range of each parameter. These parameters are identified as the boundary conditions, elasticity of concrete, lateral soil pressure and the thickness of asphalt. Only the first 3 modes of vibration of the bridge are considered.

6.4.1 Boundary Conditions

The boundary conditions (BC) of an actual bridge are often complicated. Usually they are idealized as fixed, hinged or roller supports in the analytical models. The field tests by DI3 researchers revealed that friction and dowels between the stiff

lateral diaphragm beams of the superstructure and the beams on the abutments create a very effective restraint, prohibiting any slippage and other movements. Lateral soil pressure and pavement thrust further contribute to the restraint. In an effort to simulate this restraint in the analytical model, boundary conditions of the Manoa Road Bridge are simulated using linear springs in vertical and horizontal (lateral and longitudinal) directions as described in Figure 6.9 (a and b). In addition, the lateral earth pressure on the diaphragm beam is simulated using linear lateral springs as shown in Figure 6.9 (c).

In order to examine the influence of vertical, horizontal and lateral springs on the structural behavior of the bridge and determine the sensitive ranges of these parameters, each spring stiffness was set to the powers of ten and the first three natural frequencies of the bridge were calculated. For the different spring stiffness values, the calculated frequencies are plotted in Figures 6.10, 6.11 and 6.12. It can be seen that boundary conditions do have significant influences on the dynamic characteristics of the Manoa Road Bridge.

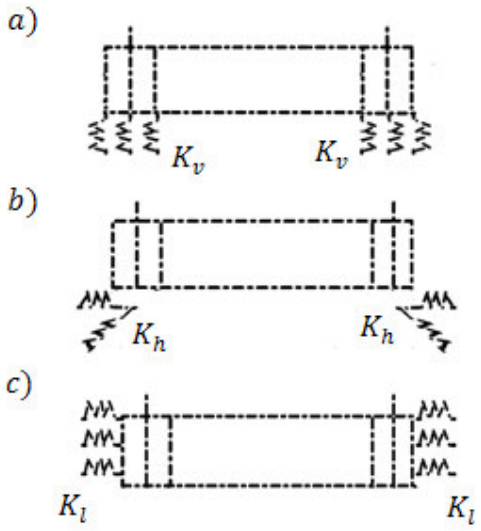

Figure 6.9 a) Vertical springs, b) Horizontal springs (lateral and longitudinal springs), c) Lateral spring due to soil pressure

As observed from Figure 6.10, the bridge response is sensitive to the variation of the vertical spring stiffness value between 0 and 10^5. However, the model produces very large vertical displacements which are not possible to observe in real structure for the range of 0 to 10^2. Hence, the sensitive range of this parameter is determined as [10^2, 10^5].

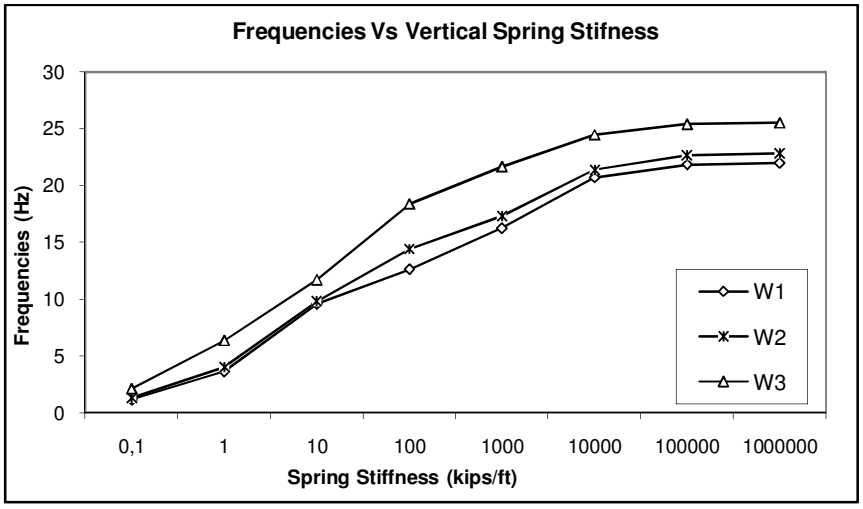

Figure 6.10 Frequencies versus Vertical Spring Stiffness

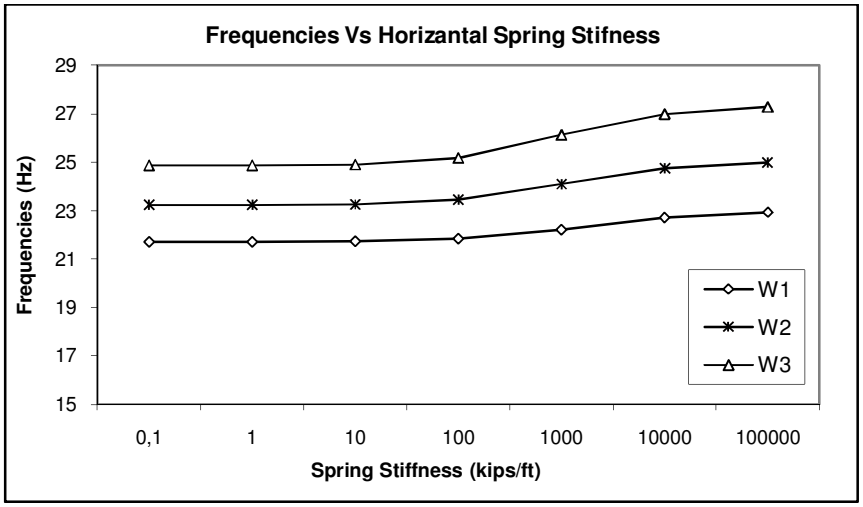

Figure 6.11 Frequencies versus Horizontal Spring Stiffness

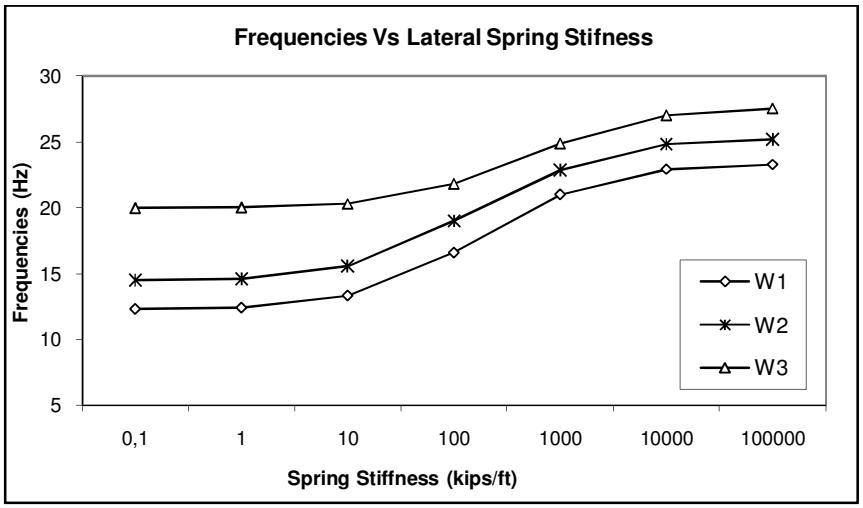

Figure 6.12 Frequencies versus Lateral Spring Stiffness

Based on the Figure 6.11, the bridge response is sensitive to the variation of the horizontal spring stiffness value between 10 and 10^5. However, very large horizontal spring stiffness reduces the flexibility of the model resulting in frequencies far larger than the ones observed in field test. Hence, the sensitive range of this parameter is set to be between [10, 10^4]. Similarly, from Figure 6.12, the bridge response is sensitive to the variation of the lateral spring stiffness value between 0 and 10^4. Hence, the sensitive range of this parameter is determined as [0, 10^4].

While generating the training set for Neural Networks, spring stiffness is expressed only in powers (of 10) so that the parameters are uniformly distributed within their sensitive ranges. For example, vertical spring stiffness is varied from 2 to 5 in the training set.

6.4.2 Modulus of Elasticity of Concrete

The modulus of elasticity of concrete plays an important role in the dynamic characteristics of the RC T-Beam bridges. It can be said that any increase in modulus of elasticity of concrete structures results in an increase in the natural frequencies of the bridge due to the stiffened structure. Therefore, it was taken as one of the parameters that significantly affect the modal parameters of the structure. Based on the field tests and the reduced elasticity modulus for concrete to account for the deterioration, the range of variation of this parameter is assumed to be between 800-4000 ksi in analytical modeling and ANN studies.

6.4.3 Thickness of Asphalt

In the FE modeling of the Manoa Road Bridge, the presence of the asphalt directly affects the mass of the bridge and thus its dynamic properties. Therefore, thickness of asphalt overlay on top of the concrete deck should also be considered in the modeling to completely reflect the dynamic characteristics of the system under study. When the asphalt thickness in Pennsylvania's RC T-beam bridge population is statistically analyzed using NBI Data, it has been found that it varies between 0 and 12 inch. Accordingly, the range of variation of this parameter is assumed to be 0-12 in the analytical model and ANN studies.

6.5 Mode shape verification

Modal analysis in structural dynamics is aimed to determine the natural frequencies and mode shapes of a structure and evaluate its responses under dynamic loading. In most cases, only a small number of lowest vibration modes dominate the responses of an engineering structure. In the present study, only the first three modes were used. However, these three modes may not appear the same under all parameter values of the bridge. The modes may switch or vanish, or in some cases new modes may appear in a modal analysis of a bridge based on it vibration characteristics governed by the assigned parameter set. For example, low values of horizontal

stiffness (K_h) introduce a new mode as the first mode of the system, shifting the first three modes of the nominal model. Therefore, it is essential to compare the mode shapes of natural frequencies using the so-called Modal Assurance Criterion (MAC) to ensure about the equivalence of modes between different models. MAC, a coefficient lying in a range between 0 and 1, is used to quantify the similarity between two mode vectors (Equation 6.1). A zero MAC indicates no correlation, whereas 1 indicates the highest correlation (i.e., identical vectors). It is important to mention that it correlates the two modes based on their shapes only, not on their magnitudes. As an example, the MAC values for a model in the training set are presented in Table 6.1. The values on the diagonal are ones, implying that the mode shapes are the same, and of the same order. Zero terms on off diagonal terms show that the mode shapes are orthogonal to each other.

$$MAC_{jk} = \frac{(\{\varphi_j\}^T\{\varphi_k\})^2}{(\{\varphi_j\}^T\{\varphi_j\})(\{\varphi_k\}^T\{\varphi_k\})} \tag{6.1}$$

where $\{\varphi_j\}$ is the j^{th} mode shape obtained from the FE model and $\{\varphi_k\}$ is the k^{th} mode shape identified from the measured accelerations.

Table 6.1 Comparison of Mode Shapes between Analytical and Experimental Results

		Experimental Modes					
		1	**2**	**3**	**4**	**5**	**6**
Analytical Modes	**1**	**0,997**	0,001	0,063	0,001	0,022	0,018
	2	0,005	**0,994**	0,001	0,084	0,000	0,001
	3	0,070	0,003	**0,997**	0,003	0,248	0,078
	4	0,002	0,124	0,003	**0,994**	0,013	0,173
	5	0,028	0,001	0,348	0,011	**0,992**	0,524
	6	0,018	0,000	0,083	0,293	0,404	**0,978**
	Max	**0,997**	**0,994**	**0,997**	**0,994**	**0,992**	**0,978**

6.6 Neural Network Modeling

6.6.1 Training Patterns

Based on the results of sensitivity analyses, five parameters have been identified as having significant impact on the static and dynamic properties of a T-beam bridge. Assigning random values to these parameters within their specified ranges, a total of 121 FE model of the Manoa Road Bridge were created individually with the aid of SAP 2000 program to generate the necessary training patterns (see Appendix C for the training data set). To obtain the static response (deflections) of the bridge analytically, two dump trucks with tandem-axle loads of 40 Kips–55 Kips per truck are simulated in all the FE models in line with actual field tests. After performing modal and static analysis of each model, first three natural frequencies were recorded considering Modal Assurance Criterion (MAC) and simulated deflections were taken at three predefined locations along the middle T-beam (Appendix C). This set was reversed to train the ANN model due to inverse nature of the problem. Frequencies and deflections are used as the inputs of the network, and the outputs are the structural parameters to be updated in the analytical model.

6.6.2 Neural Networks Model

The successful application of neural networks to a specific problem depends on two factors, namely representation and learning. Choice of an appropriate network topology and training parameters are problem-dependent and are usually determined by trial and error in the back-propagation learning algorithm. After a number of trials in NeuroSolutions 5, appropriate values of the network parameters are set as follows:

- Number of training examples = 121;
- Number of input layer neurons = 3 for Model 1 and 6 for Model 2
- Number of output layer neurons = 5

- Type of back-propagation = Levenberg-Marquardt back-propagation
- Activation function = Sigmoid function
- Normalization range = [0.2,0.8]
- Learning rate = 0,01
- Training mode = Batch mode

Based on the above network parameters, extensive study on one and two hidden layers networks was carried out and it was found that a single hidden layer with an optimum number of neurons is sufficient for modeling of this problem.

- Number of hidden layer = 1

The number of nodes in the hidden layer was varied from 4 to 15 in Neuro Solutions 5 to determine the optimum number of nodes in the hidden layer. Optimum number of nodes was found to be 9.

- Number of hidden layer neurons = 9

The architecture of the network is shown in Figure 6.13.

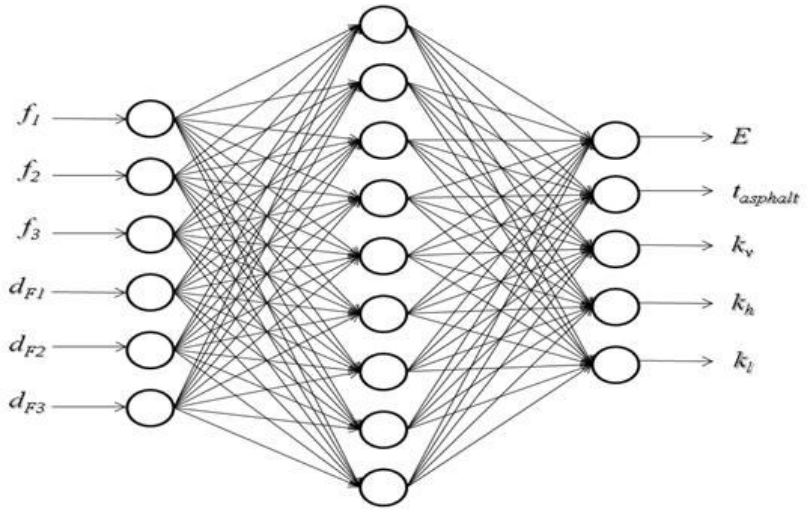

Figure 6.13 ANN Model for Calibration of Manoa Road Bridge

ANN Model

In the ANN model, the first three natural frequencies and three deflection values taken along the middle beam of the bridge (Beam F, Figure 6.4) were used as inputs to the network to predict the five output parameters to be updated in analytical model. The network was trained with the training set generated through linear analysis of analytical model and the desired outputs have been reached at 10^{th} epochs with average MSE value of 0.0124112. The error measurement indicates that the error has been reduced to an acceptable level. The field-measured data set, which consists of the first three natural frequencies and three deflection values, was presented to the trained network to obtain the predicted values of the structural parameters (Table 6.2). The second row in Table 6.2 shows the predicted values of the structural parameters. To validate the prediction of ANN based calibration procedure, the FE model of the Manoa Road Bridge was updated with the predicted values of the bridge parameters, and a modal as well as static analysis of the bridge was carried out in SAP2000 under this parameter set to obtain the analytical frequencies and deflections. The third row in Table 6.2 shows the calculated deflections and frequencies of the bridge.

Table 6.2 Calibration of Manoa Road Bridge (Linear Analysis of the Model)

Freq. and Dis. or Properties	f_1 (Hz) E (ksi)	f_2 (Hz) $t_{asphalt}$ (in)	f_3 (Hz) k_v (kips/ft)	d_{F1} (in) k_h (kips/ft)	d_{F2} (in) k_l (kips/ft)	d_{F3} (in)
Measured Freq. and Dis.	16.62	19.74	23.71	0.019	0.032	0.024
ANN Model			↓			
Properties	3364	6	1172	86	47	
SAP 2000			↓			
Calculated Freq. and Dis.	17.88	19.58	21.35	0.0216	0.0419	0.0254
Relative Error (%)	7.58	0.81	9.95	13.68	30.93	5.83

The results indicate that by using this ANN model, it is possible to reduce the differences between the measured and the calculated frequencies to less than 10% for the first three modes and to reduce the measured and the calculated deflections to less than 31% for the deflections along the central T-beam.

Although computed natural frequencies of the 3-D FE model agree well with those from field measured data, significant differences exist between the computed and the measured values of deflections. Therefore, the training set was re-generated considering that concrete does not carry tension forces. In each model of the training set, solids subjected to tension were assigned zero elasticity to prevent concrete from carrying tensions. As a result, analysis results of training patterns have been generated through non-linear analysis of the analytical model.

The same parameters (first three natural frequencies and three deflection values taken along the middle beam) were again used as inputs to the network to predict the five output parameters to be updated in analytical model.

Table 6.3 Calibration of Manoa Road Bridge (Nonlinear Analysis of the Model)

Freq. and Dis. or Properties	f_1 (Hz) E (ksi)	f_2 (Hz) $t_{asphalt}$ (in)	f_3 (Hz) k_v (kips/ft)	d_{F1} (in) k_h (kips/ft)	d_{F2} (in) k_l (kips/ft)	d_{F3} (in)
Measured Freq. and Dis.	16.62	19.74	23.71	0.019	0.032	0.024
ANN Model			↓			
Properties	3262	6	11985	1279	9	
SAP 2000			↓			
Calculated Freq. and Dis.	17.59	19.60	21.62	0.0178	0.0329	0.0213
Relative Error (%)	5.83	0.71	8.81	6.31	2.81	11.25

Using the same network parameters and architecture, the network was trained with the training set generated through non-linear analysis of the analytical model. The desired outputs were reached at 14^{th} epochs with average MSE value of 0.0060617. The error is relatively good compared the previous one. The field-measured data set, which consists of the frequencies and deflections of the Manoa Road Bridge, was fed into the trained neural network system to obtain the predicted values of bridge parameters (Table 6.3). The second row in Table 6.3 shows the predicted values of the bridge parameters. To validate the prediction of ANN based calibration procedure, the FE model of the Manoa Road Bridge was updated with the predicted values of the bridge parameters, and a modal as well as static analysis of the bridge was carried out in SAP2000 under this parameter set to obtain the analytical frequencies and deflections. The third row in Table 6.3 shows the calculated frequencies and deflections of the bridge.

A comparison of measured and calculated frequencies indicates that they do differ from each other only by 5.83 % for the first mode, 0.71 % for the second mode and 8.81 % for the third mode. A comparison of measured and calculated deflections caused by the truck loads indicates that the results of the calibrated model based on predicted bridge parameters may differ from the measured deflections by 0 to 12 %. The differences are all within tolerable limits, validating a successful prediction of the bridge parameters by neural networks.

6.7 Discussion

The purpose of this study was to demonstrate the applicability of neural network technique in prediction of the structural parameters to be updated in calibration of analytical models. Parametric sensitivity analyses are first performed in order to identify those parameters that significantly affect the dynamic and static properties of the T-beam bridges. After the structural parameters are assessed, a set of training samples are generated in such that these training samples should cover all possible combinations and ranges of parametric variation to ensure that the ANN models trained using these patterns can accurately represent the structural behavior.

Training patterns were processed by the network to establish implicit relationship between the inputs (modal parameters, deflections) and the outputs (structural parameters). Several network designs were examined, and 6-9-5 architecture with defined network parameters was identified to have a reasonable performance. The network first trained with the training set generated through linear analysis of the analytical model and desired outputs were reached at 10^{th} epochs with an average MSE value of 0.0124156. The maximum difference between the measured and the calculated frequencies for the first three modes appeared to be less than 10%. Calculated and measured deflections differ from each other as much as 31%. Then, the training set was re-generated considering that concrete does not carry tension forces. The network was trained with this training set which has been generated through non-linear analysis of the analytical model and desired outputs were reached at 14^{th} epochs with an average MSE value of 0.0060617. The maximum difference between the measured and the calculated frequencies for the first three modes is less than again 9%. However there is a significant improvement in deflections. The maximum difference between measured and the calculated deflections along the central T-beam were reduced from 31% to 12% indicating that T-beam bridges should be calibrated by taking into account the non-linear behavior of concrete.

Due to possible errors, uncertainties and discrepancies between the experiment and the analytical model, a "100% match" should not expected, hence it can concluded that the calibration of the bridge is achieved to the point that computed natural frequencies of the 3-D FE model agree well with those from field measured data. For deflections, however, slight differences exist between the computed and the measured values.

This study show that, a neural network (NN) can be trained to learn the pattern between the output and input data sets of an analytical model in reverse direction. Preparing input and output data sets for such a neural network would take considerable amount of time; however, once a neural network is successfully trained, the same system can be used efficiently and quickly for calibration of other

bridge models. The field-measured data set, which has the same format with the selected analysis output parameters, can be fed into the trained neural network system obtaining the proper input parameter that should be used in the analytical model. Following the testing of a bridge, the proper parameters to construct a calibrated analytical model can be obtained from the trained neural network within seconds.

CHAPTER 7

A RAPID CALCULATION OF LOAD RATING OF T-BEAM BRIDGES BASED ON FE MODEL AND NEURAL NETWORKS

Bridge load rating is a component of the inspection process and is used to determine the safe-load carrying capacity of the bridge. AASHTO recommends the use of a simple and practical method for rapid evaluation of load rating capacity of T-beam bridges. In this method, an individual beam is taken out as a free-body, idealized as simply-supported, and the continuity of the bridge in the transverse direction is indirectly accounted for by means of axle-load distribution factors. This approach is found to significantly underestimate the deck slab's contributions to lateral load distribution for many bridge geometries. A more accurate evaluation of load rating capacities of T-beam bridges is possible through a properly constructed, geometric replica 3D FE model since the contribution of slab is properly simulated by the model. Besides, the secondary components such as the contributions of parapets and diagrams can be accounted for. FE based method is quite a reasonable and advantageous method for load rating analysis of a single bridge. However, as far as load rating analysis of a population of bridges is concerned, the method is not practical, and computationally unmanageable due to the development of FE model of each bridge in the population. In this chapter, we develop a method based on the use of neural network and FE model together for rapid and accurate load rating analysis of a population of bridges. 104 T-beam bridge models constructed in Chapter 5 were used to generate necessary data for the training of ANN. The maximum shear and moment (demand) developed under different values of the governing parameters set (the span length and skew angle, width of bridges, beam depth and existence of reinforced parapets and end diaphragms) are recorded. After calculating the capacity of each bridge model, the load ratings are calculated with the aid of a spreadsheet program using the capacity and demand of the bridge. The training

data is prepared such that inputs are the bridge parameters and outputs are the shear and moment load rating. ANN is trained to learn this relationship in order to speed up the accurate load rating of these bridges while still strictly conforming to the AASHTO standards and provisions.

7.1 AASHTO Load Rating

The AASHTO contains simplified procedures to be used in the analysis and design of bridges. The analysis of a bridge superstructure is reduced to the analysis of single member with the introduction of wheel load distribution factors (Figure 7.1).

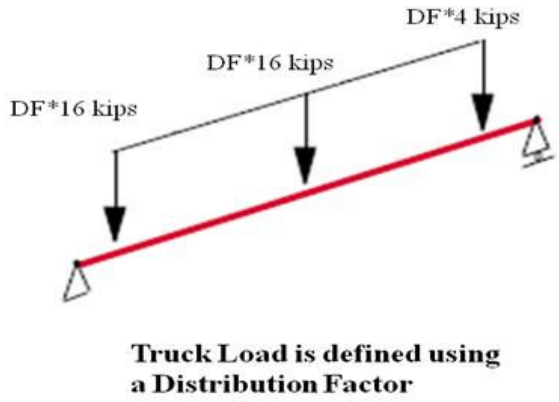

Figure 7.1 AASHTO Modeling a T-beam Bridge with HS20 Truck Loading for Load Rating

In order to load rate a bridge, AASHTO utilizes a rating factor. The rating factor (RF) is a scaling number used as a multiplier of the loading used in determining the live load effects. According to AASHTO Manual for Condition Evaluation of Bridges (1994 and updated interims), each highway bridge is rated at two levels: Inventory and Operating. The inventory rating level corresponds to the customary

design level of stresses but reflects the existing bridge and material conditions with regard to deterioration and loss of section. Operating rating level generally describe the maximum permissible live load to which the structure may be subjected. Essentially, the inventory level represents the capacity of a bridge for normal traffic, whereas the operating level corresponds to an occasional oversized load.

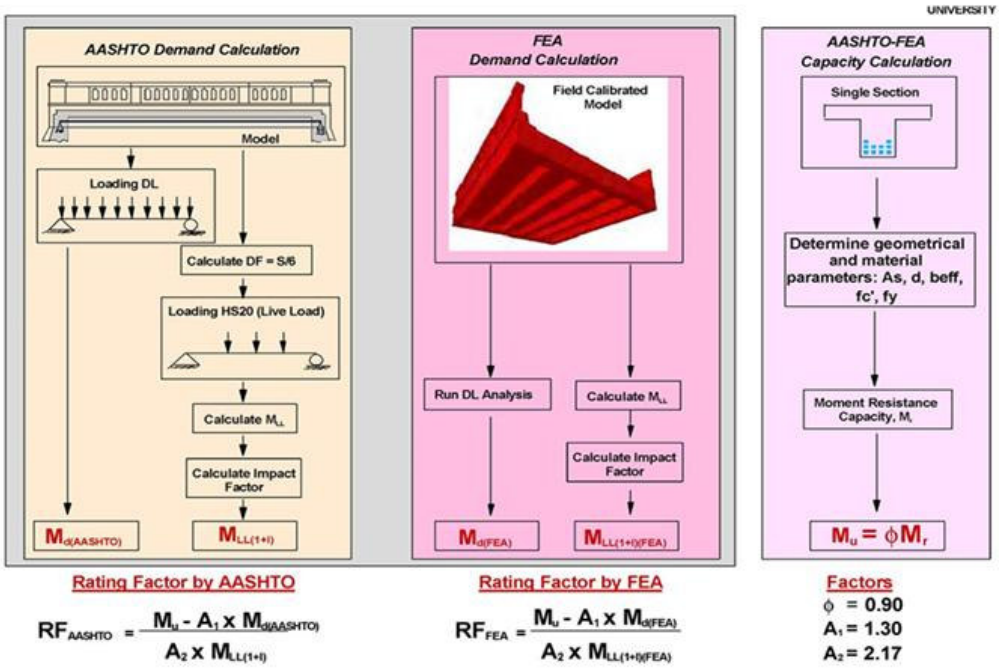

Figure 7.2 Rating Flowchart for Moment

AASHTO uses the following expression in determining the load rating of a structure. Figure 7.2 summarizes the AASHTO based bridge rating procedure.

$$RF = \frac{C - A_1 * DL}{A_2 * (1 + I) * DF * LL} \tag{7.1}$$

where

RF = Rating Factor

C = Member Capacity

DL = Dead Load Effect

LL = Live Load Effect

A_1 = Dead Load Factor

A_2 = Live Load Factor

I = Impact Factor

DF = Distribution Factor

The impact factor is a multiplier on live load intended to account for the dynamic effects of vehicles. To account for distribution of the load to adjacent members by the slab, AASHTO uses what is known as a distribution factor (DF). The distribution factor greatly affects a beam design or rating because it determines the percentage of vehicular load (moment or shear) that must be carried by the beam. Since their inception, these distribution factors have evolved or changed very little. These distribution factors have been criticized for being overly conservative.

In the AASHTO 2007 LRFD specifications for the T-beam bridges, the distribution factors are defined as a function of the spacing, span length, girder stiffness and slab thickness (Equation 7.2, 7.3, 7.5 and 7.6). In addition, there are modification factors for skewed bridges in the LRFD specifications (Equation 7.4 and 7.7).

Moment distribution factor for an interior beam with two or more design lanes loaded using Table S4.6.2.2.2b-1.

$$DF = 0{,}075 + \left(\frac{S}{9{,}5}\right)^{0{,}6} * \left(\frac{S}{L}\right)^{0{,}2} * \left(\frac{K_g}{12*L*t_s{}^3}\right)^{0{,}1} \qquad (7.2)$$

Moment distribution factor for an interior beam with one design lane loaded using Table S4.6.2.2.2b-1.

$$DF = 0{,}06 + (\frac{S}{14})^{0{,}4} * (\frac{S}{L})^{0{,}3} * \left(\frac{K_g}{12 * L * {t_s}^3}\right)^{0{,}1} \quad (7.3)$$

According to S4.6.2.2.2e, a skew correction factor for moment may be applied for bridge skews greater than 30 degrees.

$$SC = \left[1 - 0{,}25 * \left(\frac{K_g}{12 * L * {t_s}^3}\right)^{0{,}25} * (\frac{S}{L})^{0{,}5} * (\tan(\theta))^{1{,}5}\right] \quad (7.4)$$

Shear distribution factor for an interior beam with two or more design lanes loaded using Table S4.6.2.2.3a-1.

$$DF = 0{,}2 + \left(\frac{S}{12}\right) - \left(\frac{S}{35}\right)^2 \quad (7.5)$$

Calculate the shear distribution factor for an interior beam with one design lane loaded using Table S4.6.2.2.3a-1.

$$DF = 0{,}36 + \left(\frac{S}{25}\right) \quad (7.6)$$

According to S4.6.2.2.3c, a skew correction factor for support shear must be applied to the distribution factor of all skewed bridges. The value of the correction factor is calculated using Table S4.6.2.2.3c-1

$$SC = 1 + 0{,}2 * \left(\frac{12 * \mathrm{L} * \mathrm{t_s}^3}{\mathrm{K_g}}\right)^{0,3} * \tan(\theta) \quad (7.7)$$

The load ratings for 104 representative bridges from the AASHTO based analysis results are given in Appendix D.1. Appendix D.2 illustrates an example for load rating using AASHTO.

7.2 FE Based Load Rating

The additional reserve capacity and conservatism in load rating for T-beam bridges are recognized by DI3 engineers and researchers (DIITSI, 2003). There are several mechanisms that contribute to the load rating of bridges. Identifying the individual effects of those mechanisms is crucial for evaluation of the current rating process. For instance, additional capacity is brought by the existence of reinforced parapets or end diaphragms. In addition, it is possible to reflect some additional load capacity by only proper 3D modeling and still complying with AASHTO rating procedures. Figure 7.3 illustrates how two HS20 truck loads are defined for the 3D FE models for load rating. Truck loads are defined without any distribution factors.

Following expression can be used in determining the FEM based load rating of a structure. Rating calculation procedure by FE analysis is summarized in Figure 7.2.

$$RF_{FEM} = \frac{C - A_1 * DL_{FEM}}{A_2 * (1 + I) * LL_{FEM}} \quad 7.8$$

where

RF_{FEM} = FEM Based Rating Factor

C = Member Capacity

DL_{FEM} = FEM Based Dead Load Effect

LL_{FEM} = FEM Based Live Load Effect

A_1 = Dead Load Factor

A_2 = Live Load Factor

I = Impact Factor

Due to having three dimensional FEM, no distribution factor (DF) is incorporated.

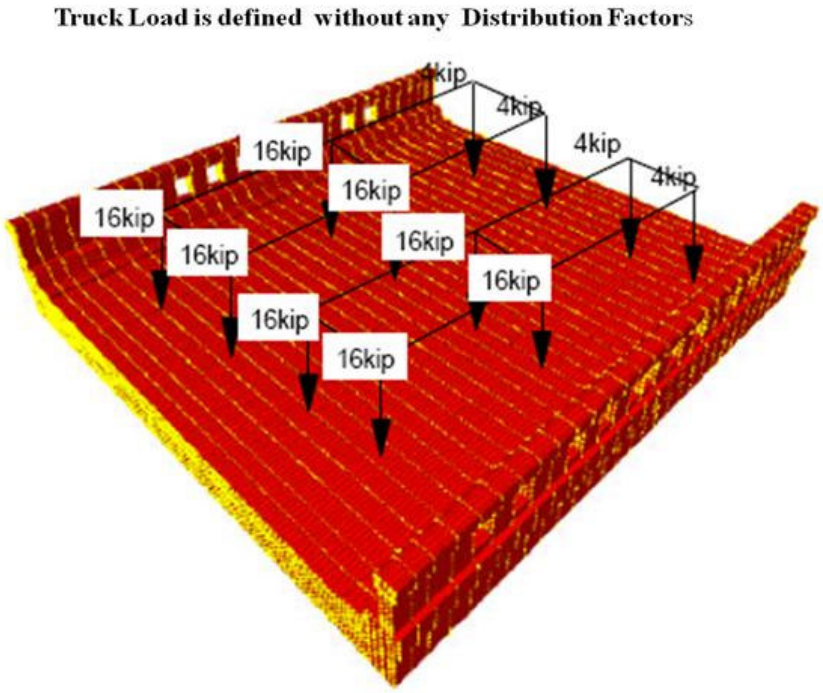

Figure 7.3 FE Modeling a T-beam Bridge with HS20 Truck Loading for Load Rating

FE based method is quite a reasonable and advantageous method for load rating analysis of a single bridge. However, as far as load rating analysis of a population of bridges is concerned, the method is not practical, and computationally unmanageable due to the development of FE model of each bridge in the

population. The load ratings for 104 representative bridges from the FE model analysis results are given in Appendix D.1. Appendix D.2 illustrates an example for load rating using FE model.

7.3 Network Modeling of FE Based Bridge Ratings

7.3.1 Bridge Data

The bridge data is prepared such that inputs are the bridge parameters identified in statistical analysis in Chapter 5 and outputs are the FEM based bridge load ratings (Inventory ratings, IR). As a result of statistical analysis, the numbers of governing independent bridge parameters are establish as only the span length and skew angle, width of bridges, beam depth and existence of reinforced parapets and end diaphragms. These parameters are used as inputs to the network. The outputs are the moment and shear load ratings obtained as discussed in previous section. In this study, the bridge data is used to establish intrinsic relationships between the bridge parameters and corresponding load ratings to speed up the FE based load rating analysis. Bridge data consisting of 104 T-beam bridges is given in Appendix D.1. Of these bridges, 75 have been assigned to training, 19 as cross-validation and 10 as test patterns in neural network modeling.

7.3.2 Neural Network Modeling

As mentioned before, the success of networks depends on network parameters and the topology. Appropriate values of the network parameters are set as follows:

- Number of training examples = 75
- Number of cross-validation examples = 19
- Number of test examples = 10
- Number of input layer neurons = 6
- Number of output layer neuron = 2
- Type of back-propagation = Levenberg-Marquardt back-propagation
- Activation function = Sigmoid function

- Normalization range = [0.2,0.8]
- Learning rate = 0,01
- Training mode = Batch mode
- Termination rule = minimum cross validation error or maximum epoch

Several architectures are tested in conjunction with the above set of network parameters to find the one having the best prediction performance. This is a similar process that is carried out in Chapter 5. A typical architecture is designated as "input nodes (n) - [hidden nodes per hidden layer (m)]-output nodes (p)". Six bridge parameters (the span length and skew angle, width of bridges, beam depth and existence of reinforced parapets and end diaphragms) form the inputs of the network and moment and shear load ratings are considered as network output. The following cases are created and studied with respect to the choice of network architecture

Case 1: Network 6-(m)-2; m varies from 4 to 12

In case 1, the architecture has one hidden layer with m nodes denoted as 6-(m)-2.

Case 2: Network 6-(m-m)-2; m varies from 4 to 12

In case 2, the architecture has two hidden layers with m nodes per layer denoted as 6-(m-m)-2

In the current study, the network performance is associated with the maximum error in load rating prediction of the network for all the testing patterns. If the maximum testing error appears to be below the tolerable level, then the performance of network is considered satisfactory. The results of the study on different network designs are shown in Figure 7.4.

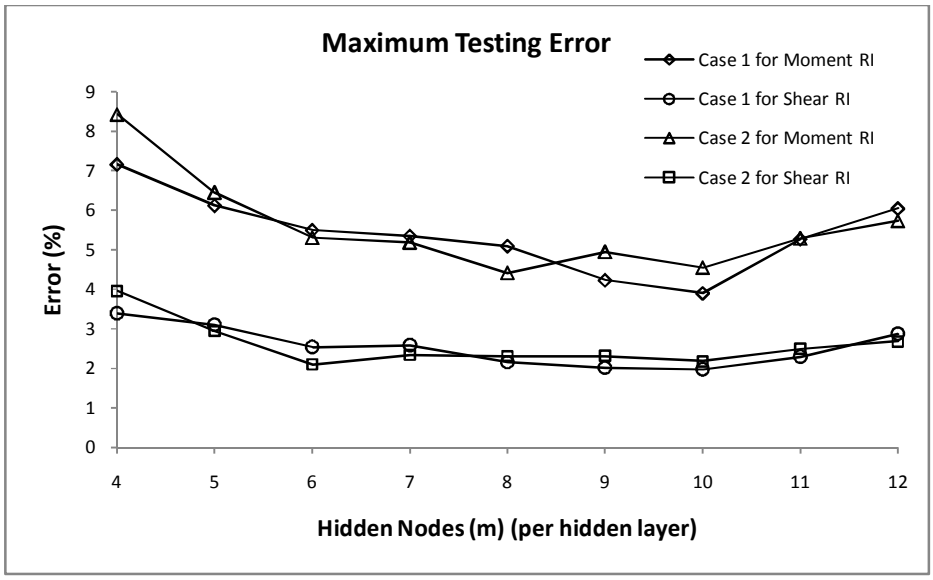

Figure 7.4 Maximum Testing Errors versus Number of Nodes in Hidden Layer(s)

It can be seen from this figure that ANN is quite useful in predicting load ratings. All the trained networks are able to predict the load ratings for all the testing patterns with a reasonable accuracy. Predictive performance of the network may be improved depending on the number of nodes in the hidden layer(s) and the number of hidden layers. A single hidden layer with an optimum number of neurons is sufficient for modeling of this problem. As seen from the Figure 7.4, the best performance in predicting load ratings is shown by Case 1 with a ten nodes, resulting in 3.89% maximum average testing error for moment load ratings and 1.97% maximum average testing error for shear load ratings for all testing patterns.

Best ANN Model

The predictive performance of the 6-10-2 architecture is better than other architectures. The neural network is presented in Figure 7.5.

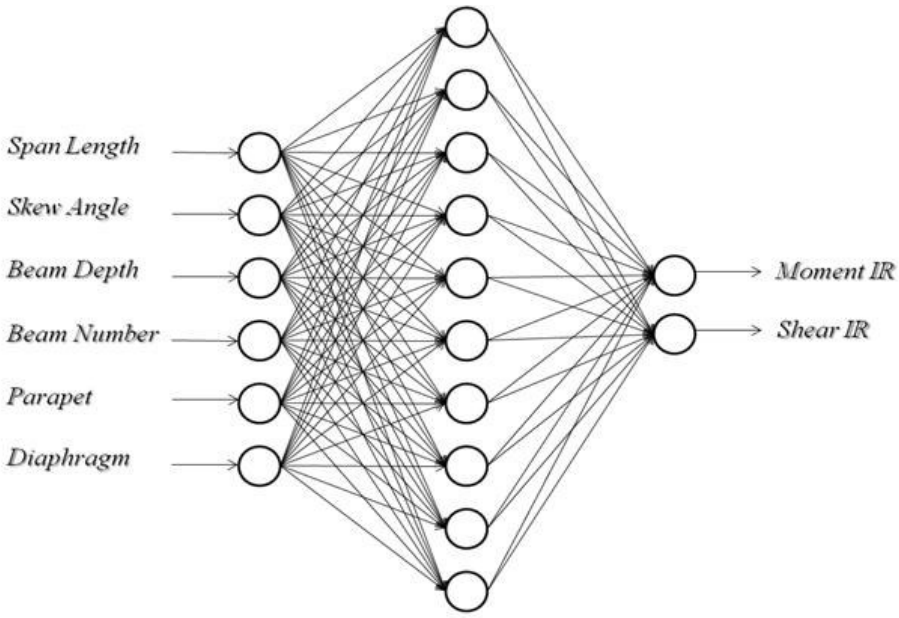

Figure 7.5 ANN Model for the Prediction of Inventory Load Ratings

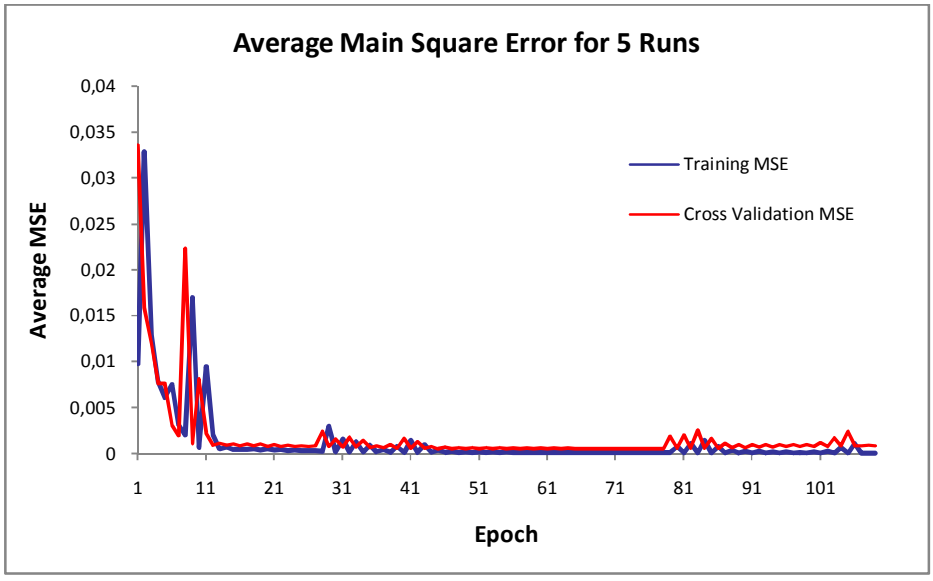

Figure 7.6 Avarage MSE versus Number of Epochs for Training the Best Network

In figure 7.6, the average MSE in training versus number of iteration is plotted. The average MSE drops drastically after 11 epochs and carries on running until minimum validation error which is reached at 59th epoch with a MSE error of 0.000495371. After training is completed, test set is used to evaluate the performance of the network. For this purpose, a total of 10 testing patterns are used to observe the prediction performance. In testing, the network predicts load ratings by generalizing what it has been trained for. The actual outputs (FEM based load ratings) and the outputs from the networks of each example are graphically represented in Figure 7.7 and 7.8.

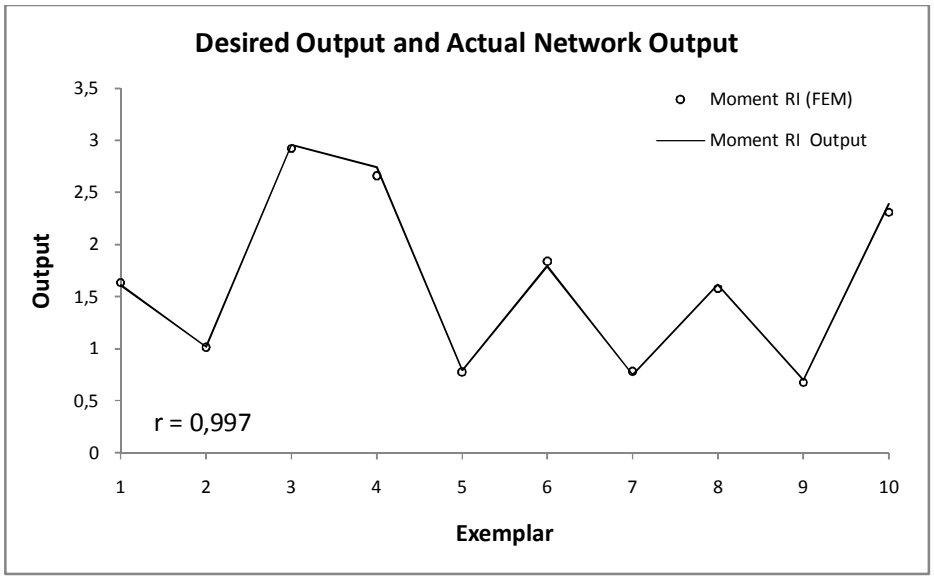

Figure 7.7 Desired Output (FEM based) and Actual output of the Best Network for Moment

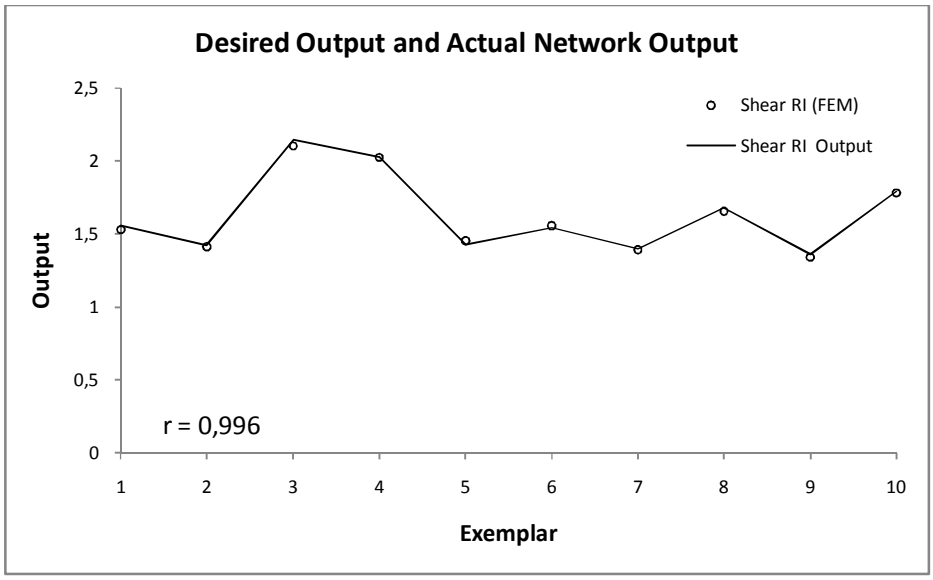

Figure 7.8 Desired Output (FEM based) and Actual output of the Best Network for Shear

From Figure 7.7 and 7.8, it is clear that the predictions of the best networks for 10 unseen patterns is quite satisfactory, resulting in maximum average testing error of 3.89% for moment load ratings and 1.97% for shear load ratings as mentioned before. This indicates that the network has learned the relation and generalizes to other patters reasonably. In addition, the linear coefficient of correlations very high between actual data and values predicted through neural network and it is 0.997 for moment load rating and 0.996 for shear load rating, indicating that proposed ANN model shows very good agreement with actual bridge data.

The load ratings for 10 testing patterns from the FE model and the corresponding AASHTO based analysis results as well as network prediction are given in Table 7.1. It is clear from the results that FEM based load ratings are higher than the AASHTO based rating, indicating that bridges inherently possess a greater load capacity. It can also be seen from this table that ANN is quite successful in predicting the load ratings from the bridge parameters.

Table 7.1 Moment and Shear Bridge Ratings for 10 Testing Patterns

	MODEL INFORMATION						AASHTO (LRFD)		FEM		ANN (FEM Based)	
Test Model	Span Length	Skew Angle	Beam Depth	Number of Beam	Parapet	Diaphragm	Moment IR	Shear IR	Moment IR	Shear IR	Moment IR	Shear IR
1	21	2	22	10	1	1	1,167	1,201	1,635	1,529	1,611	1,557
2	25	21	21	11	0	1	0,566	0,968	1,013	1,413	1,017	1,421
3	37	37	25	9	0	0	1,788	1,658	2,92	2,102	2,956	2,142
4	32	19	19	8	1	0	1,678	1,655	2,66	2,024	2,741	2,027
5	28	24	35	6	1	1	0,335	0,952	0,778	1,453	0,792	1,424
6	30	25	37	7	1	1	1,226	1,217	1,838	1,556	1,788	1,542
7	45	23	25	8	1	1	0,466	0,978	0,781	1,391	0,751	1,398
8	26	28	23	9	1	0	1,055	1,312	1,576	1,656	1,620	1,678
9	41	28	25	10	1	0	0,499	0,950	0,677	1,341	0,700	1,359
10	32	15	28	11	1	1	1,584	1,485	2,31	1,782	2,389	1,794

7.4 Discussion

The purpose of this chapter is to develop an ANN model to obtain the FEM based bridge ratings of T-beam bridges from the common bridge parameters so that the load ratings of these bridges are calculated accurately and practically. 104 T-beam bridge models constructed in Chapter 5 are used to generate necessary data for the training of ANN. Bridge data is prepared such that inputs are the bridge parameters and outputs are the FEM based shear and moment load ratings. The bridge data is divided into three sets, namely, “training” set, “cross-validation” set and “test” set. Of these bridges, 75 have been assigned to training, 19 as cross-validation and 10 as test sets in ANN modeling. ANN is trained to predict FEM based ratings from the bridge parameters. Several network designs are examined to determine one with a reasonable performance. The predictive performance of the 6-10-2 architecture with defined network parameters was found to be better than others. It produces maximum average testing error of 3.89% for moment load ratings and 1.97% for

shear load ratings in the test set, indicating that the learning and generalization performance of the ANN Model is very good. In addition, the linear coefficient of correlations is 0.997 for moment load rating and 0.996 for shear load rating in the ANN Model. This indicates that proposed ANN Model shows very good agreement with FEM based load ratings. It is clear from the results that FEM based ratings can be easily and accurately obtained using ANN Model while still strictly conforming to the AASHTO standards and provisions. The proposed ANN model is quite accurate, fast and practical.

CHAPTER 8

CONCLUSIONS

In this work, approximate analysis of RC T-beam bridges, calibration of the T-beam bridges and modeling of load ratings of these bridges are studied using neural networks. Based on the results, the following conclusions can be drawn from the study:

Approximate Analysis of RC T-Beam Bridges

- The results indicate that by selecting the right input parameters and properly constructing and training the ANN models, it is possible to establish intrinsic relationship between the bridge parameters and responses, and interpolate this relationship for other bridges with a maximum error of 3.36% for moment and 1.53% for shear. In addition, the linear coefficient of correlations between analytical data and values predicted through neural nets is very high and it is 0.998 for moment and 0.956 for shear, indicating that proposed NN models show very good agreement with actual responses.

- Sensitivity analyses with the trained neural networks provide valuable additional information on the relative influence of input parameters on the bridge systems. The most important input parameter for moment is the bridge length, while the most important input parameter for shear is skew angle. The least important input for both is parapet. In addition, moment increases with increasing span length, beam depth and the number of beam, while it decreases with increasing skew angle and existence of parapet and diaphragm. Shear increases with increasing span length, skew angle, beam

depth, the number of beam and presence of diaphragm while it decreases with the existence of parapet.

- In addition to the accuracy of outputs and the ease of use, neural networks reduce the overall time required for implementations by significant amount when compared with FE methods. The bridge responses can be obtained from the trained neural networks with a trivial computational time and effort and without a need to construct and analyze a new model for each parameter set.

Calibration of the T-Beam Bridges -Manoa Road Bridge-

- ANN model was first trained with the training set generated through linear analysis of analytical model. The results indicate that by using this ANN model, it is possible to reduce the differences between the measured and the calculated frequencies to less than 10% for the first three modes and to reduce the measured and the calculated deflections to less than 31% for the deflections along the central T-beam. Then, the same ANN Model was trained with the training set generated by considering that concrete does not carry tension forces. The maximum difference between the measured and the calculated frequencies for the first three modes is less than again 9%. However there is a significant improvement in deflections. The maximum difference between measured and the calculated deflections along the central T-beam were reduced from 31% to 12% indicating that T-beam bridges should be calibrated by taking into account the non-linear behavior of concrete.

- Due to possible errors, uncertainties and discrepancies between the experiment and the analytical model, a "100% match" should not expected, hence it can concluded that the calibration of the bridge is achieved to the point that computed natural frequencies of the 3-D FE model agree well with those from field measured data. For deflections, however, slight

differences exist between the computed and the measured values. Preparing training set would take considerable amount of time; nevertheless, once a neural network is successfully trained, the same system can be used efficiently and quickly for calibration of the bridge model during the lifetime of the structure, following testing of the actual bridge.

Modeling of Bridge Load Ratings of T-Beam Bridges

- Since 3D FE models that precisely represent PA's T-beam bridge population improve the load rating of these bridges, load ratings are calculated again more accurately by taking into account the actual geometry and detailing of the T-beam bridges. Then, ANN systems are used to model the bridge ratings based on the bridge parameters. The proposed ANN Model produces maximum average testing error of 3.89% for moment bridge ratings and 1.97% for shear bridge ratings for the test patterns. This shows that the learning and generalization performance of the ANN Model is very good. In addition, the linear coefficient of correlations is 0.997 for moment bridge ratings and 0.996 for shear bridge ratings, indicating that proposed ANN Model shows very good agreement with FEM based bridge ratings.

- Using this ANN model, the highest utilizable capacity of any T-beam bridge can be easily computed while still strictly conforming to the AASHTO standards and provisions.

Artificial Neural Networks

- The success of networks depends on network parameters and the topology.

- Levenberg- Marquardt learning rule and the sigmoid transfer function are appropriate choices for a successful network application in the current context.

- The learning and prediction performance of the network vary depending on the number of hidden layers and the number of nodes in the hidden and output layers. A single hidden layer with an optimum number of neurons is sufficient for modeling of these problems.

- While minimum MSE is a measure of learning performance, it does not guarantee the best prediction rate (generalization capability). To make sure that the network training has been satisfactorily completed and the network is capable of generalization, a set of unseen patterns must be selected and the network should be tested using these patterns.

- The proposed models are quite accurate, fast and practical for use within the range of bridge data used for training.

REFERENCES

AASHTO (1994), "LRFD Bridge Design Specifications," Washington D.C.

AASHTO (1999), "Standard Specification for Highway Bridges", Washington D.C.

AASHTO (2000), "Manual for condition evaluation of bridges." American Association of State Highway and Transportation Officials, Washington D.C.

AASHTO (2002), "Standard Specification for Highway Bridges", Washington D.C.

AASHTO (2007), "LRFD Bridge Design Specifications", 4th edition Washington D.C.

Adeli, H., (2001), "Neural Networks in Civil Engineering: 1989-2000", Computer-Aided Civil and Infrastructure Engineering, Vol. 16, PP. 126-142.

Adeli, H., Yeh, C., (1989), "Perceptron Learning in Engineering Design", Microcomputers in Civil Engineering, Vol. 4, No. 4, pp. 247-256.

Anderson, D., McNeill, G., (1992), "Artificial neural networks technology", A DACS State-of-the-Art Report, New York.

Atalla, M.J., Inman, D.J., (1998), "On Model Updating using Neural Networks", Mech. Syst. Signal Process, Vol. 12, pp. 135-161.

Barai, S.V., Pandey, P.C., (1995), "Vibration Signature Analysis Using Artificial Neural Networks", Journal of Computing in Civil Engineering, Vol. 9, No. 4, pp. 259-265.

Cattan, J., Mohammadi, J., (1997), "Analysis of Bridge Condition Rating Data Using Neural Networks", Microcomputers in Civil Engineering, Vol. 12, pp. 419-429.

Chang, C.C., Chang, T.Y.P., Xu, Y.G., (2000), "Adaptive Neural Networks for Model Updating of Structures", Smart Mater. Struct., Vol. 9, pp. 59-68.

Chen, C.H., (2005), "Structural Identification from Field Measurement Data using a Neural network", Smart Mater. Struct., Vol. 14, pp. 104-115.

Consolazio, G.R., (2000), "Iterative Equation Solver for Bridge Analysis using Neural Networks", Computer-Aided Civil and Infrastructure Engineering, Vol. 15, pp. 107-119.

Drexel Intelligent Infrastructure and Transportation Safety Institute (DIITSI), (2003), "Re-Qualification of Aged Reinforced Concrete T-Beam Bridges in Pennsylvania", Final Project Report, Drexel University, PA

Fang, X., Luo, H., Tang, J., (2005) "Structural Damage Detection Using Neural Network with Learning Rate Improvement", Computers and Structures, Vol. 83, pp. 2150-2161.

Fausett, L., (1994), "Fundamentals of Neural Networks, Architectures, Algorithms, and Applications", Prentice-Hall, New Jersey.

Fischer, M.A., Firchein, O., (1987), "Intelligence: The Eye, the Brain and the Computer", Addison-Wesley.

Halıcı, U., (2004), "Artificial Neural Networks", EE 543 Lecture Notes.

www.neurosolutions.com., last accessed: 07.06.2008

Jenkins, W.M., (1999), “A Neural Network for Structural Re-analysis”, Computers and Structures, Vol. 72, pp. 687-698.

Jenkins, W.M., (2002), “Structural Reanalysis Using a Neural Network-based Iterative Method”, Journal of Structural Engineering, Vol. 128, No. 7, pp. 946-950.

Konar, A., (1999), “Artificial Intelligence and Soft Bomputing, Behavioral and Cognitive Modelling of the Human brain”, CRC Press

Kröse, B., Smagt, P., (1996), “ An Introduction to Neural Networks”, Eighth edition, The University of Amsterdam.

LeCun, Y., 1985, "Une Procedure d'Apprentissage pour Reseau a Seuil Assymetrique.", Cognitiva, 85, 599-604, 1985

McCulloch, W.S., Pitts, W., (1943), "A Logical Calculus of Ideas Immanent in Nervous Activity", Bulletin of Mathematical Biophysics, Vol. 5, pp. 115-133.

Morshed, J., Kaluarachchi, J.J., (1998),“Application of Artificial Neural Network and Genetic Algorithm in Flow and Transport Simulations”, Advances in Water Resources Vol. 22, No. 2, pp. 45-158.

NBI, (1998), National Bridge Inventory Data (NBID), Rep.No.FHWA-PD-96-001, Washington D.C.

NBI, (2001), National Bridge Inventory Data (NBID), Washington D.C.

Oreta, A.W.C., Kawashima, K., (2003), “Neural Network Modeling of Confined Compressive Strength and Strain of Circular Concrete Columns”, Journal of Structural Engineering, Vol. 129, No. 4, pp. 554-561.

Özkaya, E., Pakdemirli, M., (2002), “Natural Frequencies of Suspension Bridges: An Artificial Neural Networks Approach”, Journal of Sound and Vibration, Vol. 257, No. 3, 596-604.

Parker D. B, (1985) "Learning-logic: Casting the Cortex of the Human Brain in Silicon", Technical Report TR-47, Center for Computational Research in Economics and Management Science, MIT, Cambridge, MA

Pearlmutter, B. A., (1990), “Dynamic Recurrent Neural Networks”, Technical Report CMU-CS-88-191, Carnegie-Mellon University, Computer Science Dept. Pittsburg, PA.

Rafiq, M.Y., Bugmann, G., Easterbrook, D.J., (2001), “Neural Network Design for Engineering Applications”, Computers and Structures, Vol. 79, pp. 1541-1552.

Rao, A.R., Kumar, B., (2007), “Predicting Re-aeration Rates Using Artificial Neural
Networks in Surface Aerators”, International Journal of Applied Environmental Sciences, Vol. 2, No. 1, pp. 155-166.

Rogers, J.R., (1994), “Simulating Structural Analysis with Neural network”, Journal of Computing in Civil Engineering, Vol. 8, No. 2, pp. 252-265.

Rumelhart, D.E., McClelland, J.L. and the PDP Research Group (1986), Parallel Distributed Processing Vols. 1 and 2, Bradford Books and MIT Press, Cambridge, Mass

Rumelhart, D.E., G. E. Hinton, and R. J. Williams, (1986), "Learning Internal Representations by Error Propagation.", in Parallel Distributed Processing: Explorations in the Microstructure of Cognition (Rumelhart D.E., and J. L. McClelland, eds.), Vol.1, Chapter 8, Cambridge, MA: MIT Press

Tang, C.W., Chen, J.C., Yen, T., (2003), "Modeling Confinement Efficiency of Reinforced Concrete Columns with Rectilinear Transverse Steel Using Artificial Neural Networks", Journal of Structural Engineering, Vol. 129, No. 6, pp. 775-783.

Turer, A., (2000), "Condition Evaluation And Load Rating Of Steel Stringer Highway Bridges using Field Calibrated 2d-Grıd And 3d-Fe Models", Ph.D. Thesis, University of Cincinnati, Department of Civil and Environmental Engineering, Cincinnati, USA.

Werbos, P. J.,(1974), Beyond Regression: New tools for Prediction and Analysis in the Behavioral Sciences, Ph.D. Thesis, Harward University, Cambridge, MA.

Yetilmezsoy, K., Demirel, S., (2008), "Artificial neural network (ANN) approach for modeling of Pb(II) adsorption from aqueous solution by Antep pistachio (Pistacia Vera L.) Shells", Journal of Hazardous Materials, Vol. 153, pp. 1288–1300.

Yun, C.B., Bahng, E.Y., (2000), "Substructural Identification Using Neural Networks", Computers and Structures, Vol. 77, pp. 41-52.

APPENDIX A

LEARNING IN ARTIFICIAL NEURAL NETWORKS

A.1 Generalized Delta Rule Algorithm

The net input to a node in the layer j is given by (Figure 3.5)

$$a_j = \sum_{i=0}^{m} w_{ji}\, u_i \tag{A1.1}$$

and the output of node j will be

$$x_j = f(a_j) \tag{A1.2}$$

Here f is the activation function and in this study following given sigmoidal function has been used

$$x_j = \frac{1}{1 + e^{-(a_j + \theta_j)/\theta_0}} \tag{A1.3}$$

Now the input to the nodes of layer k is

$$a_k = \sum w_{kj}\, x_j \tag{A1.4}$$

and its respective outputs are

$$x_k = f(a_k) \tag{A1.5}$$

In the training process of neural networks, for the input pattern $u_p = i_{pi}$ the weights adjustment will take place in the links of the neural networks for desired output t_{pk} at the output nodes. After achieving this first adjustment the network will pick up another pair of u_p and t_{pk}, and will again adjust weights for new pair. Similar way the process will go on till all the input-output pairs get exhausted. Finally network will have a single set of stabilized weights satisfying all the input-output pairs.

Usually the outputs x_{pk} will not be the same as desired output values t_{pk}. For each input-output pattern, the square of error can be given by

$$E_p = \frac{1}{2}\sum_k (t_{pk} - x_{pk})^2 \tag{A1.6}$$

and the average system error by

$$E = \frac{1}{2P}\sum_p \sum_k (t_{pk} - x_{pk})^2 \tag{A1.7}$$

Avoiding the p subscript in the eqn (A6) for convenience, then the expression will be

$$E = \frac{1}{2}\sum_k (t_k - x_k)^2 \tag{A1.8}$$

In a true gradient search for a minimum system error one has to compute the derivative of the error function E, with respect to any weight in the network and then change the weights according to the rule

$$\Delta w_{kj} = -\eta \frac{\partial E}{\partial w_{kj}} \tag{A1.9}$$

where η is learning parameter.

The partial derivative $\partial E/\partial w_{kj}$ can be given by using chain rule

$$\frac{\partial E}{\partial w_{kj}} = \frac{\partial E}{\partial a_k} \frac{\partial a_k}{\partial w_{kj}} \tag{A1.10}$$

using eqn (A4)

$$\frac{\partial a_k}{\partial w_{kj}} = \frac{\partial}{\partial w_{kj}} \sum w_{kj} x_j = x_j \tag{A1.11}$$

now δ_k can be given by

$$\delta_k = \frac{-\partial E}{\partial a_k} \tag{A1.12}$$

therefore

$$\Delta w_{kj} = \eta \delta_k x_j \tag{A1.13}$$

The weights on each line should be changed by an amount proportional to the product of the term δ_k, available to the unit receiving input along that line and the activation x_j along that line. The determination of δ_k is a recursive process. To compute $\delta_k = -\partial E/\partial a_k$, the chain rule can be used to express in terms of two factors. First the rate of change of error with respect to the output x_k and second the rate of change of the output of the node k with respect to input to that same node. Therefore

$$\delta_k = -\frac{\partial E}{\partial a_k} = -\frac{\partial E}{\partial x_k}\frac{\partial x_k}{\partial a_k} \tag{A1.14}$$

now these factors can be computed as

$$\frac{\partial E}{\partial x_k} = -(t_k - x_k) \tag{A1.15}$$

$$\frac{\partial x_k}{\partial a_k} = \tilde{f}_k(a_k) \tag{A1.16}$$

using expressions (A15) and (A16), we have

$$\delta_k = (t_k - x_k)\tilde{f}_k(a_k) \tag{A1.17}$$

for any output layer k, Δw_{kj} will be given by

$$\Delta w_{kj} = \eta(t_k - x_k)\tilde{f}_k(a_k)x_j = \eta\delta_k x_j \tag{A1.18}$$

Similarly for the internal units

$$\Delta w_{ji} = \eta\delta_j x_i \tag{A1.19}$$

$$\delta_j = \tilde{f}_j(a_j)\sum_k \delta_k w_{kj} \tag{A1.20}$$

The application of the backpropagation algorithm involves two phases. In the first phase the input is presented and propagated forward through the network to compute the output value of each unit. In the backward phase the δ s for all the units are computed. Once these two phases are complete, one can compute for each weight the Δw s.

In summary here we add one more subscript p to denote the pattern number, we have

$$\Delta_p w_{ji} = \eta \delta_{pj} x_{pi} \tag{A1.21}$$

If j are the nodes of the output layer then

$$\delta_{pj} = (t_{pj} - x_{pj}) \tilde{f}_j(a_{pj}) \tag{A1.22}$$

or if j are nodes of internal or hidden units then

$$\delta_{pj} = \tilde{f}_j(a_{pj}) \sum_k \delta_{pk} w_{kj} \tag{A1.23}$$

The backpropagation is basically a gradient descent algorithm. In multilayer networks, the error surfaces will be complex with several local minima. It is possible that the gradient descent procedure may not reach the global minimum, but get trapped in one of the many local minima.

One way to increase the learning rate without leading to oscillation is to modify the backpropagation algorithm by including the momentum term α as below

$$\Delta w_{ji}(n+1) = \eta(\delta_j x_i) + \alpha \Delta w_{ji}(n) \tag{A1.24}$$

where n is the presentation number and α is the constant that determines the effect of the previous weight changes on the current direction of movement in the weight space. This provides a kind of momentum in the weight space that effectively filters out the high frequency variations of the error surface in the weight space.

A.2 Correlation Coefficient

The size of the mean square error (MSE) can be used to determine how well the network output fits the desired output, but it doesn't necessarily reflect whether the two sets of data move in the same direction. For instance, by simply scaling the network output, we can change the MSE without changing the directionality of the data. The correlation coefficient (*r*) solves this problem. By definition, the correlation coefficient between a network output *x* and a desired output *t* is:

$$r = \frac{\frac{\sum_i (x_i - \bar{x})(t_i - \bar{t})}{N}}{\sqrt{\frac{\sum_i (t_i - \bar{t})^2}{N}} \sqrt{\frac{\sum_i (x_i - \bar{x})^2}{N}}} \qquad (A1.25)$$

The correlation coefficient is confined to the range [-1,1]. When r =1 there is a perfect positive linear correlation between *x* and *t*, that is, they covary, which means that they vary by the same amount. When r = -1, there is a perfectly linear negative correlation between *x* and *t*, that is, they vary in opposite ways (when *x* increases, *t* decreases by the same amount). When r = 0 there is no correlation between *x* and *t*, i.e. the variables are called uncorrelated. Intermediate values describe partial correlations. For example a correlation coefficient of 0.88 means that the fit of the model to the data is reasonably good.

APPENDIX B

BRIDGE DATA FOR APPROXIMATE ANALYSIS

Table B.1 Generated Models and Corresponding Analysis Results

	MODEL INFORMATION						ANALYSIS OUTPUTS	
Model	**Span Length**	**Skew Angle**	**Beam Depth**	**Number of Beam**	**Parapet**	**Diaphragm**	**FEM Moment**	**FEM Shear**
1	26	32	26	5	1	1	718,234	23,234
2	36	39	33	5	0	1	1427,633	26,588
3	32	12	40	5	1	1	1134,555	23,939
4	22	26	24	5	1	1	640,897	21,43
5	29	14	24	5	1	1	754,005	21,238
6	24	15	31	5	1	1	739,897	21,868
7	29	23	34	5	1	1	972,534	22,873
8	49	32	25	5	1	1	1113,118	23,075
9	49	25	29	5	1	1	1296,697	23,898
10	40	28	31	5	1	0	1189,578	23,508
11	41	6	31	5	1	0	1195,406	21,58
12	20	10	31	5	0	1	743,601	20,672
13	47	7	23	5	0	1	1943,912	22,738
14	21	45	21	5	0	1	608,804	22,401
15	39	21	19	5	0	0	1500,546	22,39
16	20	27	38	5	0	0	753,835	21,135
17	41	6	31	5	0	0	1745,813	23,221
18	26	0	24	6	1	1	810,057	20,438
19	28	28	32	6	1	1	1023,79	23,271
20	50	22	38	6	1	1	2289,972	25,314
21	23	31	39	6	1	1	866,842	22,607
22	51	25	36	6	1	0	2148,386	24,249
23	28	27	20	6	1	0	825,016	20,755
24	29	0	23	6	1	0	985,28	19,907
25	54	28	22	6	0	1	2902,305	24,559
26	54	4	29	6	0	1	3086,096	24,296
27	25	12	31	6	0	1	1023,414	22,46
28	37	1	19	6	0	0	1839,272	21,62
29	36	4	20	7	1	1	1117,098	21,187
30	26	36	28	7	1	1	909,456	24,137
31	49	17	33	7	1	1	2109,775	25,351
32	35	39	39	7	1	0	1541,666	26,969
33	27	35	21	7	1	0	875,648	23,081
34	52	11	19	7	1	0	1346,455	20,624
35	34	0	30	7	1	0	1397,282	22,821
36	21	35	19	7	0	1	707,919	22,129
37	24	3	23	7	0	1	882,953	20,896
38	32	39	27	7	0	1	1317,915	26,326
39	55	39	20	7	0	1	2415,02	25,892
40	42	26	39	7	0	0	2138,326	25,757
41	50	8	25	7	0	0	2649,935	23,607
42	49	28	19	8	1	1	1306,137	22,183
43	24	44	33	8	1	1	827,929	24,388

Table B.1 (continued).

44	33	30	25	8	1	1	1150,534	24,13
45	33	10	25	8	1	0	1299,422	22,82
46	37	2	35	8	1	0	1677,228	24,028
47	36	21	19	8	1	0	1177,831	21,291
48	48	39	21	8	1	0	1451,435	22,644
49	47	31	32	8	1	0	1953,888	25,298
50	25	17	38	8	0	1	956,251	23,451
51	55	45	20	8	0	1	1923,636	26,172
52	34	32	21	8	0	1	1321,827	24,238
53	48	15	39	8	0	0	2494,788	26,221
54	53	23	25	9	1	1	1951,25	23,955
55	40	8	36	9	1	1	1735,088	25,074
56	38	40	22	9	1	1	1212,005	26,49
57	21	10	30	9	1	1	776,331	21,46
58	31	14	25	9	1	1	1124,206	22,82
59	52	2	31	9	1	0	2380,562	24,999
60	36	45	38	9	1	0	1480,588	27,727
61	30	5	22	9	1	0	1125,145	22,306
62	33	35	23	9	1	0	1151,799	24,614
63	28	31	38	9	0	1	1133,351	24,705
64	42	27	29	9	0	1	1829,805	26,196
65	49	32	21	9	0	1	2106,361	25,133
66	37	37	25	9	0	0	1430,889	25,227
67	30	37	22	9	0	0	1078,143	24,468
68	27	18	39	9	0	0	1148,586	23,851
69	22	15	40	9	0	0	881,849	22,301
70	37	26	25	10	1	1	1342,869	24,512
71	31	24	25	10	1	1	1111,678	23,628
72	48	24	36	10	1	1	2068,198	26,707
73	44	41	33	10	1	1	1710,487	28,277
74	21	2	22	10	1	1	751,17	20,427
75	40	8	39	10	1	0	1904,678	25,63
76	30	45	38	10	1	0	1230,696	26,426
77	38	38	38	10	1	0	1690,701	26,704
78	54	43	32	10	0	1	2301,866	28,344
79	40	22	39	10	0	1	1729,635	26,377
80	41	44	36	10	0	1	1629,005	28,442
81	49	1	33	10	0	1	2532,279	25,295
82	35	19	40	10	0	0	1638,345	25,532
83	31	11	24	10	0	0	1271,526	22,171
84	33	16	28	10	0	0	1398,857	23,351
85	52	14	24	10	0	0	2535,614	24,077
86	29	40	26	10	0	0	1050,448	24,585
87	51	45	31	10	0	0	2069,741	27,872
88	21	43	22	11	1	1	631,585	22,641
89	38	38	31	11	1	1	1396,37	27,518
90	51	7	27	11	1	1	2107,604	24,509
91	54	25	23	11	1	0	2041,764	23,467
92	30	5	32	11	1	0	1234,07	23,082
93	54	0	19	11	1	0	1888,665	22,205
94	32	41	32	11	1	0	1245,423	26,479
95	46	19	37	11	1	0	2142,325	25,905
96	50	31	26	11	0	1	2085,061	26,16
97	35	26	32	11	0	0	1544,681	25,335
98	53	38	28	11	0	0	2207,442	26,034
99	28	21	21	11	0	0	1016,031	22,29
100	46	34	31	11	0	0	1976,295	26,141
101	37	26	22	11	0	1	1378,852	24,062
102	28	28	19	11	1	1	903,853	23,266
103	26	3	25	8	0	0	966,723	21,02
104	35	22	19	8	0	0	1438,956	22,614
105	47	0	19	8	1	1	1351,672	21,544
106	41	32	31	8	0	1	1836,371	26,046

Table B.1 (continued).

107	21	4	39	7	0	0	874,132	21,283
108	52	44	25	7	1	1	1557,353	26,437
109	24	5	24	6	0	0	942,194	20,753
110	49	19	28	6	0	0	2837,365	24,62
111	34	7	20	6	0	1	1586,351	22,023
112	35	4	35	6	1	0	1555,862	23,539
113	45	17	19	6	1	0	1111,021	18,842
114	31	21	25	11	1	1	1117,09	23,529
115	25	21	21	11	0	1	877,846	22,527
116	30	39	28	6	0	0	1289,762	24,862
117	32	14	40	7	0	0	1579,935	24,289
118	42	24	32	8	0	1	1956,106	25,401
119	50	15	29	11	1	0	2241,165	25,602
120	54	10	20	8	1	1	1521,141	22,252
121	32	19	19	8	1	0	1081,079	21,809
122	32	32	39	5	0	1	1293,81	25,637
123	53	0	19	7	1	1	1357,467	20,659
124	41	44	36	10	0	1	1629,005	28,376
125	37	26	20	10	0	1	1390,765	23,593
126	38	40	40	6	1	0	1701,652	26,4
127	31	17	38	9	0	0	1359,581	24,062
128	42	20	33	8	1	1	1745,81	23,998
129	49	14	20	7	0	1	2471,707	23,707
130	28	19	38	5	1	0	951,964	23,059
131	49	17	27	11	0	0	2322,649	24,914
132	42	26	25	9	0	0	1820,374	24,057
133	22	26	23	6	0	1	849,231	22,034
134	31	19	32	5	1	1	976,878	22,895
135	28	24	35	6	1	1	1079,69	23,202
136	30	25	37	7	1	1	1217,701	24,6
137	45	23	25	8	1	1	1606,977	23,719
138	26	28	23	9	1	0	930,698	23,055
139	41	28	25	10	1	0	1566,541	24,375
140	32	15	28	11	1	1	1256,158	23,935

APPENDIX C

TRAINING SET OF MANOA ROAD BRIDGE

Table C.1 Generated Models and Analysis Results for Manoa Road Bridge

	ANALYSIS OUTPUTS						MODEL INFORMATION				
Model	**f_1 (Hz)**	**f_2 (Hz)**	**f_3 (Hz)**	**d_{F1} (in)**	**d_{F2} (in)**	**d_{F3} (in)**	**E (ksi)**	**$t_{asphalt}$ (in)**	**K_v (10^x) (kips/ft)**	**K_h (10^x) (kips/ft)**	**K_l (10^x) (kips/ft)**
1	20,03	21,46	23,01	0,017	0,038	0,021	2500	5	4,78	3	2,6
2	17,21	18,58	20,08	0,022	0,048	0,027	2000	0	4	2,85	1,85
3	14,35	15,4	16,53	0,034	0,074	0,041	1100	12	4,48	3,48	1,3
4	21,3	22,82	24,42	0,015	0,034	0,019	3000	2	2,78	1,3	3,95
5	19,85	21,2	22,69	0,018	0,036	0,021	3300	7	3,78	1	1,48
6	18,41	19,58	20,86	0,02	0,045	0,025	2200	4	4,85	1	2,48
7	18,88	20,18	21,69	0,019	0,044	0,024	2000	3	4,85	1,9	3,7
8	18,07	19,26	20,57	0,021	0,046	0,026	2100	3	3,6	1,9	2,95
9	13,01	14,01	15,06	0,042	0,082	0,049	1300	8	2,9	1,78	1,7
10	14,56	15,72	16,92	0,033	0,067	0,039	1600	11	2,95	2,3	1,85
11	14,39	15,66	16,72	0,034	0,065	0,041	1900	11	2	2,7	1,78
12	21,11	22,94	24,87	0,015	0,034	0,019	3000	11	3,95	3,95	1,85
13	17,37	18,44	19,6	0,023	0,05	0,028	2000	8	4,6	1	1,9
14	15,05	16,55	18,09	0,029	0,06	0,035	1800	0	2,9	2,85	1,6
15	21,24	22,77	24,48	0,015	0,035	0,019	2800	6	4,78	1,9	3,48
16	21,66	23,55	25,51	0,015	0,032	0,018	3400	10	3,95	3,3	1,6
17	22,55	24,24	26,21	0,013	0,031	0,016	3000	8	4,3	3,3	3,95
18	24	25,79	27,73	0,012	0,027	0,014	3900	2	4,78	2,9	2,95
19	20,75	22,22	23,71	0,016	0,035	0,02	3100	10	2,78	1	3,48
20	19,78	21,18	22,79	0,018	0,04	0,021	2300	9	3,95	1,85	3,78
21	18,15	19,36	20,74	0,021	0,048	0,026	1700	9	3,3	3,78	3,3
22	15,62	16,78	17,94	0,029	0,059	0,035	1800	5	2,48	2,7	2,3
23	17,41	18,63	20,15	0,022	0,05	0,027	1700	0	4,6	1,7	3,78
24	19,98	21,31	22,75	0,017	0,038	0,021	2700	9	4,7	1	2,6
25	21,15	22,71	24,42	0,015	0,035	0,019	2800	3	4,48	3,3	2,7
26	19,21	20,61	22,16	0,018	0,04	0,022	2500	0	2,7	2	3,7
27	20,26	21,99	23,81	0,017	0,037	0,02	2700	3	3,9	3,95	1,9
28	17,16	18,23	19,39	0,024	0,05	0,028	2100	1	4	1	1,3
29	22,33	24,55	26,8	0,014	0,03	0,017	3800	7	3,48	3,9	1,85
30	19,69	22,01	24,21	0,018	0,036	0,021	3300	10	3	3,7	1
31	19,41	20,2	20,89	0,019	0,039	0,024	2700	2	2	2,7	3,7
32	18,03	19,21	20,5	0,021	0,047	0,026	2100	5	3,85	1,3	2,85
33	21,09	22,56	24,24	0,015	0,036	0,019	2500	7	2,9	3,9	3,9
34	21,92	23,56	25,42	0,014	0,033	0,017	3000	3	3,7	2	4
35	20,35	21,79	23,39	0,017	0,038	0,02	2500	6	3,9	2,95	3,3
36	15,71	16,82	18,04	0,028	0,062	0,034	1300	11	5	3,95	1,9
37	15,45	16,64	17,89	0,029	0,063	0,035	1400	11	3,7	3,3	1,7
38	18,35	19,54	20,84	0,021	0,045	0,025	2100	9	5	1	2,78
39	12,84	13,53	14,31	0,043	0,093	0,052	800	12	2,95	1,9	2,85
40	21,8	23,67	25,58	0,014	0,031	0,017	3600	4	3,95	2,95	1
41	18,23	19,57	21,03	0,02	0,043	0,024	2300	0	4,95	2,3	1,7
42	15,04	16,98	18,81	0,03	0,054	0,035	3400	2	2,3	1,3	1,9
43	15,71	16,88	18,09	0,028	0,058	0,034	1800	10	2,85	2,48	2,3

Table C.1 (continued).

44	16,67	17,74	19,01	0,025	0,057	0,03	1400	1	5	2,3	3,7
45	18,15	20,34	22,28	0,021	0,041	0,025	3300	8	2,6	2,95	1
46	14,73	15,57	16,52	0,032	0,07	0,039	1200	6	5	1	2,48
47	18,64	19,87	21,23	0,02	0,044	0,024	2200	8	4	1,78	2,95
48	17,42	18,61	19,89	0,022	0,048	0,027	2000	0	2,48	1	3,6
49	19,8	21,2	22,71	0,018	0,039	0,021	2500	6	4,3	2,85	2,6
50	12,19	13,11	14,03	0,047	0,099	0,057	800	5	2,3	4	1,85
51	20,72	22,31	23,98	0,016	0,034	0,019	3500	4	3,7	2,3	1,9
52	17,04	18,14	19,42	0,024	0,055	0,029	1400	2	4,85	3,6	3,3
53	20,58	22,96	25,22	0,016	0,033	0,02	3600	7	2,95	3,85	1,48
54	16,54	17,58	18,72	0,025	0,055	0,031	1700	11	3,7	1	2,78
55	18,13	19,43	20,84	0,021	0,047	0,025	1900	9	3,95	3,48	2,48
56	16,22	17,23	18,35	0,027	0,059	0,033	1400	8	2,7	1,6	3,9
57	16,87	17,93	19,08	0,024	0,052	0,029	1900	10	3,95	1	2,3
58	17,12	18,25	19,43	0,024	0,05	0,029	2100	4	2,7	1,9	2,95
59	13,3	14,28	15,33	0,039	0,085	0,047	900	4	4,3	3,78	1
60	22,91	24,62	26,59	0,013	0,03	0,016	3100	9	3,78	3,7	3,7
61	13,67	14,43	15,36	0,037	0,085	0,046	800	8	4,78	1,95	3,48
62	20,64	22,21	23,99	0,015	0,034	0,019	3000	0	3,78	1	3,3
63	13,8	14,62	15,5	0,037	0,078	0,044	1100	11	4,6	1,7	1,3
64	22,24	23,89	25,77	0,014	0,032	0,017	2900	7	3,7	3,6	3,7
65	23,36	25,09	27	0,013	0,028	0,015	3600	1	4,7	1	3,48
66	21,41	22,9	24,53	0,015	0,033	0,018	3100	12	4,48	1	3
67	19,24	20,59	22,03	0,019	0,04	0,023	2700	4	3,3	1	3
68	19,49	20,85	22,38	0,018	0,042	0,022	2100	9	4,7	3,6	3
69	18,65	20,24	21,97	0,019	0,041	0,023	2400	0	3,85	3,3	2
70	19,41	20,73	22,18	0,018	0,042	0,022	2100	9	2,9	3,78	3,3
71	19,68	21,08	22,66	0,018	0,04	0,022	2300	7	3,95	1	3,7
72	16,72	18,48	20,3	0,024	0,045	0,028	3300	0	3	1	2
73	17,29	18,51	19,78	0,023	0,049	0,028	2200	3	3,78	2	0
74	17,62	18,75	20	0,022	0,047	0,027	2400	10	3,78	1	0
75	21,57	23,18	24,94	0,015	0,034	0,018	2800	6	3,78	3,78	3
76	21,98	23,61	25,43	0,014	0,032	0,017	3100	2	3,9	1	3,7
77	18,89	20,19	21,67	0,019	0,044	0,024	2000	6	3,48	3	3,6
78	20,96	23,17	25,37	0,015	0,033	0,019	3400	11	3,48	3,9	0
79	17,22	18,53	19,93	0,022	0,047	0,027	2300	0	3,78	2	1
80	20,97	23,12	25,22	0,015	0,033	0,019	3500	1	3	3,78	2
81	21,64	23,16	24,64	0,015	0,032	0,018	3600	3	2,6	3	3
82	18,41	19,63	20,92	0,02	0,044	0,025	2300	4	4,7	2	1
83	18,92	20,24	21,73	0,019	0,044	0,024	2100	4	3,48	1,3	3,78
84	22,59	24,27	26,19	0,013	0,031	0,016	3200	2	4,48	2	3,78
85	21,24	22,78	24,44	0,015	0,034	0,019	3000	8	3	1	3,78
86	21,26	22,53	23,7	0,015	0,034	0,019	2800	7	2,3	3,9	3,6
87	22,25	23,89	25,79	0,014	0,032	0,017	2800	6	4,6	4	3,48
88	22,26	23,92	25,78	0,014	0,032	0,017	3100	5	4	2,7	3,7
89	18,44	19,95	21,55	0,02	0,045	0,024	2100	11	4,6	3,9	0
90	20,02	21,38	22,9	0,017	0,04	0,021	2200	8	2,78	3,9	3,78
91	19,83	21,28	22,81	0,018	0,037	0,021	3200	11	3,78	2	0
92	20,73	22,62	24,58	0,016	0,035	0,019	3000	6	3,95	3,78	0
93	21,92	23,62	25,42	0,014	0,032	0,017	3300	9	4,7	3	2
94	17,88	19,08	20,33	0,022	0,046	0,026	2200	2	4,3	2	0
95	19,86	21,88	23,8	0,017	0,036	0,021	3200	5	2,78	3,6	2
96	21,96	24,07	26,24	0,014	0,031	0,017	3500	12	3,85	4	0
97	17,9	20,04	22,06	0,021	0,044	0,026	2700	2	2,9	3,6	0
98	21,03	22,55	24,33	0,015	0,036	0,019	2400	4	4,48	4	3,6
99	17,73	19,63	21,51	0,022	0,042	0,026	3600	10	3	2	0
100	20,55	22,02	23,56	0,016	0,035	0,02	3100	6	3	1	3,3
101	17,93	19,23	20,67	0,022	0,043	0,026	2900	4	3,48	1	0
102	21,74	23,34	25,13	0,015	0,033	0,018	3000	8	3,85	2	3,7
103	21,21	22,85	24,82	0,014	0,033	0,018	2800	0	4,6	3	3,7
104	16,25	17,98	19,69	0,026	0,05	0,031	2900	12	2,9	2	0
105	12,68	14,88	16,65	0,042	0,071	0,048	3200	5	2	1	0
106	19,32	20,78	22,35	0,018	0,038	0,022	2700	0	2,85	2,9	3
107	19,89	21,28	22,75	0,017	0,039	0,021	2600	11	3	2,7	3,3
108	20,11	21,41	22,68	0,017	0,036	0,021	3100	5	2,48	1,9	3,3

Table C.1 (continued).

109	15,34	17,14	18,98	0,029	0,054	0,034	3100	12	2,7	1	1,7
110	15,09	16,61	18,07	0,031	0,057	0,036	2600	1	2,3	2	2
111	20,16	21,53	22,93	0,017	0,037	0,021	2800	12	2,7	2,7	3,3
112	19,18	21,29	23,23	0,019	0,037	0,023	3500	8	2,7	3	1,7
113	16,18	17,82	19,46	0,027	0,05	0,031	2900	7	2,6	2	2
114	20,89	22,38	23,94	0,016	0,035	0,019	3000	2	3	2,7	3,3
115	19,08	20,37	21,69	0,019	0,041	0,023	2600	2	2,7	1	3,3
116	16,52	18,43	20,28	0,025	0,047	0,03	3400	3	2,6	2	1,7
117	17,09	18,8	20,58	0,024	0,045	0,028	3300	6	2,95	1,7	1,7
118	18,38	19,78	21,25	0,021	0,042	0,025	2900	7	2,85	2	2,7
119	17,4	19,12	20,92	0,023	0,044	0,027	3400	9	2,9	1,7	2
120	16,52	18,43	20,19	0,025	0,05	0,03	2600	9	2,78	2,7	0
121	14,78	16,25	17,57	0,032	0,057	0,038	2900	7	2	1,9	2

APPENDIX D

BRIDGE RATING CALCULATION

D.1 Bridge Data for Load Rating

Table D.1 Generated Models and Corresponding Load Ratings

	MODEL INFORMATION							RATING FACTORS		
Model	**Span Length**	**Skew Angle**	**Beam Depth**	**Number of Beam**	**Parapet**	**Diaphragm**	**Moment RI (AASHTO)**	**Moment RI (FEM)**	**Shear RI (AASHTO)**	**Shear RI (FEM)**
1	26	32	26	5	1	1	1,511	3,131	1,314	1,730
2	36	39	33	5	0	1	1,083	1,679	1,271	1,656
3	32	12	40	5	1	1	1,628	3,163	1,764	2,211
4	22	26	24	5	1	1	1,684	3,259	1,401	1,812
5	29	14	24	5	1	1	1,042	2,583	1,251	1,779
6	24	15	31	5	1	1	2,073	3,870	1,682	2,088
7	29	23	34	5	1	1	1,622	3,142	1,588	2,081
8	49	32	25	5	1	1	0,229	1,423	0,868	1,599
9	49	25	29	5	1	1	0,334	1,417	1,020	1,674
10	40	28	31	5	1	0	0,723	1,961	1,187	1,810
11	41	6	31	5	1	0	0,677	1,890	1,271	1,962
12	20	10	31	5	0	1	2,497	3,902	1,905	2,254
13	21	45	21	5	0	1	1,644	2,804	1,182	1,585
14	20	27	38	5	0	0	3,088	5,031	2,133	2,563
15	41	6	31	5	0	0	0,677	0,960	1,271	1,759
16	26	0	24	6	1	1	1,299	2,397	1,404	1,847
17	28	28	32	6	1	1	1,613	2,749	1,519	1,965
18	50	22	38	6	1	1	0,531	0,985	1,292	1,853
19	23	31	39	6	1	1	2,965	4,431	1,976	2,406
20	51	25	36	6	1	0	0,450	0,943	1,206	1,853
21	28	27	20	6	1	0	0,851	1,763	1,057	1,632
22	29	0	23	6	1	0	0,980	1,758	1,284	1,809
23	36	4	20	7	1	1	0,447	1,062	1,002	1,484
24	26	36	28	7	1	1	1,683	2,628	1,371	1,716
25	49	17	33	7	1	1	0,440	0,829	1,176	1,623
26	35	39	39	7	1	0	1,430	2,071	1,499	1,851
27	27	35	21	7	1	0	1,042	1,751	1,074	1,462
28	52	11	19	7	1	0	-0,020	0,548	0,753	1,435
29	34	0	30	7	1	0	1,021	1,572	1,407	1,797
30	21	35	19	7	0	1	1,365	1,980	1,162	1,504
31	24	3	23	7	0	1	1,440	1,945	1,410	1,762
32	32	39	27	7	0	1	1,066	1,454	1,150	1,471
33	49	28	19	8	1	1	0,041	0,552	0,708	1,326
34	24	44	33	8	1	1	2,498	3,707	1,589	1,944
35	33	30	25	8	1	1	0,840	1,522	1,108	1,521
36	33	10	25	8	1	0	0,840	1,278	1,205	1,586
37	37	2	35	8	1	0	1,031	1,491	1,501	1,879
38	36	21	19	8	1	0	0,398	0,846	0,888	1,423

Table D.1 (continued).

39	48	39	21	8	1	0	0,132	0,630	0,725	1,386
40	47	31	32	8	1	0	0,495	0,861	1,105	1,588
41	25	17	38	8	0	1	2,399	3,685	1,921	2,247
42	34	32	21	8	0	1	0,604	0,815	0,937	1,324
43	26	3	25	8	0	0	1,371	1,924	1,428	1,827
44	40	8	36	9	1	1	0,894	1,394	1,443	1,817
45	38	40	22	9	1	1	0,482	1,044	0,863	1,211
46	21	10	30	9	1	1	2,298	3,530	1,800	2,103
47	31	14	25	9	1	1	0,962	1,548	1,234	1,610
48	36	45	38	9	1	0	1,338	2,028	1,401	1,749
49	30	5	22	9	1	0	0,852	1,241	1,192	1,507
50	33	35	23	9	1	0	0,769	1,285	1,010	1,379
51	28	31	38	9	0	1	2,066	2,975	1,737	2,092
52	42	27	29	9	0	1	0,568	0,737	1,095	1,449
53	37	37	25	9	0	0	0,659	0,959	0,995	1,398
54	30	37	22	9	0	0	0,895	1,313	1,027	1,393
55	37	26	25	10	1	1	0,630	1,094	1,051	1,437
56	31	24	25	10	1	1	0,962	1,561	1,184	1,557
57	48	24	36	10	1	1	0,551	0,877	1,247	1,630
58	44	41	33	10	1	1	0,655	1,144	1,121	1,467
59	40	8	39	10	1	0	0,993	1,376	1,541	1,883
60	30	45	38	10	1	0	1,937	2,715	1,569	1,919
61	38	38	38	10	1	0	1,149	1,644	1,402	1,794
62	40	22	39	10	0	1	0,993	1,477	1,477	1,851
63	41	44	36	10	0	1	0,912	1,426	1,241	1,587
64	31	11	24	10	0	0	0,906	1,154	1,211	1,623
65	33	16	28	10	0	0	0,990	1,303	1,284	1,696
66	29	40	26	10	0	0	1,245	1,848	1,185	1,568
67	51	45	31	10	0	0	0,350	0,515	0,956	1,349
68	21	43	22	11	1	1	1,737	2,865	1,241	1,612
69	38	38	31	11	1	1	0,868	1,483	1,170	1,487
70	30	5	32	11	1	0	1,418	2,030	1,567	1,925
71	32	41	32	11	1	0	1,353	2,017	1,317	1,651
72	46	19	37	11	1	0	0,652	0,890	1,330	1,714
73	35	26	32	11	0	0	1,041	1,409	1,328	1,704
74	28	21	21	11	0	0	0,920	1,274	1,128	1,509
75	46	34	31	11	0	0	0,504	0,640	1,073	1,490
76	28	28	19	11	1	1	0,782	1,290	1,013	1,343
77	35	22	19	8	0	0	0,437	0,507	0,899	1,321
78	47	0	19	8	1	1	0,085	0,533	0,847	1,337
79	41	32	31	8	0	1	0,702	0,923	1,150	1,545
80	52	44	25	7	1	1	0,155	0,793	0,779	1,294
81	35	4	35	6	1	0	1,167	1,786	1,538	1,975
82	45	17	19	6	1	0	0,131	0,960	0,793	1,686
83	31	21	25	11	1	1	0,962	1,524	1,199	1,562
84	42	26	25	9	0	0	0,431	0,507	0,973	1,412
85	30	39	28	6	0	0	1,281	1,667	1,238	1,629
86	42	24	32	8	0	1	0,667	0,849	1,205	1,616
87	31	19	32	5	1	1	1,332	2,826	1,467	1,973
88	32	32	39	5	0	1	1,669	2,538	1,625	2,003
89	41	44	36	10	0	1	0,912	1,426	1,241	1,591
90	37	26	20	10	0	1	0,408	0,524	0,883	1,281
91	38	40	40	6	1	0	1,236	1,893	1,456	1,936
92	31	17	38	9	0	0	1,629	2,309	1,700	2,109
93	42	20	33	8	1	1	0,699	1,193	1,255	1,764
94	28	19	38	5	1	0	1,957	3,691	1,803	2,241
95	25	21	21	11	0	1	1,167	1,635	1,201	1,529
96	32	19	19	8	1	0	0,566	1,013	0,968	1,413
97	28	24	35	6	1	1	1,788	2,920	1,658	2,102
98	30	25	37	7	1	1	1,678	2,660	1,655	2,024
99	45	23	25	8	1	1	0,335	0,778	0,952	1,453
100	26	28	23	9	1	0	1,226	1,838	1,217	1,556
101	41	28	25	10	1	0	0,466	0,781	0,978	1,391
102	32	15	28	11	1	1	1,055	1,576	1,312	1,656
103	37	26	22	11	0	1	0,499	0,677	0,950	1,341
104	21	2	22	10	1	1	1,584	2,310	1,485	1,782

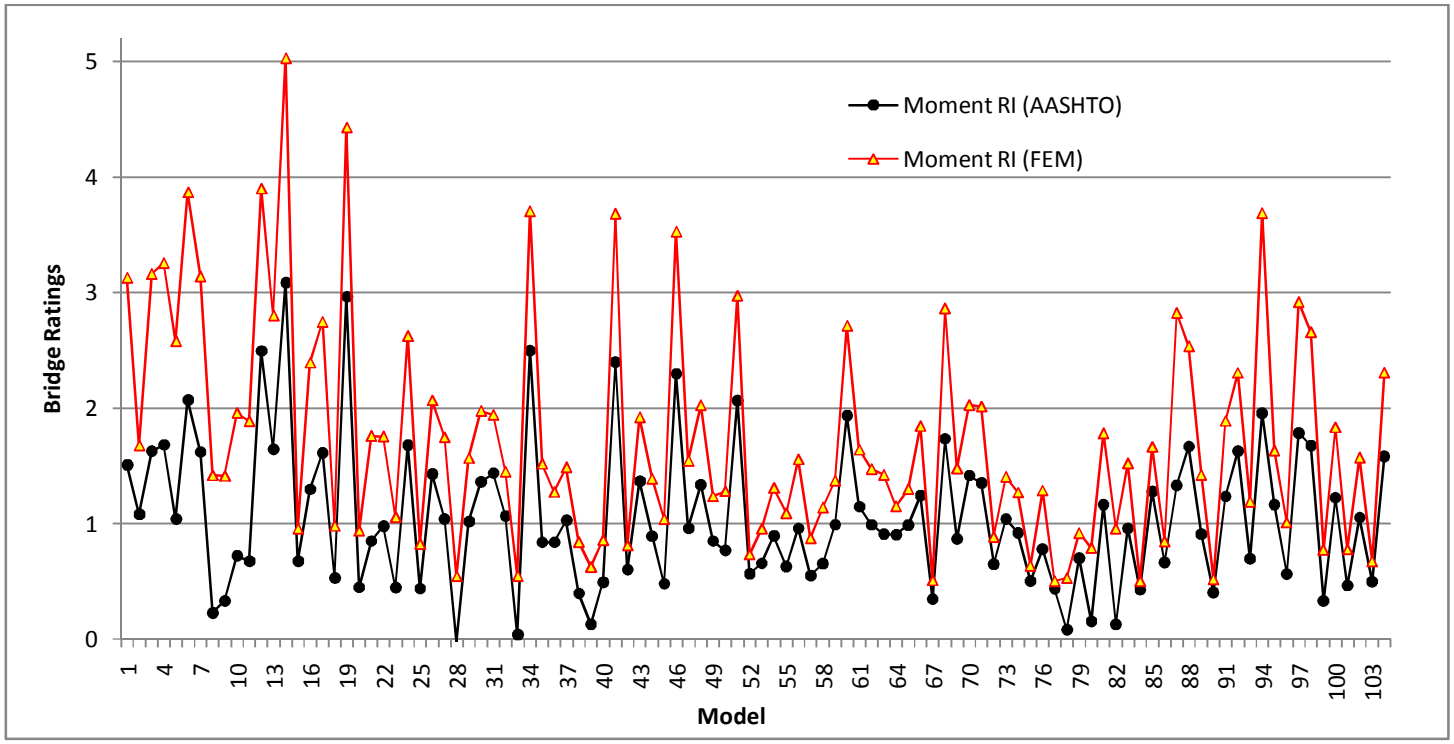

Figure D.1 FEM and AASHTO (LRFD) Based Bridge Ratings of Generated Models for Moment

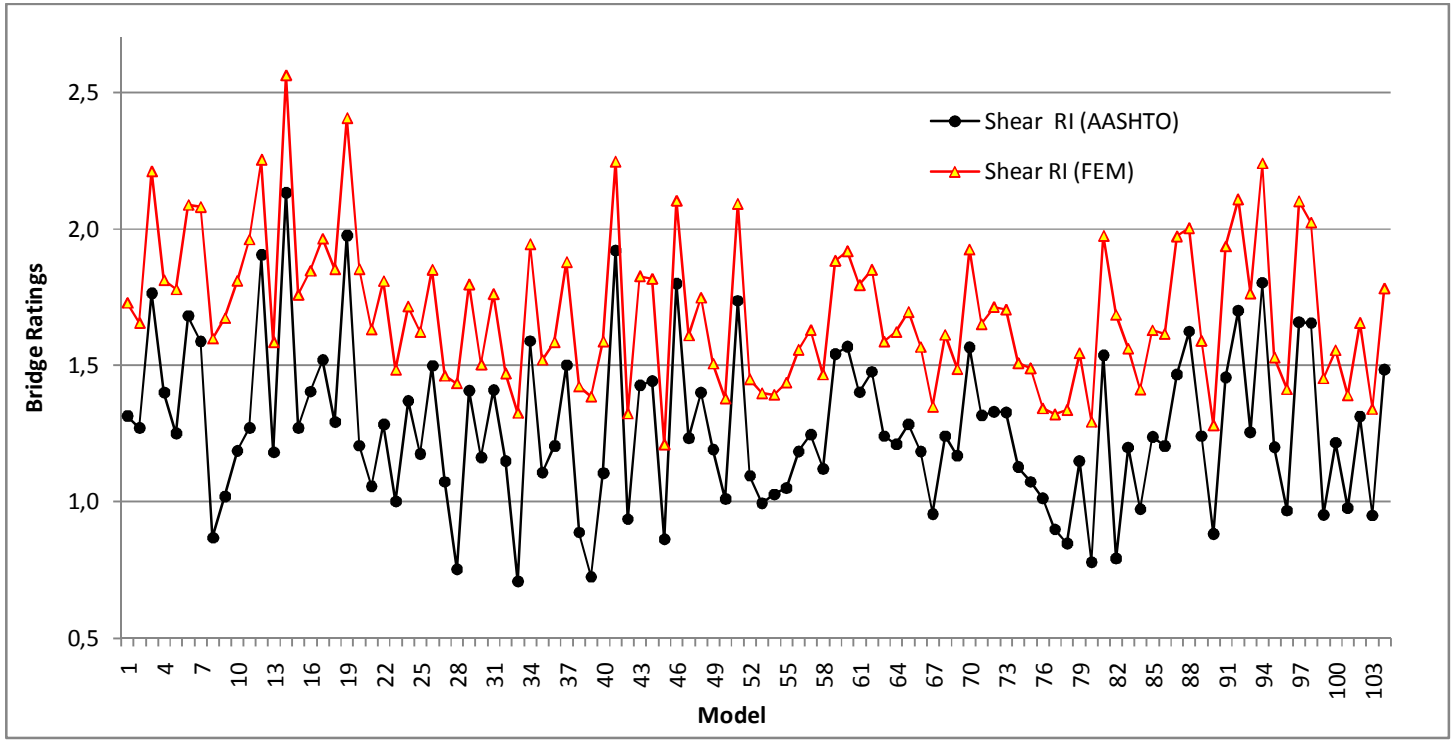

Figure D.2 FEM and AASHTO (LRFD) Based Bridge Ratings of Generated Models for Shear

D.2 AASHTO LRFD Based and FEM Based Rating Factor Calculation:

Example Model #1:

References:

1) AASHTO Manual for Condition Evaluation of Bridges. Second Edition 1994,rev.2000

2) AASHTO LRFD Bridge Design Specifications (2007)

Bridge: Span 26 ft, Skew 32 deg. , Depth 26 in. , Number of beam 5, parapet and diaphragm exist.

Truck: HS20

LOAD FACTOR RATING FOR MOMENT:

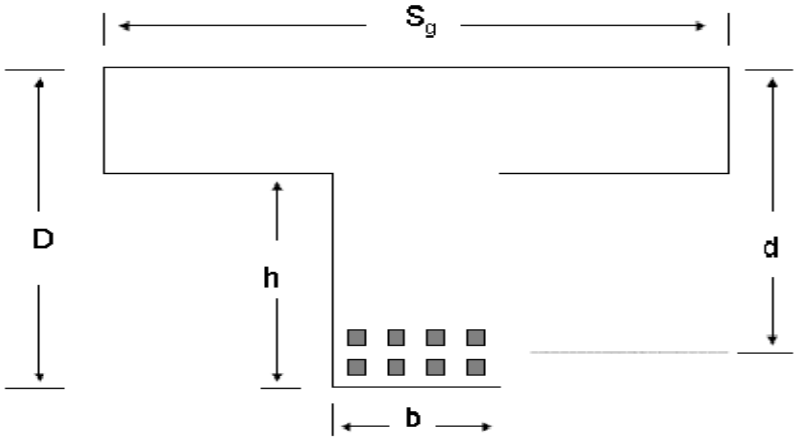

Note: Slab thickness and wearing surface thickness are taken as 8.5" and 4.5" respectively on every bridge

Notation :

Fy = Steel yield stress (ksi)

fc = Concrete compressive strength (ksi)

b = T – beam web width (in)

D = T – Beam depth (in)

d = T – Beam adjusted depth (in)

w_{ws} = unit wearing surface weight (kip/ft3)

w_c = unit concrete weight (kip/ft3)

A_s = Total steel area (in2)

h = T – Beam web height (in)

L = Span Length(ft)

S_g = Beam spacing (ft)

Dead Load Moment Calculation:

Calculate Dead Load Due to Concrete:

DL_c = Deadload due to concrete (kip/ft)

DL_ws = Deadload due to wearing surface (kip/ft)

DL = DL_c + DL_ws

DL_c = Unit Concrete Weight x [Flange Area + Web Area]

DL_ws = Unit Wearing Surface Weight x [Wearing Surface Section Area]

b = 15.5 h = 17.5 S_g = 60

w_c = 0.150 w_{ws} = 0.140

$$DL_c = w_c\left[\left(\frac{8.5}{12}\right) * \left(\frac{S_g}{12}\right) + \left(\frac{b}{12}\right) * \left(\frac{h}{12}\right)\right] \qquad DL_c = 0.814$$

$$DL_{ws} = w_{ws}\left[\left(\frac{4.5}{12}\right) * \left(\frac{S_g}{12}\right)\right] \qquad DL_{ws} = 0.2625$$

$$DL = DL_c + DL_{ws} \qquad DL = 1.076$$

Calculate Moment Due to Dead Load:

MDL = Moment due to dead load (kip − ft)

L = Span Length according to AASHTO 3.24.1 (ft)

L = 26

$$MDL = DL * \frac{L^2}{8} \qquad MDL = 90.95$$

Impact Factor Calculation:

I = Impact factor in accordance with AASHTO 6.7.4

$$I = \frac{50}{(L + 125)}$$

If $I > 0.30, it\ can\ be\ taken\ as\ 0.30$ ($AASHTO$ 3.8.2.1)

I = 0.3

Distribution Factor Calculation:

DF = Distribution factor for live loads in accordance with AASHTO 2007

Calculate n, the modular ratio between the beam and the deck.

$n = E_B/E_D$

$= 3600/3600$

$= 1$

Calculate e_g, the distance between the center of gravity of the beam and the deck.

$e_g = NA_{YT} + t_s/2$

$= 8{,}75 + 8{,}5/2$

$= 13$ in

Calculate K_g, the longitudinal stiffness parameter

$K_g = n(I + Ae_g^2)$

$= 1*[39918{,}32 + 781{,}25\ (13)^2]$

$= 171949{,}6\ \text{in}^4$

According to S4.6.2.2.2e, a skew correction factor for moment may be applied for bridge skews greater than 30 degrees.

$$SC = \left[1 - 0{,}25 * \left(\frac{K_g}{12 * L * {t_s}^3}\right)^{0{,}25} * \left(\frac{S}{L}\right)^{0{,}5} * (\tan(\theta))^{1{,}5}\right]$$

$$SC = 0{,}947293$$

Moment distribution factor for an interior beam with two or more design lanes loaded using Table S4.6.2.2.2b-1.

$$DF = \left[0{,}075 + \left(\frac{S}{9{,}5}\right)^{0{,}6} * \left(\frac{S}{L}\right)^{0{,}2} * \left(\frac{K_g}{12 * L * {t_s}^3}\right)^{0{,}1}\right] * SC$$

$$DF = 0{,}533491$$

Moment distribution factor for an interior beam with one design lane loaded using Table S4.6.2.2.2b-1.

$$DF = \left[0{,}06 + \left(\frac{S}{14}\right)^{0,4} * \left(\frac{S}{L}\right)^{0,3} * \left(\frac{K_g}{12*L*t_s^{\,3}}\right)^{0,1}\right] * SC$$

$$DF = 0{,}438546$$

Live Load Moment Calculation:

MLL = Live Load Moment without impact per wheel line $(kip - ft)$

MLL values are taken from the table given in the Appendix A.of the AASHTO (2002) manual

$MLL = 222.2$

Impact and Distribution factors are to be incorporated to use the live load in rating equation

MLL_I = Factored live load moment by distribution and impact factors

DF = Moment distribution factor for an interior beam with two or more design lanes loaded using

$MLL\_I = MLL * DF * (1 + I)$

$MLL\_I = 154.10$

Moment Capacity Calculation (same for FEM based Rating Analysis):

$beff$ = Effective slab width (in)

AASHTO 8.10.1.1

$b_{eff1} = \frac{L * 12}{4}$ $\quad b_{eff1} = 78$

$b_{eff2} = S_g$ $\quad b_{eff2} = 60$

$b_{eff3} = 8.5 * 12$ $\quad b_{eff3} = 102$

Option 2 (beff2) controls the effective slab width. Therefore beff = beff2

$b_{eff} = 60$

a = Depth of rectangular stress block (in)

As = 12.50 total steel area in the tension region (in2)

Fy = 33 steel yield stress (ksi)

fc = 3 concrete compressive strength (ksi)

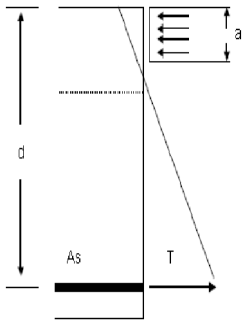

$a = \frac{A_s * f_y}{0.85 * f_c * b_{eff}}$ $\quad a = 2.696$

Calculate d (adjusted depth) for the section:

Location of the center of gravity for steel rebars from the bottom fiber:

$2.696 + \frac{3.75}{2} = 4.57$

$D = 26$

$d = D - 4.57 = 21.43$

Calculate Moment Capacity for the section:

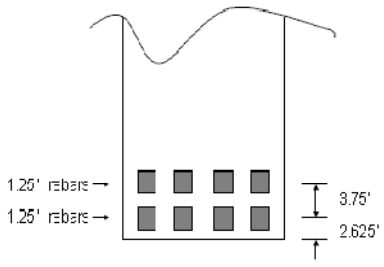

MR = Moment capacity (kip − ft)

$M_R = (A_s * f_y)\left(\frac{d}{12} - \frac{a}{12 * 2}\right)$

$M_R = 692.72$

MU = Ultimate moment capacity (kip − ft)

$\varphi = 0.9$

$MU = \varphi * MR$

$MU = 623.45$

Rating Calculation:

IR = Inventory Rating

$A_1 = 1.30$

$A_2 = 2.17$

$$IR = \frac{M_U - A_1 * M_{DL}}{A_2 * M_{LL\_I}}$$

OR = Inventory Rating

$A_1 = 1.30$

$A_2 = 1.30$

$$OR = \frac{M_U - A_1 * M_{DL}}{A_2 * M_{LL\_I}}$$

$IR = 1{,}511 \qquad OR = 2{,}522$

FEM BASED RATING FOR MOMENT:

Dead Load Moment Calculation

Same moment due to dead load found by LRFD dead load moment calculations is used.

MDL = 90.95

Live Load Moment Calculation:

MLL_FEM: Moment due to Live Load at the critical location(kip − ft)

MLL values are taken from the table given in the Appendix A.of the AASHTO (2002) manual

$\mathrm{MLL} = 222.2$

$\mathrm{FEM\_Moment\_DF} = 0{,}269365$

$\mathrm{MLL\_I\_FEM} = \mathrm{MLL} * \mathrm{FEM\_Moment\_DF} * (1 + \mathrm{I})$

$\mathrm{MLL\_I\_FEM} = 77.81$

Moment Capacity Calculation:

MU = Ultimate moment capacity (kip − ft).

Same capacity found by LRFD Moment capacity calculations is used.

$MU = 623.45$

FEM Based Moment Rating Calculation:

IR = Inventory Rating

$A_1 = 1.30$

$A_2 = 2.17$

$$FEM\_IR = \frac{M_U - A_1 * M_{DL\_FEM}}{A_2 * M_{LL\_I\_FEM}}$$

OR = Inventory Rating

$A_1 = 1.30$

$A_2 = 1.30$

$$FEM\_OR = \frac{M_U - A_1 * M_{DL\_FEM}}{A_2 * M_{LL\_I\_FEM}}$$

$FEM\_IR = 2.992$ $FEM\_OR = 4.995$

LOAD FACTOR RATING FOR SHEAR:

Notation :

s = Stirup spacing (in)

Av = Stirup area (in2)

Ab = Bent − up rebar area (in2)

Dead Load Shear Calculation:

Critical shear location needs to be determined:

X = Critical shear location, distance from the face of the bearing (ft)

X should be taken as the larger of $0.5 * d * cot(\theta)$ or d from the internal face of the bearing. (AASHTO 5.8.3.2)

θ denotes the angle between the section normal and the shear plane and is equal to 45 degrees

$$X_1 = 0.5 * d * \frac{1}{12} * \frac{\cos\left(45 * \frac{\pi}{180}\right)}{\sin\left(45 * \frac{\pi}{180}\right)}$$

$$X_2 = \frac{d}{12}$$

$X_1 = 0.896$

$X_2 = 1.792$

X_2 governs, therefore $X = X_2$

$X = X_2$

VDL $=$ Shear due to dead load (kip)

$$VDL = DL * \left[\left(\frac{L}{12}\right) - X\right]$$

$$VDL = 12.06$$

Distribution Factor Calculation:

DF $=$ Distribution factor for live loads in accordance with AASHTO 2007

According to S4.6.2.2.3c, a skew correction factor for support shear must be applied to the distribution factor of all skewed bridges. The value of the correction factor is calculated using Table S4.6.2.2.3c-1

$$SC = 1 + 0{,}2 * \left(\frac{12 * L * t_s^3}{K_g}\right)^{0,3} * \tan(\theta)$$

$$SC = 1{,}129099$$

Shear distribution factor for an interior beam with two or more design lanes loaded using Table S4.6.2.2.3a-1.

$$DF = \left[0{,}2 + \left(\frac{S}{12}\right) - \left(\frac{S}{35}\right)^2\right] * SC$$

$$DF = 0{,}673235$$

Calculate the shear distribution factor for an interior beam with one design lane loaded using Table S4.6.2.2.3a-1.

$$DF = \left[0{,}36 + \left(\frac{S}{25}\right)\right] * SC \qquad DF = 0{,}632295$$

Live Load Shear Calculation:

$\mathrm{VLL} = \text{Shear due to live load (kip)}$

VLL values are taken from the table given in the Appendix A of the AASHTO (2002) manual

$VLL = 46.8$

Impact and Distribution factors are to be incorporated to use the live load in rating equation

$\mathrm{VLL\_I} = \text{Live load shear with impact and distribution factor (kip)}$

Shear distribution factor for an interior beam with two or more design lanes loaded using Table S4.6.2.2.3a-1.

$DF = 0{,}673235$

$\mathrm{VLL\_I} = \mathrm{VLL} * \mathrm{DF} * (1 + \mathrm{I})$

$VLL\_I = 40.96$

Shear Capacity Calculation:

$\mathrm{Vc} = \text{Shear capacity of the concrete (kip)}$

$\mathrm{Vs1} = \text{Shear capacity of stirrups (kip)}$

$\mathrm{Vs2} = \text{Shear capacity of bent} - \text{up rebars (kip)}$

$\mathrm{Vt} = \text{Total shear capacity of the section (kip)}$

$\mathrm{Vu} = \text{Ultimate shear capacity of the section (kip)}$

$\mathrm{Vt} = \mathrm{Vc} + \mathrm{Vs1} + \mathrm{Vs2}$

$\mathrm{Vu} = 0.85 * \mathrm{Vt}$

Calculate Vc, Vs1, Vs2:

$$V_c = \frac{\left(2 * \sqrt{f_c} * b * d\right)}{1000}$$

$V_c = 36.51$

Av $= 0.393$ total area of the stirups in the section (in2)

s $= 6$ stirup spacing (in)

$$V_{S1} = A_v * f_y * \frac{d}{s}$$

$V_{S1} = 46.47$

Avb $= 3.125$

$$\propto = 45 * \frac{\pi}{180}$$

$V_{S2} = A_{vb} * F_y * \sin \propto$

$V_{S2} = 72.92$

$V_t = V_c + V_{S1} + V_{S2}$

$V_t = 155.90$

$V_U = 0.85 * V_t$

$V_U = 132.51$

Rating Calculation:

IR $=$ Inventory Rating

$A_1 = 1.30$

$A_2 = 2.17$

$$IR = \frac{V_U - A_1 * V_{DL}}{A_2 * V_{LL\_I}}$$

$\mathrm{OR} = \text{Inventory Rating}$

$A_1 = 1.30$

$A_2 = 1.30$

$$OR = \frac{V_U - A_1 * V_{DL}}{A_2 * V_{LL\_I}}$$

$IR = 1.314$

$OR = 2.194$

FEM BASED RATING FOR SHEAR:

Dead Load Shear Calculation:

Same shear due to dead load found by LRFD dead load shear calculations is used.

$VDL = 12.06$

Live Load Shear Calculation:

$\mathrm{VLL\_FEM}: \text{Shear due to Live Load at the critical location } (\mathrm{kip} - \mathrm{ft})$

VLL values are taken from the table given in the Appendix A of the AASHTO (2002) manual

$VLL = 46.8$

$\mathrm{FEM\_Shear\_DF} = 0{,}496453$

$\mathrm{VLL\_I\_FEM} = \mathrm{VLL} * \mathrm{FEM\_Shear\_DF} * (1 + \mathrm{I})$

$\mathrm{VLL\_I\_FEM} = 30.20$

Shear Capacity Calculation:

Vu = Ultimate shear capacity (kip − ft).

Same capacity found by LFD shear capacity calculations is used.

$V_U = 132.51$

FEM Based Shear Rating Calculation:

IR = Inventory Rating

$A_1 = 1.30$

$A_2 = 2.17$

$$FEM\_IR = \frac{V_U - A_1 * V_{DL\_FEM}}{A_2 * V_{LL\_I\_FEM}}$$

OR = Inventory Rating

$A_1 = 1.30$

$A_2 = 1.30$

$$FEM\_OR = \frac{V_U - A_1 * V_{DL\_FEM}}{A_2 * V_{LL\_I\_FEM}}$$

$FEM\_IR = 1.783$

$FEM\_OR = 2.975$